PUBLIC POWER CORPORATION

ATHENS, GREECE

NISYROS GEOTHERMAL DEVELOPMENT
NISYROS WELL NIS-2
Production Characteristics
and Fluid Composition

OS-86038

ORKUSTOFNUN
NATIONAL ENERGY AUTHORITY

VIRKIR CONSULTING GROUP LTD.

REYKJAVÍK, ICELAND

NISYROS GEOTHERMAL DEVELOPMENT

NISYROS WELL NIS-2

Production Characteristics

and Fluid Composition

CS - 86038

**Work under contract no 1650002, March 1985
for the Public Power Corporation of Greece**

SUMMARY OF RESULTS AND RECOMMENDATIONS FOR FURTHER WORK

NISYROS WELL NIS-2
Production Characteristics and Fluid Composition

SUMMARY OF RESULTS AND RECOMMENDATIONS FOR FURTHER WORK

The work described in this report was carried out under contract No. 1650002, March 1985, between the Public Power Corporation of Greece and the joint venture of the Virkir Consulting Group and the National Energy Authority, Iceland. This work encompassed evaluation of the production characteristics of, and the composition of fluids from, well NIS-2 on Nisyros. Pertinent data were collected during a flow test lasting from March 17 to June 18, 1985.

FLOW CHARACTERISTICS

Total Discharge and Wellhead Pressure: The well was discharged to a silencer and the mass flow measured regularly. The wellhead pressure declined rapidly during the first week due to initial stabilization; the mass flow increased, however. After 20 days of discharge the mass flow increased suddenly from about 14 kg/s to about 23 kg/s and the wellhead pressure from about 9 bar-g to about 14 bar-g. Subsequently the flow and wellhead pressure declined slightly, but during the last 60 days of the test they remained in the range 20.3 kg/s - 21.2 kg/s and 11.2 bar-g - 11.9 bar-g, respectively. The sudden increase was accompanied by a discharge of rock chips and mud, indicating the opening of a new aquifer or the widening of an existing one.

Discharge Enthalpy: After one week of discharge the enthalpy was about 1600 kJ/kg, dropped to around 1400 kJ/kg when the sudden increase in mass flow occurred, and remained stable thereafter.

Steam Production: During the last 30 days of the flow test, after the well had stabilized, the calculated average steam discharge was 5.2 kg/s at a separation pressure of 15 bar-g. This figure is based on mass flow data when the wellhead pressure was between 11 bar-g and 12 bar-g. Steam flow of 5.2 kg/s is barely sufficient for the generation of $2MW_e$ of electric power in a single-stage condensing turbine. This steam flow rate is expected to decrease during long-term production.

FLUID COMPOSITION

Brine Composition: Downhole chloride concentrations are about 50000 mg/kg and total dissolved solids about 85000 mg/kg. This is more than

double the salinity of seawater. After flashing to atmospheric pressure, the concentration of chloride rises to 82000 mg/kg and that of total dissolved solids to 140000 mg/kg. The high temperature and the high salinity of the Nisyros brine suggest that it may contain heavy metals in concentrations above acceptable limits for surface disposal.

Gas in Steam: The concentration of gas in the steam was measured regularly during the test. Early samples showed high gas concentrations of 4.4% by weight, but after the sudden change in output the gas concentrations became lower. During the last month of discharge, the calculated concentration of gas in steam at 15 bar-g was about 1.9% by weight. This is high but acceptable for power generation. The main noncondensible gas constituents are carbon dioxide (97.7% by volume), hydrogen sulfide (1.65%), methane (0.45%), and hydrogen (0.10%).

RESERVOIR CHARACTERISTICS

Aquifer Temperature: It was not possible to make downhole logs of temperature and pressure due to bent air-lift tubing in the well. From chemical analyses of the discharged fluids, the aquifer temperature was estimated to be 290°C.

Permeability: From the decrease in wellhead pressure during the flow test the permeability thickness product was estimated to be 0.7 darcy m. This is similar to the permeability of the Milos M-2 well. This approach is not optimal, but had to be adopted, because downhole pressure recovery could not be measured. The skin factor was estimated to be -2 before the the sudden increase in mass flow, when it improved to -5.

Boiling in the Reservoir: Downhole pressure, temperature, and steam fraction profiles in the discharging well were modelled, because downhole pressure and temperature could not be measured. The results indicate boiling to the bottom of the well. During the latter part of the flow test period the calculated pressure at the main inflow into the well was below about 30 bar-g. From this it is concluded that the main pressure drop from undisturbed conditions to wellhead occurs in the aquifer (60 bar), and, accordingly, it is expected that steam flow will vary little with wellhead pressure.

SCALING TENDENCIES

Silica: The silica concentration is about 640 mg/kg downhole but rises to around 1040 mg/kg when the fluids are flashed to atmospheric pressure. Amorphous silica supersaturation is attained if the steam pressure falls below 14.8 bar-g. Silica can thus be expected to precipitate in equipment operated below this pressure. Design of wellhead parts and steam separators should take this into account. Coprecipitation with sulfides could lower the solubility.

Calcite: Upon flashing, the brine becomes supersaturated with respect to calcite. The precipitation is expected to be most intense at the level of first boiling and will thus be concentrated in the aquifer. Calcite scaling will probably not induce operational problems.

Sulfides: The brine is high in iron and probably also in some other base metals. These metals will be precipitated as sulfides upon boiling of the brine. Tests are required to establish the scaling rate.

STEAM SEPARATION AND TURBINE INLET PRESSURE

As the brine is highly saline, carry-over of water droplets from the wellhead separator will be unacceptably high for the operation of the turbines. A second separator is therefore necessary. The wellhead separator should be operated at 15 bar-g but the second separator at a lower pressure. For this separation to be effective the steam must be scrubbed with condensate. Selection of turbine inlet pressure should take into account results of scaling studies and anticipated long-term decline in wellhead pressure.

RECOMMENDATIONS FOR FURTHER WORK

The test on well NIS-2 in 1985 lasted for three months and focused on establishing various well flow parameters and the chemical composition of the discharged fluid. No scaling or corrosion studies were performed, the well was not logged, and viable methods of waste water disposal were not assessed. The present steam flow is barely sufficient for producing 2 MW_e of electric power. Basing a power station on a single well is risky and possibly difficult operationally, so drilling of new production wells is advisable. Siting of new wells should be preceeded by an assessment of all available reservoir data, including the disciplines of geology, geophysics, geochemistry, and reservoir engineering.

In order that a sound decision to erect a 2 MW$_e$ power plant on the island of Nisyros can be made, we recommend the following additional studies on well NIS-2:

1. Logging of downhole temperature and pressure, which entails that the air-lift tube be removed.

2. Logging with go-devils to see whether a significant amount of scale has formed inside the casing.

3. Discharging the well for a longer period (up to 12 months) to establish the long-term production characteristics.

4. Measurements of downhole pressure recovery after the flow test to determine permeability and skin factor.

5. Carrying out tests to establish scaling and corrosion rates.

6. Monitoring of the chemical composition of brine, and of gas in steam. Selected brine samples should be collected for trace element analysis.

Furthermore, we recommend the following investigations:

7. Assessment of possible methods of waste water disposal, including treatment for disposal into the sea, ponding and infiltration, and reinjection into the reservoir following silica removal.

8. Evaluation of all available reservoir and well production data, encompassing the disciplines of geology, geophysics, geochemistry, reservoir engineering, and process engineering, in order to site new wells. The available data may turn out to be insufficient, in which case further measurements are advisable before new wells are sited.

CONTENTS

LIST OF TABLES

LIST OF FIGURES

1   INTRODUCTION

This report describes part of the work carried out under contract No.
1650002, March 1985, between the Public Power Corporation of Greece
(PPC) and the joint venture of the Virkir Consulting Group and the
National Energy Authority (Virkir/NEA), Iceland.

The scope of the work for the contract was to:

1. Provide well testing program for NIS-1 and NIS-2.
2. Assist in setting up a field lab.
3. Provide procedures for chemical sampling and analysis.
4. Interpret the results of the output test.
5. Suggest data to be included in tender documents.
6. Provide technical advice for the possible drilling of reinjection
   wells.

Nisyros is an island in the Dodecanese. The island is a volcano, which
has collapsed, forming a caldera. The soil and bedrock on the caldera
floor have been considerably altered by hydrothermal activity. The
wells are located inside the caldera as shown in Figure 1.1.

Well NIS-2 was drilled to a depth of 1547 m and was completed on Octo-
ber 8th, 1983. The well was cased with 9 5/8" cemented casing down to
1050 m and lined with 7" liner. The well profile is shown in Figure
1.1.

The water and steam flow from the well were monitored by PPC person-
nel, and samples were collected for chemical analysis. The analyses
were performed in part by PPC in the field, and in part by the Insti-
tute of Geology and Mineral Exploration (IGME) in Athens. Two refer-
ence brine samples and twelve gas samples were analyzed by the con-
tractor.

Sverrir Thorhallsson and Halldor Armannsson travelled to Nisyros on
behalf of the consultants and assisted PPC personnel in discharging
the well and in setting up a field laboratory. They also provided pro-
cedures for chemical sampling and analysis and instructed site scien-
tists. The test started March 17, and ended on June 18, 1985.

Omar Sigurdsson travelled to Nisyros and supervised an injection test
of well NIS-1. The result of this test has been submitted to PPC in a
separate report.

Trausti Hauksson interpreted the results of the output measurements,
and Jon Orn Bjarnason and Stefan Arnorsson the results of the chemical
analyses.

Figure 1.1 Well location and well profile.

NISYROS WELL N-2
WELL PROFILE

(Based on Di Paola)
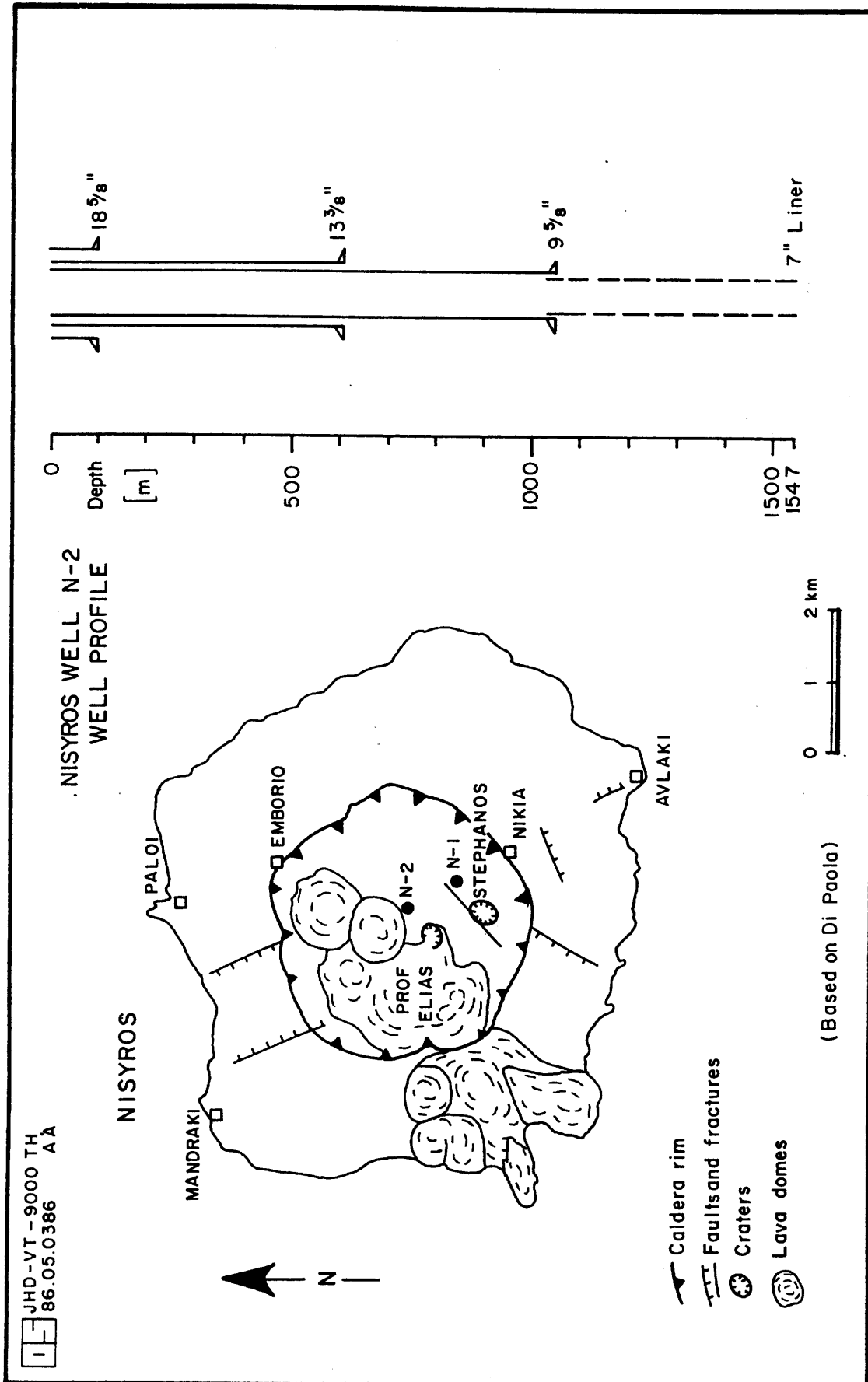
2 FLOW TESTS

2.1 Introduction

Well NIS-2 on Nisyros was subjected to flow tests for three months in the second quarter of 1985. The well was opened slightly on March 17, 1985, to bleed off gas and to allow the well to heat up slowly. The wellhead pressure was 48 bar-g initially, and increased to 51 bar-g in a matter of minutes. Because of this, the master valve was opened fully and the well discharged through a 2 1/2" lip pressure pipe, causing the wellhead pressure to decrease rapidly to about 19 bar-g in seven days. On March 24 the flow was diverted to a 4" lip pipe, causing the wellhead pressure to decline further, to 10 bar-g. The mass flow was approximately constant in the period up to April 6, approximately 14-15 kg/s. During this period the wellhead pressure decreased from 10 bar-g to 9 bar-g and the discharge enthalpy from about 1700 kJ/kg to about 1550 kJ/kg.

On April 6, an abrupt change occurred in the flow characteristics. Wellhead pressure increased to about 14 bar-g, mass flow to about 23 kg/s, but the discharge enthalpy decreased to about 1400 kJ/kg. This change was accompanied by a discharge of rock chips and mud, indicating that an aquifer that had been clogged during drilling was reopened due to the pressure decrease in the discharging well.

After this sudden change the well output decreased to about 21 kg/s in one week, but thereafter it remained relatively stable for the remaining 60 days of the test. The well was shut down on June 18.

2.2 Method of measurement

The mass flow and the discharge enthalpy were obtained by measurements of critical lip pressure and water flow through a rectangular weir. The lip pressure pipes were as required by the method of Russell James. This method is empirical and based on experiments on dilute geothermal waters. It is, therefore, not possible to estimate the effect of salinity on the Russell James equation. Thus an unknown error is introduced when the equation is applied to the very saline brines of Nisyros. We consider, however, that this error will not significantly affect the calculated steam flow.

The Russell James equation is as follows:

$$m = 1.441 \; 10^6 \; \frac{d^2 \; P_c^{0.96}}{H^{1.102}} \quad \text{(kg/s)}$$

P_c : Critical lip pressure (barg)

d : Lip diameter (m)

H : Enthalpy (kJ/kg)

The following equation (ASME 1971) was employed to calculate brine volume flow from measured water level in the weir box:

$$q = 2/3 \; C \; R_w \; \sqrt{2 \; g \; h} \quad \text{(m}^3\text{/s)}$$

R_w : weir width (m) + 0.0025

h : head (m) + 0.0009

C : flow coefficient

The flow coefficient is a function of weir width (Rw), channel width (Lc), crest height (P), and head (h). For this particular case of Rw = 0.2 m, Lc = 0.64 m, and P = 0.25 m, the flow coefficient is 0.59.

Because a salinity correction cannot be applied to the Russell James method, no correction for the effect of salinity on the enthalpy and the density of the brine was applied either. Consequently, all the following calculations are based on the thermodynamic properties of pure water and steam.

For calculating the fluid enthalpy, a combined mass and energy balance is used and the enthalpy found by iteration.

$$mH = m_f \; H_f + (m - m_f) H_g$$

m : total flow

m_f : mass flow of brine at atmospheric pressure (kg/s)

H_f : enthalpy of brine at atmospheric pressure (kJ/kg)

H_g : enthalpy of steam at atmospheric pressure (kJ/kg)

2.3 Results of flow measurements

The results of the flow measurements are shown in Table 2.1. Primary data for rectangular weir and critical lip pressure measurements are shown, as are the calculated enthalpy (Htot) and total flow (Qtot). Results of measurements of wellhead pressure, total flow, and enthalpy are shown in Figure 2.1.

The properties of the well flow changed suddenly on April 6. Discharge enthalpy decreased from about 1550 kJ/kg to about 1400 kJ/kg and mass flow increased from about 14 kg/s to about 23 kg/s. This change was caused by an inflow of lower enthalpy fluid af approximately 1180 kJ/kg. After this change the wellhead pressure declined gradually from 14 bar-g to 11 bar-g, which can be explained by drawdown in the reservoir. The mass flow and enthalpy remained constant, however, during the last 60 days of the test.

The graph of total flow vs. wellhead pressure is shown in Figure 2.2. The production characteristic curve was rather flat prior to the change on April 6 indicating that the major flow constriction is in the aquifer. Data are lacking to establish the production characteristic curve after the change on April 6, but we expect it to be relatively flat also.

2.4 Well model

Downhole pressure, temperature, and steam fraction profiles in the flowing well were modelled on the basis of four selected discharge measurements; the first just after initiation of the well discharge, the second and third just before and after the sudden change in output, and the fourth just before shutdown (Figs. 2.3, 2.4, and 2.5).

The calculations are based on the empirical equations of Armand and Treacher for the pressure drop and the slip ratio in two phase flow. The effect of salinity of 65000 mg/kg (NaCl) and gas concentration of 3000 mg/kg (CO_2) on the thermodynamic properties is taken into account in the calculation.

The calculations show that the well fluid flashes to the bottom of the well during flow. The main inflow is believed to be at a depth of 1080 m because circulation loss occurred at that depth during drilling. The calculated steam fraction was 47% by weight at this depth shortly after initiation of the discharge. During the first twenty days the steam fraction fell to 32% indicating increased inflow of lower enthalpy fluids (see curve 2 in Fig 2.5). This is an unusual behavior

of a well producing from a flashing aquifer where the steam fraction usually increases with time because the relative permeability favors flow of the steam phase. After the output increase of April 6, the steam fraction fell further to 20% at 1080 m depth and remained constant thereafter.

The calculated pressure at the aquifer depth of 1080 m was 28 bar-g at the end of the test. The undisturbed aquifer pressure for the well was not measured, but if one assumes hydrostatic pressure of cold seawater, this aquifer pressure is 90 bar-g, and the inflow is therefore choked during discharge. If the inflow is through a fracture, one can estimate the fracture width by assuming critical flow and using the equation of Russell James. Such calculations give a fracture cross sectional area of 7 cm^2, corresponding to a horizontal fracture width of 1.1 mm. This result is only indicative but is consistent with the low permeability of the producing formation.

2.5 Wellhead pressure decrease

Because of a bend in the air-lift tubing used initially to stimulate the well, logging equipment could not be lowered into the well for downhole measurements of the pressure recovery after shutdown. Determination of reservoir transmissivity from wellhead pressure decrease must therefore be relied upon, although such an approach is not optimal. Figure 2.6 shows changes in wellhead pressure divided by output, plotted versus the logarithm of the time, from the beginning of the test. The slope of this curve is 25 kPa/(kg/s) per log cycle during both discharge periods. From the well modelling it was found that the pressure change at 1080 m is 40% greater than the wellhead pressure change. Thus the slope should be increased by 40%, giving a value of 35.

The reservoir transmissivity is obtained from the following equation:

$$\frac{kh}{\mu} = \frac{2.3 \, \upsilon}{4 \, \pi \, m}$$

$\dfrac{kh}{\mu}$: transmissivity (m^3/Pas)

m : slope Pa/(kg/s)/log cycle

υ : specific volume of fluid (m^3/kg)

The specific volume of fluid in the aquifer is assumed to be that of water at 290°C, which is 0.00136 m^3/kg. This gives the transmissivity

as:

$$\frac{kh}{\mu} = \frac{2.3 \times 0.00136}{4 \pi 35000} = 7.1 \ 10^{-9}$$

This is considerably higher than the transmissivity of NIS-1 (2×10^{-9} m^3/Pas).

The permeability thickness (kh) can be obtained by multiplying the transmissivity by the viscosity of water at 290°C. This gives the following:

$$kh = 6.5 \cdot 10^{-13} \ m^3 \quad (0.65 \ darcy \ m)$$

This compares favorably with the Milos reservoir, where kh, derived similarly from wellhead pressure decrease, is 0.3-0.6 darcy m for well M-2.

The skin factor was estimated by means of the equation

$$s = 1.151 \ (\frac{\Delta P}{m} - \log \ (\frac{k}{\phi \ \mu \ c_t \ r_w^2} \ ) \ -5.29)$$

using a viscosity (μres) of 9.1×10^{-5} Pas, a formation storativity (ϕcth) of 4×10^{-8} m/Pa, and a transmissivity (kh/μ) of 7.1×10^{-9} m^3/Pas. The above value for the storativity is taken from an injection test on well NIS-1.

We have estimated the ratio ΔP/flow to be 120 kPa/(kg/s) and 90 kPa/(kg/s), respectively, before and after the sudden change in well performance on April 6. Here ΔP denotes the pressure difference between undisturbed aquifer conditions and those of the inflow into the well. By inserting these values into the above equation, the skin factor was found to have improved from about -2 to about -5.

2.6 Steam and brine flow

The calculated flow of steam at a separation pressure of 15 bar-g is shown in Table 2.2 for all measurements. Steam flow was nearly constant at 5.1 kg/s before the sudden increase in mass flow on April 6. Shortly afterwards, the steam flow increased to 6.2 kg/s. Subsequently it declined gradually and at the termination of the test it was 5.2 kg/s.

After initial stabilization the well is expected to produce 5.2 kg/s of high pressure steam separated at 15 bar-g, and 3.0 kg/s of low pressure steam (at atmospheric pressure). The effluent brine will be 12.5 kg/s. During long-term production, the steam flow is expected to decrease below 5.2 kg/s, the rate of decline depending on the reservoir properties. Experience from some exploited geothermal reservoirs in other parts of the world tends to show a long-term decline of approximately 10% - 20% in five years.

The wellhead pressure declined considerably during the flow test and had reached 11.4 bar-g at the end. It is considered advisable to operate the well at a higher pressure (around 15 bar-g, see section 4.4) in order to reduce or prevent silica scaling. As the production characteristic curve for the well is expected to be rather flat, the increased wellhead pressure should not cause the steam flow rate to be reduced significantly.

Table 2.1 Data from flow test 1985.

Date	Time	WHP bar-g	Rectangular weir			Crh mm	Tbrine C	Crit. D mm	Lip PC bar-g	Calculated		Remarks	No:
			wh mm	Rw mm	Chw mm					Qtot kg/s	Htot kJ/kg		
850317	1830	31.00	34.	200.	640.	250.	100.0	75.0	2.50	6.56	1904.8		1
850319	1345	23.70	35.	200.	640.	250.	100.0	75.0	4.80	9.44	2124.1		2
850321	1100	21.00	40.	200.	640.	250.	100.0	75.0	4.40	9.41	2002.7		3
850324	1600	18.50	63.	200.	640.	250.	100.0	97.6	2.30	12.20	1662.1	4" lip	4
850325	1200	16.90	63.	200.	640.	250.	100.0	97.6	2.20	·11.98	1644.2		5
850326	1200	16.50	67.	200.	640.	250.	100.0	97.6	2.30	12.66	1606.4		6
850327	0900	12.50	67.	200.	640.	250.	100.0	97.6	2.70	13.51	1673.5		7
850327	1200	10.80	67.	200.	640.	250.	100.0	97.6	3.25	14.67	1752.4		8
850327	1700	10.20	70.	200.	640.	250.	100.0	97.6	3.20	14.92	1707.5		9
850329	0900	9.80	69.	200.	640.	250.	100.0	97.6	2.90	14.17	1677.7		10
850329	1800	10.00	69.	200.	640.	250.	100.0	97.6	3.00	14.38	1692.3		11
850330	0900	9.80	71.	200.	640.	250.	100.0	97.6	2.80	14.20	1636.8		12
850330	1700	9.90	71.	200.	640.	250.	100.0	97.6	2.80	14.20	1636.8		13
850331	0900	9.90	72.	200.	640.	250.	100.0	97.6	2.70	14.11	1608.4		14
850331	1800	9.80	72.	200.	640.	250.	100.0	97.6	2.90	14.54	1639.4		15
850401	1000	9.70	73.	200.	640.	250.	100.0	97.6	2.80	14.45	1611.6		16
850401	1800	9.50	73.	200.	640.	250.	100.0	97.6	2.80	14.45	1611.6		17
850402	1100	9.50	74.	200.	640.	250.	100.0	97.6	2.70	14.36	1583.3		18
850402	1700	9.40	74.	200.	640.	250.	100.0	97.6	2.70	14.36	1583.3		19
850403	0900	9.20	76.	200.	640.	250.	100.0	97.6	2.60	14.40	1542.2		20
850403	1700	9.20	75.	200.	640.	250.	100.0	97.6	2.70	14.49	1570.9		21
850404	0800	9.20	75.	200.	640.	250.	100.0	97.6	2.60	14.27	1554.6		22
850404	1500	9.20	75.	200.	640.	250.	100.0	97.6	2.60	14.27	1554.6		23
850404	1900	9.20	75.	200.	640.	250.	100.0	97.6	2.60	14.27	1554.6		24
.850405	1200	9.00	76.	200.	640.	250.	100.0	97.6	2.60	14.40	1542.2		25
850405	1800	9.00	76.	200.	640.	250.	100.0	97.6	2.65	14.51	1550.5		26
850406	0800	9.10	76.	200.	640.	250.	100.0	97.6	2.60	14.34	1548.4		27
850406	1545	13.50	116.	200.	640.	250.	100.0	97.6	4.20	23.40	1367.7	Cuttings/bent./FeS	28
850406	1645	14.20	113.	200.	640.	250.	100.0	97.6	4.30	23.15	1404.2	Cuttings	29
850406	1800	14.00	113.	200.	640.	250.	100.0	97.6	4.50	23.57	1426.8	Cuttings	30
850407	1000	13.80	115.	200.	640.	250.	100.0	97.6	4.10	23.03	1364.1	.Cuttings	31
850407	1400	13.90	115.	200.	640.	250.	100.0	97.6	4.20	23.24	1375.9	Cuttings	32
850408	1300	13.50	119.	200.	640.	250.	100.0	97.6	4.20	23.86	1343.5	Cuttings	33 .
850408	1900	13.50	119.	200.	640.	250.	100.0	97.6	4.20	23.86	1343.5	Cuttings	34
850409	0700	13.54	113.	200.	640.	250.	100.0	97.6	4.20	22.94	1392.6	Cuttings	35
850409	1700	13.50	111.	200.	640.	250.	100.0	97.6	4.20	22.63	1409.5	Cuttings	36
850410	1000	13.20	110.	200.	640.	250.	100.0	97.6	4.10	22.27	1406.2	Cuttings	37
850410	1500	13.40	110.	200.	640.	250.	100.0	97.6	4.20	22.48	1418.1	Cuttings	38
850411	1000	13.10	109.	200.	640.	250.	100.0	97.6	4.00	21.91	1402.8	Some cuttings	39
850411	1700	13.00	109.	200.	640.	250.	100.0	97.6	4.00	21.91	1402.8		40
850412	1400	13.10	111.	200.	640.	250.	100.0	97.6	4.00	22.21	1385.6		41
850413	0900	13.00	109.	200.	640.	250.	100.0	97.6	4.00	21.91	1402.8		42
850413	1200	12.90	109.	200.	640.	250.	100.0	97.6	4.00	21.91	1402.8	·	43
850413	1500	12.90	105.	200.	640.	250.	100.0	97.6	4.00	21.32	1438.2		44
850413	1700	12.90	103.	200.	640.	250.	100.0	97.6	4.00	21.03	1456.3		45
850413	2000	12.90	106.	200.	640.	250.	100.0	97.6	4.00	21.47	1429.2		46
850414	0900	13.00	107.	200.	640.	250.	100.0	97.6	4.00	21.61	1420.3		47
850414	1200	12.90	107.	200.	640.	250.	100.0	97.6	3.90	21.40	1408.0		48
850414	1500	12.90	107.	200.	640.	250.	100.0	97.6	3.90	21.40	1408.0		49
850414	1900	12.90	107.	200.	640.	250.	100.0	97.6	3.90	21.40	1408.0		50
850414	2000	12.90	107.	200.	640.	250.	100.0	97.6	3.90	21.40	1408.0		51
850415	1000	12.90	110.	200.	640.	250.	100.0	97.6	3.90	21.85	1381.8		52
850415	1400	12.90	110.	200.	640.	250.	100.0	97.6	3.90	21.85	1381.8		53
850415	1800	12.90	110.	200.	640.	250.	100.0	97.6	3.90	21.85	1381.8		54
850416	0800	12.80	108.	200.	640.	250.	100.0	97.6	3.80	21.34	1386.5		55

Table 2.1 (cont.)

Date	Time	WHP bar-g	Rectangular weir wh mm	Rw mm	Chw mm	Crh mm	Tbrine C	Crit. D mm	Lip PC bar-g	Calculated Qtot kg/s	Htot kJ/kg	Remarks	No:
850416	0900	12.80	108.	200.	640.	250.	100.0	97.6	3.90	21.55	1399.2		56
850416	1200	12.80	107.	200.	640.	250.	100.0	97.6	3.80	21.19	1395.4		57
850416	1500	12.80	108.	200.	640.	250.	100.0	97.6	3.80	21.34	1386.5		58
850416	1600	12.80	107.	200.	640.	250.	100.0	97.6	3.80	21.19	1395.4		59
850416	1900	12.80	107.	200.	640.	250.	100.0	97.6	3.80	·21.19	1395.4		60
850416	2000	12.80	107.	200.	640.	250.	100.0	97.6	3.80	21.19	1395.4		61
850416	2100	12.80	107.	200.	640.	250.	100.0	97.6	3.80	21.19	1395.4		62
850418	0800	12.70	108.	200.	640.	250.	100.0	97.6	3.70	21.13	1373.7		63
850418	1300	12.70	108.	200.	640.	250.	100.0	97.6	3.70	21.13	1373.7		64
850418	1700	12.70	108.	200.	640.	250.	100.0	97.6	3.70	21.13	1373.7		65
850419	0800	12.60	108.	200.	640.	250.	100.0	97.6	3.70	21.13	1373.7		66
850419	1200	12.60	108.	200.	640.	250.	100.0	97.6	3.70	21.13	1373.7		67
850419	1800	12.60	107.	200.	640.	250.	100.0	97.6	3.70	20.98	1382.5		68
850420	0900	12.60	108.	200.	640.	250.	100.0	97.6	3.70	21.13	1373.7		69
850420	1300	12.60	107.	200.	640.	250.	100.0	97.6	3.70	20.98	1382.5		70
850421	0700	12.60	108.	200.	640.	250.	100.0	97.6	3.70	·21.13	1373.7		71
850421	1000	12.60	108.	200.	640.	250.	100.0	97.6	3.70	21.13	1373.7		72
850421	1300	12.60	108.	200.	640.	250.	100.0	97.6	3.70	21.13	1373.7		73
850422	0800	12.50	106.	200.	640.	250.	100.0	97.6	3.80	21.04	1404.3		74
850422	1400	12.50	106.	200.	640.	250.	100.0	97.6	3.70	20.83	1391.4		75
850422	1900	12.50	106.	200.	640.	250.	100.0	97.6	3.70	20.83	1391.4		76
850423	0700	12.40	107.	200.	640.	250.	100.0	97.6	3.80	21.19	1395.4		77
850423	1100	12.40	106.	200.	640.	250.	100.0	97.6	3.80	21.04	1404.3		78
850424	0900	12.40	107.	200.	640.	250.	100.0	97.6	3.80	21.19	1395.4		79
850424	1300	12.30	108.	200.	640.	250.	100.0	97.6	3.80	21.34	1386.5		80
850424	1900	12.30	107.	200.	640.	250.	100.0	97.6	3.80	21.19	1395.4		81
850425	0900	12.30	107.	200.	640.	250.	100.0	97.6	3.70	20.98	1382.5		82
850425	1400	12.20	106.	200.	640.	250.	100.0	97.6	3.70	20.83	1391.4		83
850426	1200	12.00	105.	200.	640.	250.	100.0	97.6	3.60	20.47	1387.3		84
850426	1900	12.50	105.	200.	640.	250.	100.0	97.6	3.60	20.47	1387.3		85
850427	0900	12.20	105.	200.	640.	250.	100.0	97.6	3.70	20.69	1400.4		86
850427	1700	12.20	105.	200.	640.	250.	100.0	97.6	3.70	20.69	1400.4		87
850428	1000	12.30	105.	200.	640.	250.	100.0	97.6	3.70	20.69	1400.4		88
850428	1600	12.30	105.	200.	640.	250.	100.0	97.6	3.70	20.69	1400.4		89
850429	1400	12.30	105.	200.	640.	250.	100.0	97.6	3.70	20.69	1400.4		90
850430	1100	12.20	105.	200.	640.	250.	100.0	97.6	3.70	20.69	1400.4		91
850430	1800	12.30	105.	200.	640.	250.	100.0	97.6	3.70	20.69	1400.4		92
850501	1000	12.20	105.	200.	640.	250.	100.0	97.6	3.70	20.69	1400.4		93
850506	1200	12.00	104.	200.	640.	250.	100.0	97.6	3.80	20.75	1422.3		94
850506	2000	11.90	104.	200.	640.	250.	100.0	97.6	3.80	20.75	1422.3		95
850507	1000	12.00	104.	200.	640.	250.	100.0	97.6	3.70	20.54	1409.4		96
850507	1600	12.00	104.	200.	640.	250.	100.0	97.6	3.70	20.54	1409.4		97
850508	1200	12.00	104.	200.	640.	250.	100.0	97.6	3.70	20.54	1409.4		98
850508	1800	12.00	104.	200.	640.	250.	100.0	97.6	3.70	20.54	1409.4		99
850509	0800	11.90	104.	200.	640.	250.	100.0	97.6	3.80	20.75	1422.3		100
850509	1200	11.90	104.	200.	640.	250.	100.0	97.6	3.80	20.75	1422.3		101
850510	0900	11.90	104.	200.	640.	250.	100.0	97.6	3.70	20.54	1409.4		102
850510	1700	11.90	104.	200.	640.	250.	100.0	97.6	3.70	20.54	1409.4		103
850511	1200	11.90	104.	200.	640.	250.	100.0	97.6	3.70	20.54	1409.4		104
850512	1000	11.80	104.	200.	640.	250.	100.0	97.6	3.70	20.54	1409.4		105
850513	1000	11.60	104.	200.	640.	250.	100.0	97.6	3.70	20.54	1409.4		106
850514	1000	11.60	104.	200.	640.	250.	100.0	97.6	3.70	20.54	1409.4		107
850515	1200	11.50	104.	200.	640.	250.	100.0	97.6	3.70	20.54	1409.4		108
850516	1100	11.40	104.	200.	640.	250.	100.0	97.6	3.70	20.54	1409.4		109
850517	0800	11.50	104.	200.	640.	250.	100.0	97.6	3.70	20.54	1409.4		110

Table 2.1 (cont.)

Date	Time	WHP bar-g	wh mm	Rw mm	Chw mm	Crh mm	Tbrine C	D mm	PC bar-g	Qtot kg/s	Htot kJ/kg	Remarks	No:
			Rectangular weir					Crit. Lip		Calculated			
850517	1200	11.40	104.	200.	640.	250.	100.0	97.6	3.70	20.54	1409.4		111
850518	0800	11.70	104.	200.	640.	250.	100.0	97.6	3.60	20.33	1396.3		112
850519	1100	11.50	104.	200.	640.	250.	100.0	97.6	3.60	20.33	1396.3		113
850520	0800	11.40	104.	200.	640.	250.	100.0	97.6	3.60	20.33	1396.3		114
850521	0900	11.30	103.	200.	640.	250.	100.0	97.6	3.50	.19.97	1392.0		115
850522	0800	11.30	103.	200.	640.	250.	100.0	97.6	3.50	19.97	1392.0		116
850523	0900	11.30	103.	200.	640.	250.	100.0	97.6	3.50	19.97	1392.0		117
850523	1400	11.20	105.	200.	640.	250.	100.0	97.6	3.50	20.26	1373.8		118
850524	1200	11.60	109.	200.	640.	250.	100.0	97.6	3.50	20.86	1338.4		119
850525	1000	11.70	109.	200.	640.	250.	100.0	97.6	3.60	21.07	1351.8		120
850525	1900	12.00	109.	200.	640.	250.	100.0	97.6	3.50	20.86	1338.4		121
850526	0900	11.60	110.	200.	640.	250.	100.0	97.6	3.40	20.79	1316.0		122
850526	1400	11.70	110.	200.	640.	250.	100.0	97.6	3.50	21.01	1329.7		123
850527	0800	11.90	110.	200.	640.	250.	100.0	97.6	3.50	21.01	1329.7		124
850528	1000	11.80	110.	200.	640.	250.	100.0	97.6	3.60	21.22	1343.1		125
850528	1400	11.80	110.	200.	640.	250.	100.0	97.6	3.60	21.22	1343.1		126
850529	1100	11.70	109.	200.	640.	250.	100.0	97.6	3.50	20.86	1338.4		127
850529	1400	11.70	109.	200.	640.	250.	100.0	97.6	3.50	20.86	1338.4		128
850530	0700	11.80	109.	200.	640.	250.	100.0	97.6	3.60	21.07	1351.8		129
850530	1100	11.80	109.	200.	640.	250.	100.0	97.6	3.60	21.07	1351.8		130
850530	1800	11.80	109.	200.	640.	250.	100.0	97.6	3.50	20.86	1338.4		131
850531	0900	11.70	109.	200.	640.	250.	100.0	97.6	3.60	21.07	1351.8		132
850531	1300	11.70	109.	200.	640.	250.	100.0	97.6	3.50	20.86	1338.4		133
850601	0900	11.80	109.	200.	640.	250.	100.0	97.6	3.60	21.07	1351.8		134
850601	1700	11.70	109.	200.	640.	250.	100.0	97.6	3.50	20.86	1338.4		135
850603	0900	11.80	109.	200.	640.	250.	100.0	97.6	3.50	20.86	1338.4		136
850604	1000	11.70	108.	200.	640.	250.	100.0	97.6	3.60	20.92	1360.5		137
850605	1000	11.60	108.	200.	640.	250.	100.0	97.6	3.50	20.71	1347.1		138
850606	1000	11.60	109.	200.	640.	250.	100.0	97.6	3.50	20.86	1338.4		139
850607	0700	11.60	111.	200.	640.	250.	100.0	97.6	3.50	21.16	1321.2		140
850607	1000	11.50	109.	200.	640.	250.	100.0	97.6	3.50	20.86	1338.4		141
850608	0900	11.60	102.	200.	640.	250.	100.0	97.6	3.50	19.83	1401.3		142
850609	1000	11.50	102.	200.	640.	250.	100.0	97.6	3.50	19.83	1401.3		143
850610	1000	11.50	102.	200.	640.	250.	100.0	97.6	3.50	19.83	1401.3		144
850611	1000	11.40	103.	200.	640.	250.	100.0	97.6	3.50	19.97	1392.0		145
850612	1000	11.40	102.	200.	640.	250.	100.0	97.6	3.50	19.83	1401.3		146
850613	1000	11.20	108.	200.	640.	250.	100.0	97.6	3.60	20.92	1360.5		147
850614	1500	11.30	109.	200.	640.	250.	100.0	97.6	3.50	20.86	1338.4		148
850615	1000	11.20	107.	200.	640.	250.	100.0	97.6	3.50	20.56	1356.0		149
850616	0800	11.20	108.	200.	640.	250.	100.0	97.6	3.60	20.92	1360.5		150
850616	1700	11.20	107.	200.	640.	250.	100.0	97.6	3.50	20.56	1356.0		151
850617	1000	11.20	105.	200.	640.	250.	100.0	97.6	3.50	20.26	1373.8		152
850618	0900	11.20	108.	200.	640.	250.	100.0	97.6	3.50	20.71	1347.1		153

WHP: Wellhead pressure
wh: Water level
Rw: Weir width
Chw: Channel width
Crh: Crest height

Tbrine: Temperature of brine in weir box
D: Critical lip diameter
PC: Critical lip pressure
Qtot: Total mass flow
Htot: Specific enthalpy of total flow

Table 2.2 Calculated production of steam.

Date	Time	Wellhead Pressure (barg)	Total flow (kg/s)	En- thalpy (kJ/kg)	Steam at 15 barg (kg/s)	Steam at 0 barg (kg/s)	Brine at 0 barg (kg/s)	Remarks
85.03.17	18:30	31.00	6.6	1905.	3.5	0.6	2.4	
85.03.19	13:45	23.70	9.4	2124.	6.2	0.6	2.6	
85.03.21	11:00	21.00	9.4	2003.	5.6	0.7	3.1	
85.03.24	16:00	18.50	12.2	1662.	5.1	1.4	5.7	4" lip
85.03.25	12:00	16.90	12.0	1644.	4.9	1.4	5.7	
85.03.26	12:00	16.50	12.7	1606.	4.9	1.5	6.3	
85.03.27	09:00	12.50	13.5	1673.	5.7	1.5	6.3	
85.03.27	12:00	10.80	14.7	1752.	6.8	1.5	6.4	
85.03.27	17:00	10.20	14.9	1708.	6.6	1.6	6.7	
85.03.29	09:00	9.80	14.2	1678.	6.0	1.6	6.6	
85.03.29	18:00	10.00	14.4	1692.	6.2	1.6	6.6	
85.03.30	09:00	9.80	14.2	1637.	5.7	1.7	6.8	
85.03.30	17:00	9.90	14.2	1637.	5.7	1.7	6.8	
85.03.31	09:00	9.90	14.1	1608.	5.5	1.7	7.0	
85.03.31	18:00	9.80	14.5	1639.	5.9	1.7	7.0	
85.04.01	10:00	9.70	14.4	1612.	5.6	1.7	7.1	
85.04.01	18:00	9.50	14.4	1612.	5.6	1.7	7.1	
85.04.02	11:00	9.50	14.4	1583.	5.4	1.7	7.2	
85.04.02	17:00	9.40	14.4	1583.	5.4	1.7	7.2	
85.04.03	09:00	9.20	14.4	1542.	5.1	1.8	7.5	
85.04.03	17:00	9.20	14.5	1571.	5.3	1.8	7.4	
85.04.04	08:00	9.20	14.3	1555.	5.1	1.8	7.4	
85.04.04	15:00	9.20	14.3	1555.	5.1	1.8	7.4	
85.04.04	19:00	9.20	14.3	1555.	5.1	1.8	7.4	
85.04.05	12:00	9.00	14.4	1542.	5.1	1.8	7.5	
85.04.05	18:00	9.00	14.5	1551.	5.2	1.8	7.5	
85.04.06	08:00	9.10	14.3	1548.	5.1	1.8	7.4	
85.04.06	15:45	13.50	23.4	1368.	6.2	3.4	13.9	Cuttings/bent./FeS
85.04.06	16:45	14.20	23.1	1404.	6.5	3.2	13.4	Cuttings
85.04.06	18:00	14.00	23.6	1427.	6.9	3.2	13.4	Cuttings
85.04.07	10:00	13.80	23.0	1364.	6.0	3.3	13.7	Cuttings
85.04.07	14:00	13.90	23.2	1376.	6.2	3.3	13.7	Cuttings
85.04.08	13:00	13.50	23.9	1344.	6.0	3.5	14.4	Cuttings
85.04.08	19:00	13.50	23.9	1344.	6.0	3.5	14.4	Cuttings
85.04.09	07:00	13.54	22.9	1393.	6.3	3.2	13.4	Cuttings
85.04.09	17:00	13.50	22.6	1409.	6.4	3.2	13.0	Cuttings
85.04.10	10:00	13.20	22.3	1406.	6.3	3.1	12.9	Cuttings
85.04.10	15:00	13.40	22.5	1418.	6.5	3.1	12.9	Cuttings
85.04.11	10:00	13.10	21.9	1403.	6.2	3.1	12.7	Some cuttings
85.04.11	17:00	13.00	21.9	1403.	6.2	3.1	12.7	
85.04.12	14:00	13.10	22.2	1386.	6.1	3.1	13.0	
85.04.13	09:00	13.00	21.9	1403.	6.2	3.1	12.7	
85.04.13	12:00	12.90	21.9	1403.	6.2	3.1	12.7	
85.04.13	15:00	12.90	21.3	1438.	6.4	2.9	12.0	
85.04.13	17:00	12.90	21.0	1456.	6.5	2.8	11.7	
85.04.13	20:00	12.90	21.5	1429.	6.3	2.9	12.2	

Table 2.2 (cont.)

Date	Time	Wellhead Pressure (barg)	Total flow (kg/s)	En- thalpy (kJ/kg)	Steam at 15 barg (kg/s)	Steam at 0 barg (kg/s)	Brine at 0 barg (kg/s)	Remarks
85.04.14	09:00	13.00	21.6	1420.	6.3	3.0	12.3	
85.04.14	12:00	12.90	21.4	1408.	6.1	3.0	12.3	
85.04.14	15:00	12.90	21.4	1408.	6.1	3.0	12.3	
85.04.14	19:00	12.90	21.4	1408.	6.1	3.0	12.3	
85.04.14	20:00	12.90	21.4	1408.	6.1	3.0	12.3	
85.04.15	10:00	12.90	21.9	1382.	5.9	3.1	12.8	
85.04.15	14:00	12.90	21.9	1382.	5.9	3.1	12.8	
85.04.15	18:00	12.90	21.9	1382.	5.9	3.1	12.8	
85.04.16	08:00	12.80	21.3	1387.	5.8	3.0	12.5	
85.04.16	09:00	12.80	21.6	1399.	6.0	3.0	12.5	
85.04.16	12:00	12.80	21.2	1395.	5.9	3.0	12.3	
85.04.16	15:00	12.80	21.3	1387.	5.8	3.0	12.5	
85.04.16	16:00	12.80	21.2	1395.	5.9	3.0	12.3	
85.04.16	19:00	12.80	21.2	1395.	5.9	3.0	12.3	
85.04.16	20:00	12.80	21.2	1395.	5.9	3.0	12.3	
85.04.16	21:00	12.80	21.2	1395.	5.9	3.0	12.3	
85.04.18	08:00	12.70	21.1	1374.	5.6	3.0	12.5	
85.04.18	13:00	12.70	21.1	1374.	5.6	3.0	12.5	
85.04.18	17:00	12.70	21.1	1374.	5.6	3.0	12.5	
85.04.19	08:00	12.60	21.1	1374.	5.6	3.0	12.5	
85.04.19	12:00	12.60	21.1	1374.	5.6	3.0	12.5	
85.04.19	18:00	12.60	21.0	1383.	5.7	3.0	12.3	
85.04.20	09:00	12.60	21.1	1374.	5.6	3.0	12.5	
85.04.20	13:00	12.60	21.0	1383.	5.7	3.0	12.3	
85.04.21	07:00	12.60	21.1	1374.	5.6	3.0	12.5	
85.04.21	10:00	12.60	21.1	1374.	5.6	3.0	12.5	
85.04.21	13:00	12.60	21.1	1374.	5.6	3.0	12.5	
85.04.22	08:00	12.50	21.0	1404.	5.9	2.9	12.2	
85.04.22	14:00	12.50	20.8	1391.	5.7	2.9	12.2	
85.04.22	19:00	12.50	20.8	1391.	5.7	2.9	12.2	
85.04.23	07:00	12.40	21.2	1395.	5.9	3.0	12.3	
85.04.23	11:00	12.40	21.0	1404.	5.9	2.9	12.2	
85.04.24	09:00	12.40	21.2	1395.	5.9	3.0	12.3	
85.04.24	13:00	12.30	21.3	1387.	5.8	3.0	12.5	
85.04.24	19:00	12.30	21.2	1395.	5.9	3.0	12.3	
85.04.25	09:00	12.30	21.0	1383.	5.7	3.0	12.3	
85.04.25	14:00	12.20	20.8	1391.	5.7	2.9	12.2	
85.04.26	12:00	12.00	20.5	1387.	5.6	2.9	12.0	
85.04.26	19:00	12.50	20.5	1387.	5.6	2.9	12.0	
85.04.27	09:00	12.20	20.7	1400.	5.8	2.9	12.0	
85.04.27	17:00	12.20	20.7	1400.	5.8	2.9	12.0	
85.04.28	10:00	12.30	20.7	1400.	5.8	2.9	12.0	
85.04.28	16:00	12.30	20.7	1400.	5.8	2.9	12.0	
85.04.29	14:00	12.30	20.7	1400.	5.8	2.9	12.0	
85.04.30	11:00	12.20	20.7	1400.	5.8	2.9	12.0	
85.04.30	18:00	12.30	20.7	1400.	5.8	2.9	12.0	

Table 2.2 (cont.)

Date	Time	Wellhead Pressure (barg)	Total flow (kg/s)	En- thalpy (kJ/kg)	Steam at 15 barg (kg/s)	Steam at 0 barg (kg/s)	Brine at 0 barg (kg/s)	Remarks
85.05.01	10:00	12.20	20.7	1400.	5.8	2.9	12.0	
85.05.06	12:00	12.00	20.8	1422.	6.0	2.9	11.8	
85.05.06	20:00	11.90	20.8	1422.	6.0	2.9	11.8	
85.05.07	10:00	12.00	20.5	1409.	5.9	2.9	11.8	
85.05.07	16:00	12.00	20.5	1409.	5.9	2.9	11.8	
85.05.08	12:00	12.00	20.5	1409.	5.9	2.9	11.8	
85.05.08	18:00	12.00	20.5	1409.	5.9	2.9	11.8	
85.05.09	08:00	11.90	20.8	1422.	6.0	2.9	11.8	
85.05.09	12:00	11.90	20.8	1422.	6.0	2.9	11.8	
85.05.10	09:00	11.90	20.5	1409.	5.9	2.9	11.8	
85.05.10	17:00	11.90	20.5	1409.	5.9	2.9	11.8	
85.05.11	12:00	11.90	20.5	1409.	5.9	2.9	11.8	
85.05.12	10:00	11.80	20.5	1409.	5.9	2.9	11.8	
85.05.13	10:00	11.60	20.5	1409.	5.9	2.9	11.8	
85.05.14	10:00	11.60	20.5	1409.	5.9	2.9	11.8	
85.05.15	12:00	11.50	20.5	1409.	5.9	2.9	11.8	
85.05.16	11:00	11.40	20.5	1409.	5.9	2.9	11.8	
85.05.17	08:00	11.50	20.5	1409.	5.9	2.9	11.8	
85.05.17	12:00	11.40	20.5	1409.	5.9	2.9	11.8	
85.05.18	08:00	11.70	20.3	1396.	5.7	2.9	11.8	
85.05.19	11:00	11.50	20.3	1396.	5.7	2.9	11.8	
85.05.20	08:00	11.40	20.3	1396.	5.7	2.9	11.8	
85.05.21	09:00	11.30	20.0	1392.	5.5	2.8	11.6	
85.05.22	08:00	11.30	20.0	1392.	5.5	2.8	11.6	
85.05.23	09:00	11.30	20.0	1392.	5.5	2.8	11.6	
85.05.23	14:00	11.20	20.3	1374.	5.4	2.9	12.0	
85.05.24	12:00	11.60	20.9	1338.	5.2	3.1	12.6	
85.05.25	10:00	11.70	21.1	1352.	5.4	3.1	12.6	
85.05.25	19:00	12.00	20.9	1338.	5.2	3.1	12.6	
85.05.26	09:00	11.60	20.8	1316.	4.9	3.1	12.8	
85.05.26	14:00	11.70	21.0	1330.	5.1	3.1	12.8	
85.05.27	08:00	11.90	21.0	1330.	5.1	3.1	12.8	
85.05.28	10:00	11.80	21.2	1343.	5.3	3.1	12.8	
85.05.28	14:00	11.80	21.2	1343.	5.3	3.1	12.8	
85.05.29	11:00	11.70	20.9	1338.	5.2	3.1	12.6	
85.05.29	14:00	11.70	20.9	1338.	5.2	3.1	12.6	
85.05.30	07:00	11.80	21.1	1352.	5.4	3.1	12.6	
85.05.30	11:00	11.80	21.1	1352.	5.4	3.1	12.6	
85.05.30	18:00	11.80	20.9	1338.	5.2	3.1	12.6	
85.05.31	09:00	11.70	21.1	1352.	5.4	3.1	12.6	
85.05.31	13:00	11.70	20.9	1338.	5.2	3.1	12.6	
85.06.01	09:00	11.80	21.1	1352.	5.4	3.1	12.6	
85.06.01	17:00	11.70	20.9	1338.	5.2	3.1	12.6	
85.06.03	09:00	11.80	20.9	1338.	5.2	3.1	12.6	
85.06.04	10:00	11.70	20.9	1361.	5.4	3.0	12.5	
85.06.05	10:00	11.60	20.7	1347.	5.2	3.0	12.5	

Table 2.2 (cont.)

Date	Time	Wellhead Pressure (barg)	Total flow (kg/s)	En- thalpy (kJ/kg)	Steam at 15 barg (kg/s)	Steam at 0 barg (kg/s)	Brine at 0 barg (kg/s)	Remarks
85.06.06	10:00	11.60	20.9	1338.	5.2	3.1	12.6	
85.06.07	07:00	11.60	21.2	1321.	5.1	3.1	13.0	
85.06.07	10:00	11.50	20.9	1338.	5.2	3.1	12.6	
85.06.08	09:00	11.60	19.8	1401.	5.6	2.8	11.5	
85.06.09	10:00	11.50	19.8	1401.	5.6	2.8	11.5	
85.06.10	10:00	11.50	19.8	1401.	5.6	2.8	11.5	
85.06.11	10:00	11.40	20.0	1392.	5.5	2.8	11.6	
85.06.12	10:00	11.40	19.8	1401.	5.6	2.8	11.5	
85.06.13	10:00	11.20	20.9	1361.	5.4	3.0	12.5	
85.06.14	15:00	11.30	20.9	1338.	5.2	3.1	12.6	
85.06.15	10:00	11.20	20.6	1356.	5.3	3.0	12.3	
85.06.16	08:00	11.20	20.9	1361.	5.4	3.0	12.5	
85.06.16	17:00	11.20	20.6	1356.	5.3	3.0	12.3	
85.06.17	10:00	11.20	20.3	1374.	5.4	2.9	12.0	
85.06.18	09:00	11.20	20.7	1347.	5.2	3.0	12.5	

Figure 2.1 Wellhead pressure, flow, and enthalpy vs. time.
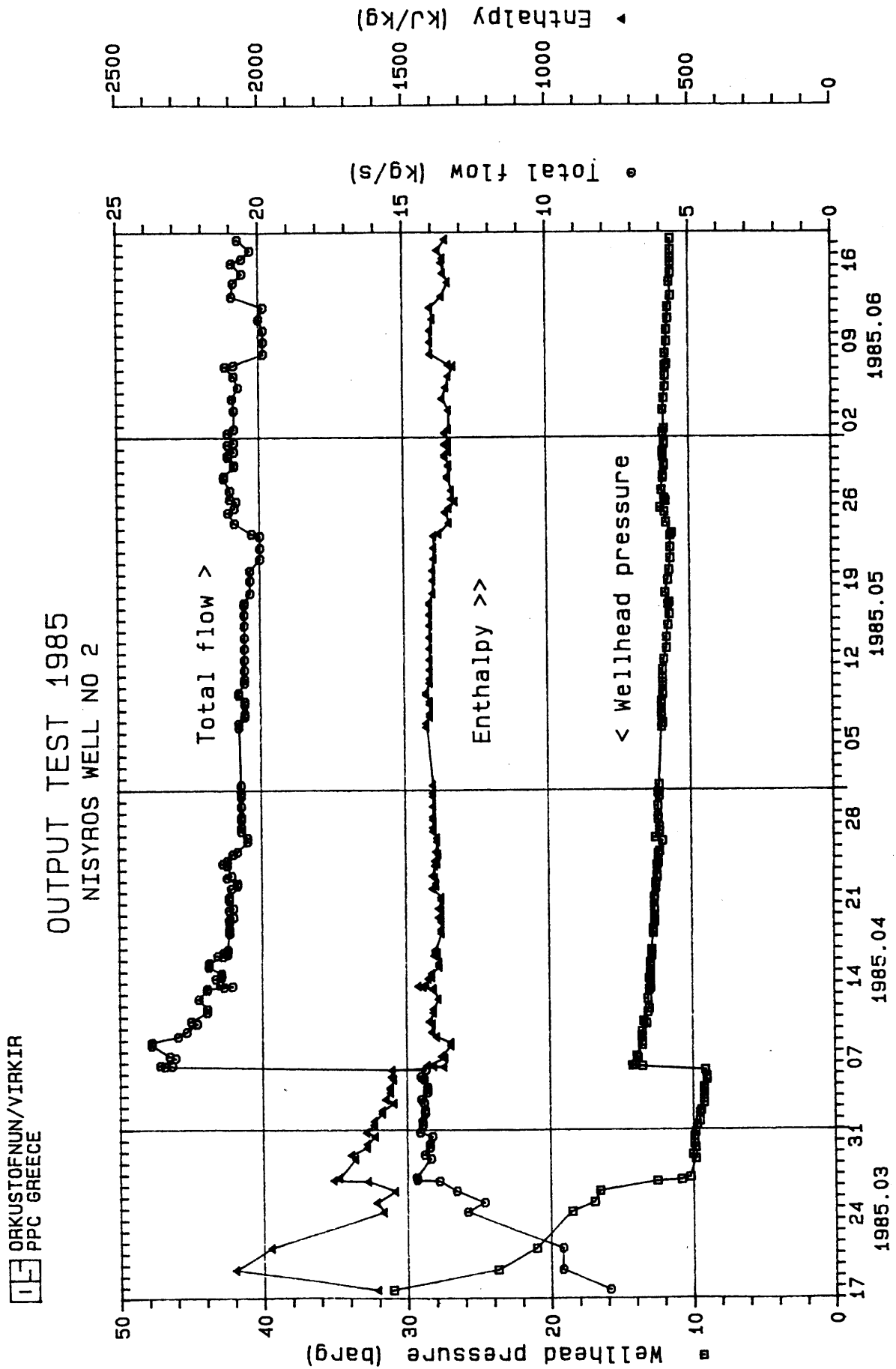
Figure 2.2 Total flow vs. pressure.

OUTPUT TEST 1985
NISYROS WELL NO 2

ORKUSTOFNUN/VIRKIR
PPC GREECE
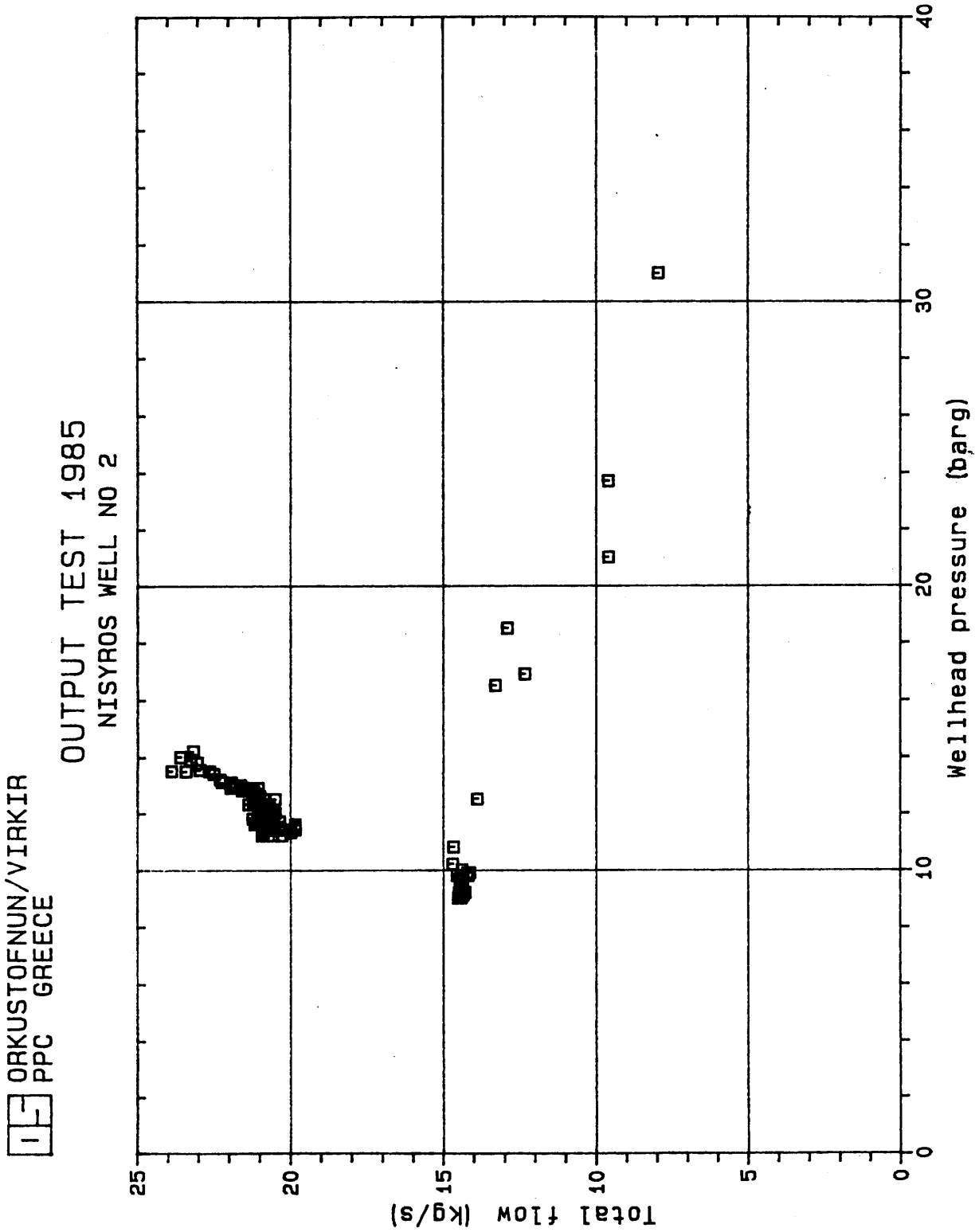
Figure 2.3 Computed pressure profiles.

NISYROS WELL NO 2
COMPUTED PRESSURE PROFILES IN TEST 1985

1: 85.03.17 18:30   3: 85.04.06 15:45
2: 85.04.06 08:00   4: 85.06.18 17:00
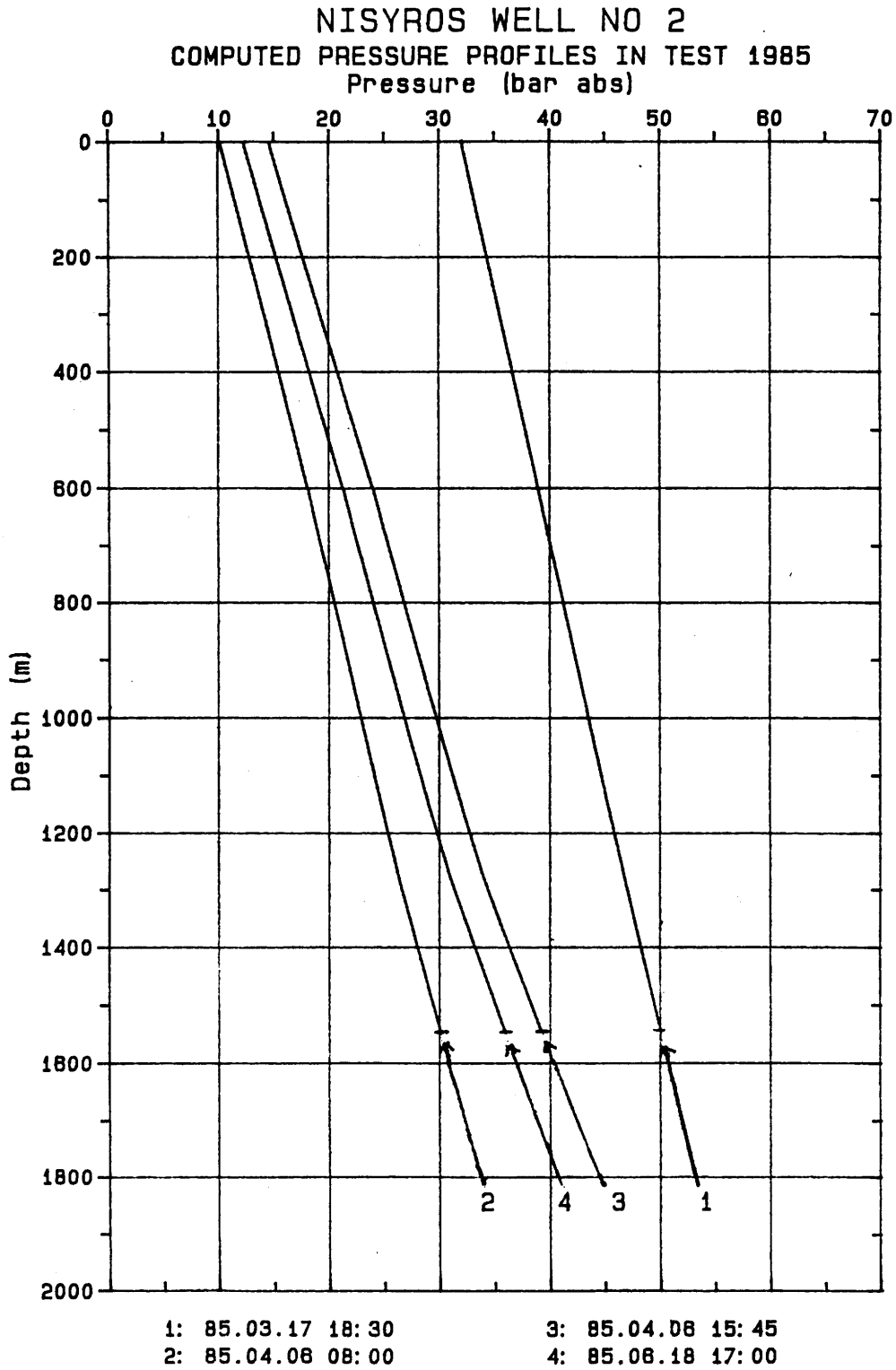
Figure 2.4 Computed temperature profiles.

NISYROS WELL NO 2
COMPUTED TEMPERATURE PROFILES IN TEST 1985
Temperature (C)

1: 85.03.17 18:30   3: 85.04.06 15:45
2: 85.04.06 08:00   4: 85.06.18 17:00
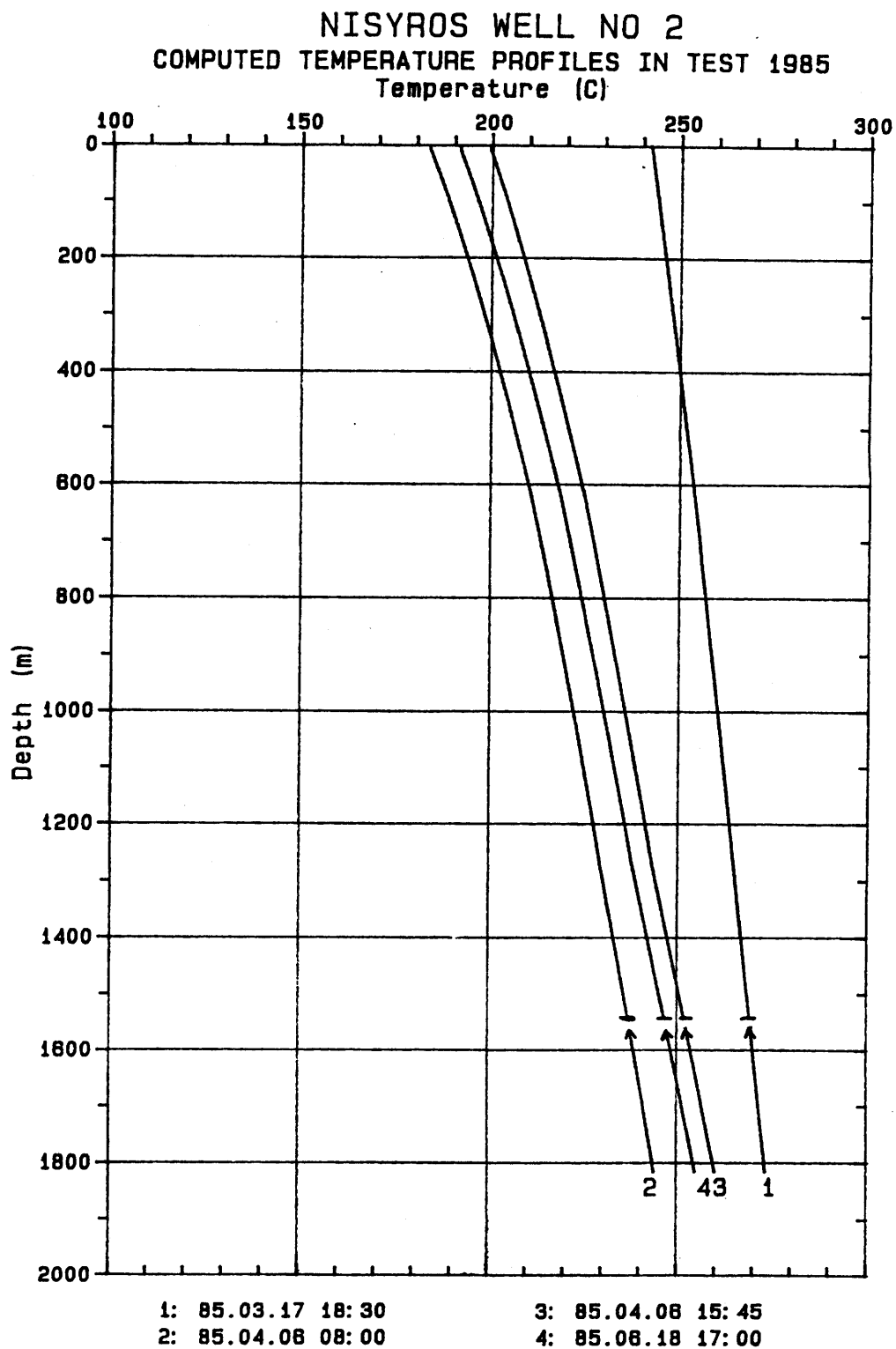
Figure 2.5 Computed steam fraction profiles.

NISYROS WELL NO 2
COMPUTED STEAM FRACTION PROFILES IN TEST 1985
Steam fraction (kg/kg)

1: 85.03.17 18:30   3: 85.04.06 15:45
2: 85.04.06 08:00   4: 85.06.18 17:00
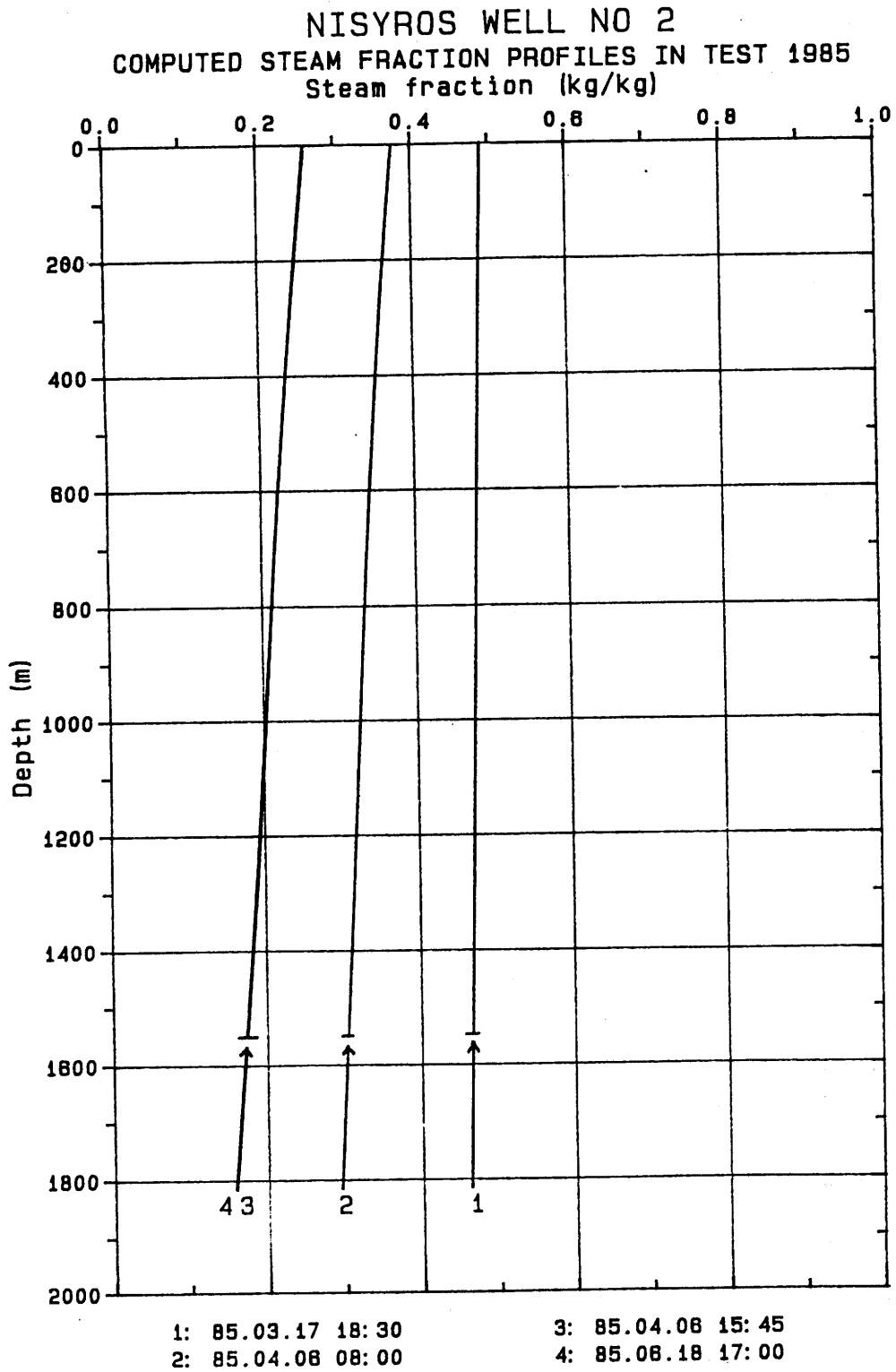
Figure 2.6 Changes in wellhead pressure vs. log time.
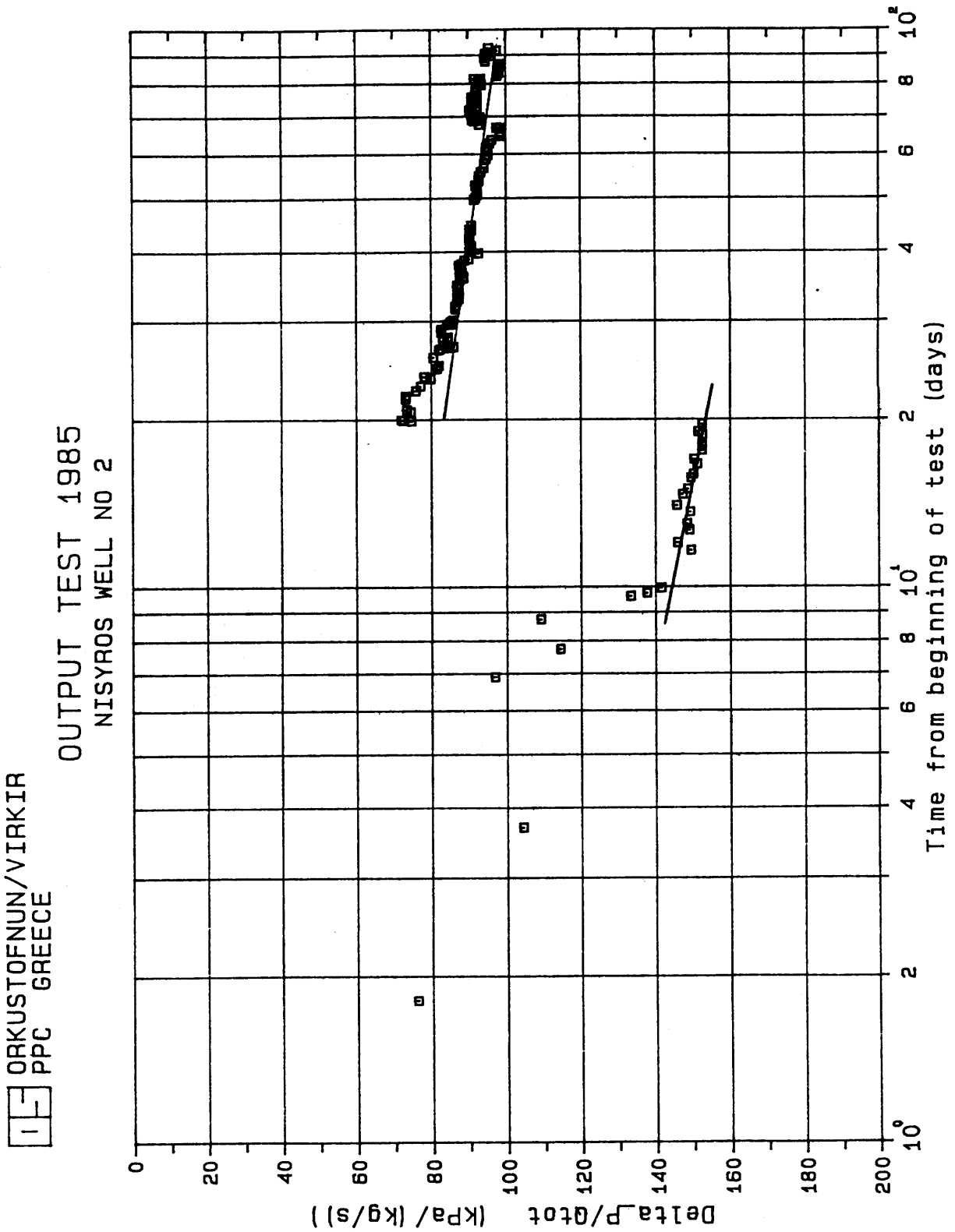
3   WATER LEVEL MEASUREMENTS IN WELL NIS-1

The water level was measured regularly in well NIS-1 during the flow test of well NIS-2. Well NIS-2 was first discharged on March 17, 1985 and shut in on June 18, 1985. The flow test results for well NIS-2 are shown in Figure 2.1. The first water level measurement in well NIS-1 was carried out in March, but the exact date is uncertain. It is assumed that this first measurement represents the static water level in well NIS-1. This level was then 155.10 m below the well-head. The water level was next measured on April 7, 1985, and shows a small drawdown (18 cm) from the previous measurement. This difference may not be significant. By that time the output of well NIS-2 had changed as described above. After this the water level was measured regularly every day or every other day to the end of the output test of well NIS-2. The water level readings are given in Table 3.1 and shown in Figure 3.1. As can be seen from Figure 3.1, there is a regular trend to lower water levels during the output test of well NIS-2. It is not clear, however, whether this is due to interference from NIS-2, because information on water level recovery is lacking.

If one assumes that the water level changes in well NIS-1 are due to interference from well NIS-2, they can be used to obtain global values for the reservoir formation transmissivity and storativity. A semi-logarithmic plot of the water level is shown in Figure 3.2 along with the calculated water level (solid curve), using flow rates for well NIS-2 as shown in Figure 2.1. The water level is calculated from the exponential integral function (Theis solution). The distance between wells NIS-1 and NIS-2 is approximately 780 m. These values yield the following results:

> A static water level at 153.71 m depth,
> coefficient of formation transmissivity $T = 0.0010$ m^2/s,
> coefficient of formation storage $S = 0.0028$.

These values are very high and should be taken with great caution. They compare with similar values obtained in the best liquid dominated reservoirs in the world, but do not reflect the observed behavior of wells NIS-1 and NIS-2. The implied global permeability thickness product from the above value of the transmissivity between wells NIS-1 and NIS-2 is $kh = 13$ Dm (darcy meters), compared to the estimated $kh = 0.7$ Dm for well NIS-2 and $kh = 0.2$ Dm for well NIS-1. The implied formation storage is $\phi cth = 39 \times 10^{-8}$ m/Pa, which is about ten times greater than that obtained from injection tests on NIS-1. This large discrepancy between the implied global values and those obtained for NIS-1 and NIS-2 suggests that it is unlikely that the water level

changes observed in well NIS-1 are due to interference. Furthermore, as a two-phase zone developed during the flow test in the production zone around well NIS-2, it is doubtful that an interference can be observed over a distance of 780 m.

Table 3.1 Water level measurements in well NIS-1.

NISYROS WELL-1

WATER LEVEL MEASUREMENTS

Date	Water level m	Remarks
850317	155.10	OUTPUT TEST OF NIS-2
850407	155.28	
850408	155.40	
850409	155.50	
850410	155.65	
850411	155.70	
850413	155.76	
850415	155.87	
850417	156.14	
850418	156.23	
850419	156.38	
850420	156.43	
850421	156.48	
850422	156.53	
850423	156.61	
850424	156.70	
850425	156.80	
850426	156.93	
850427	156.99	
850428	157.07	
850429	157.09	
850430	157.12	
850501	157.08	
850502	157.18	
850503	157.29	
850504	157.40	
850505	157.40	
850506	157.49	
850507	157.58	
850508	157.64	
850509	157.70	
850510	157.75	
850511	157.87	
850512	157.98	
850514	158.02	
850515	158.10	
850516	158.20	
850517	158.25	
850518	158.40	
850519	158.48	
850520	158.37	
850521	158.42	
850522	158.48	
850523	158.49	
850524	158.49	
850525	158.50	
850526	158.41	
850527	158.35	
850528	158.28	
850529	158.25	
850530	158.32	
850531	158.35	
850601	158.37	
850602	158.42	
850603	158.59	
850604	158.63	
850605	158.54	
850606	158.59	
850607	158.59	
850608	158.70	
850609	158.73	
850610	158.73	
850611	158.74	
850612	158.66	
850613	158.73	
850614	158.73	
850615	158.80	
850616	158.90	
850617	158.92	
850618	158.80	
850619	158.95	
850620	158.91	

Figure 3.1 Water level in well NIS-1 vs. time.
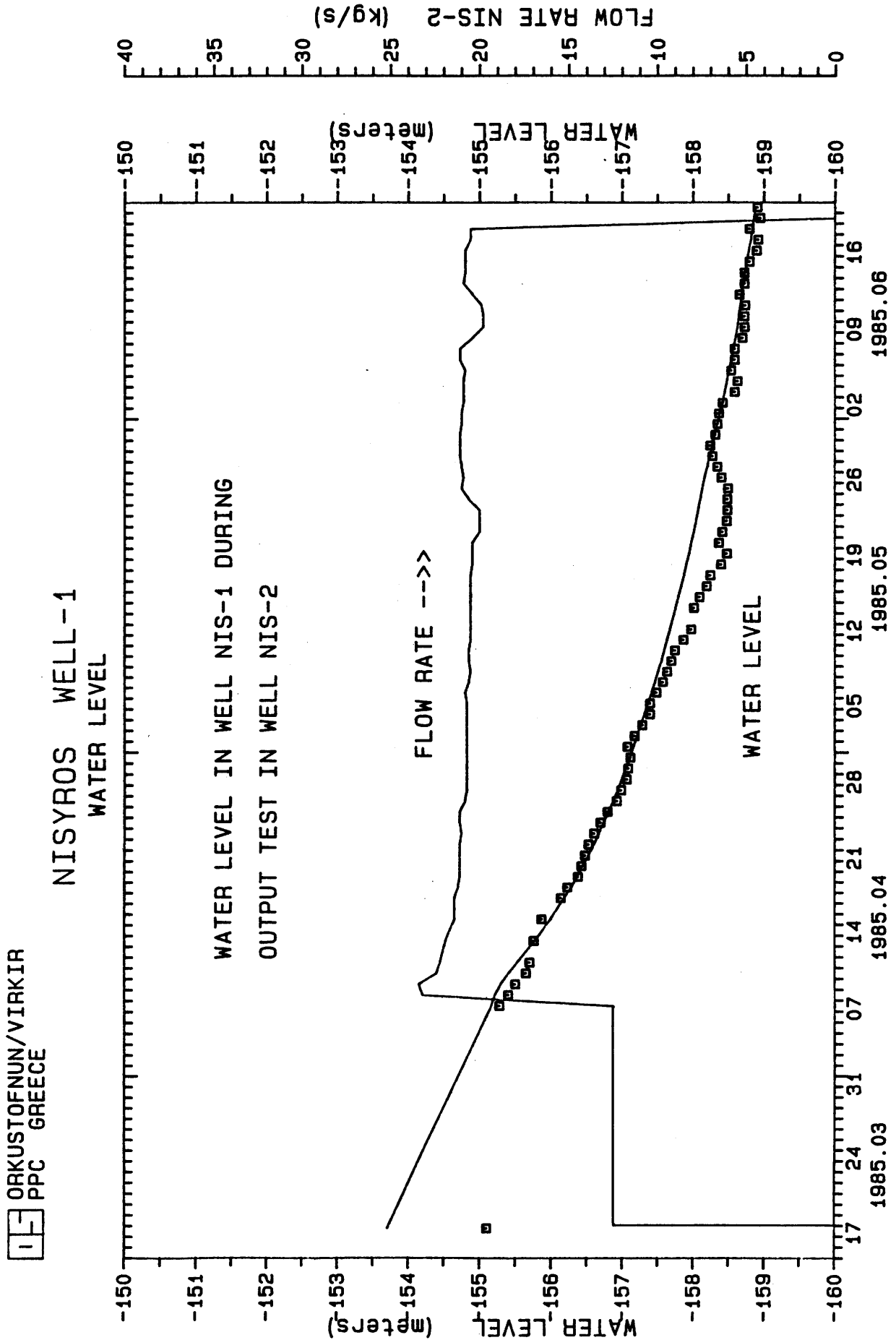
Figure 3.2 Water level in well NIS-1 vs. log time.
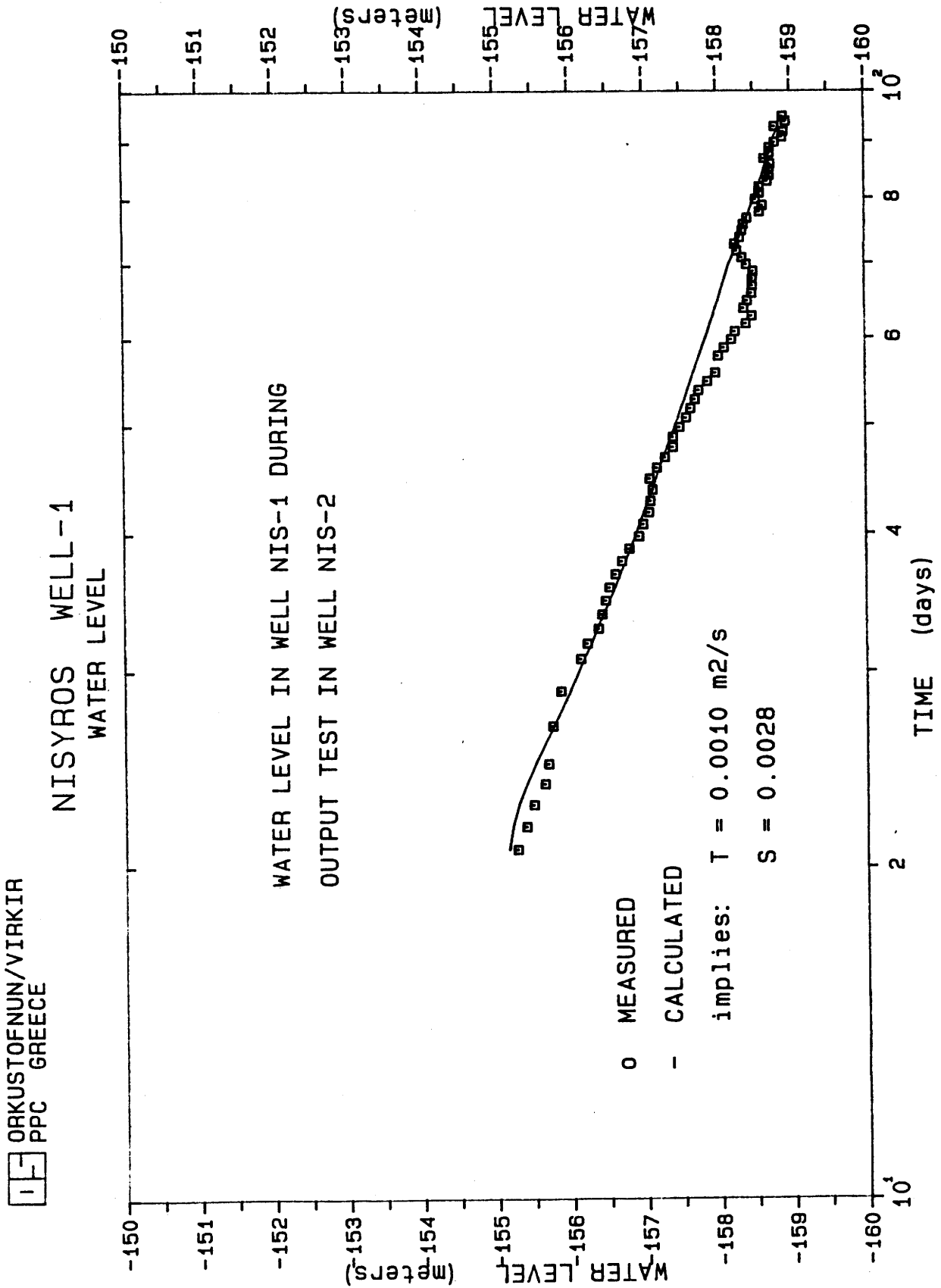
4   CHEMISTRY OF THE GEOTHERMAL FLUIDS

4.1 Samples for chemical analysis

Complete samples of geothermal fluids, including gas, brine, and con-
densate, were collected from a high-pressure line, while additional
samples of brine were collected from the silencer at atmospheric pres-
sure. During the consultant visit of Armannsson, five high-pressure
samples were drawn and the concentration of their volatile constit-
uents determined. The results were communicated in a short interim
report by Armannsson in 1985. The collection of, and the determination
of volatile constituents in, the remaining samples was carried out by
PPC. To aid PPC personnel in this, a description of the sampling pro-
cedures was provided by Virkir/NEA. The volatiles referred to here
comprise dissolved CO_2, dissolved H_2S, and pH, both in brine and con-
densate, as well as the total concentration of CO_2 and H_2S in steam.
Numerous brine samples were also analyzed for silica and chloride by
PPC.

Many of the brine samples were analyzed at the Institute of Geology
and Mineral Exploration in Athens (IGME) and the following constit-
uents determined: SiO_2, Na, Ca, Mg, K, Cl, SO_4, Fe, B, F, Li, Sr, Mn,
and total dissolved solids.

Two brine samples collected under pressure were brought to Iceland and
analyzed by NEA for reference. A total of twelve gas samples were also
analyzed by gas chromatography at NEA.

The analytical results are presented in Appendix 1. They exhibit con-
siderable scatter. Many of the analyses show a poor balance between
cations and anions. Therefore, it is suspected that some of the fluc-
tuations, at least, may be due to analytical imprecision. The analyt-
ical results are discussed at some length in Appendix 2, where those
samples that are likely to be of the best quality are identified. The
best samples (Table 4.1) were relied upon in the interpretation given
in the following sections.

4.2 Calculation of the deep water composition

The samples collected at the wellhead were drawn at different pres-
sures, and are thus not immediately comparable. To make the results
comparable and to obtain information about the downhole conditions,
one must first compute the so-called "deep water composition", i.e.
the concentration of the various solutes in the water phase in the

reservoir.

In order to calculate the deep water composition, it is necessary to know the steam fraction of the fluid at the pressure of collection as well as the steam fraction of the downhole fluid that enters the well. These steam fractions are found from the enthalpy of the fluid and the aquifer temperature. The procedure for computing these fractions and the deep water composition is described below.

The specific enthalpy, H_t, of the two phase mixture at the wellhead is given by

$$(1) \qquad H_t = X_s H_s + X_w H_w,$$

where H_s and H_w are the specific enthalpies of saturated steam and saturated water at the collection pressure, respectively, and X_s and X_w are the steam and water (mass) fractions at the same pressure. For a given pressure, H_s and H_w may be found from ordinary steam tables. The fractions are clearly related by

$$(2) \qquad X_s + X_w = 1.$$

By eliminating X_s from the above two equations and solving for X_w one finds that

$$(3) \qquad X_w = (H_t - H_s)/(H_w - H_s).$$

The specific enthalpy, H_t, is typically measured by the Russell James method, as described in the section on output measurements. The concentration, C_t, of a dissolved chemical in total flow is

$$(4) \qquad C_t = X_s C_s + X_w C_w,$$

or

$$(5) \qquad C_t = (1 - X_w) C_s + X_w C_w,$$

where C_s and C_w denote the concentration of the substance in the steam and water phases, respectively, at the point of collection.

To a good approximation, the enthalpy can be taken to be constant in the well, i.e. one may assume that the total enthalpy at the point of inflow is identical to that measured at the wellhead. This is rather generally true for the flow of fluids in pipes, provided that heat loss through the pipe walls, as well as gravity and kinetic energy contributions, can be neglected, as they can here.

Sometimes, the inflow into a well consists of saturated water only. In such a case the total enthalpy is equal to the enthalpy of water at the temperature and pressure in the inflow. Since the enthalpy of water varies quite slowly with pressure at constant temperature, the inflow enthalpy can then be taken equal to that of saturated water at the downhole temperature.

Often, however, the fluid entering the well is a mixture of water and steam. Such is the case for well NIS-2. The enthalpy of the mixture may then be written in terms of the enthalpies of saturated water and saturated steam at the downhole temperature as follows:

(6) $\qquad Ht = Xd\ Hd + Xx\ Hx,$

where Xd and Xx are the mass fractions of water ("deep water") and steam ("excess steam"), respectively, in the inflow. Hd and Hx are the corresponding specific enthalpies of saturated water and saturated steam at the inflow temperature. If this temperature is known, these enthalpies may be found from steam tables. The fractions Xd and Xx must, of course, sum to unity:

(7) $\qquad Xd + Xx = 1$

They can be found by solving equations (6) and (7) simultaneously.

If one assumes there to be no chemical sources or sinks, such as scale formation or dissolution in the wellbore, the concentration of a particular solute in total flow is the same at the inflow as it is at the wellhead. This concentration, Ct, is a weighted sum of the concentrations in the inflow water and steam phases, thus:

(8) $\qquad Ct = Xd\ Cd + Xx\ Cx.$

Here, of course, Cd is the concentration in the deep water of the substance under consideration, and Cx is its concentration in the "excess" steam that flows into the well.

If the solute is nonvolatile, then $Cs = Cx = 0$. Elimination of Ct between equations (5) and (8) therefore yields:

(9) $\qquad Cd = Xw\ Cw/Xd.$

In the sections which treat the deep water composition, the deep water concentrations of nonvolatile solutes are computed from equation (9).

If, on the other hand, the solute is volatile the situation is rather

more complicated. Then most of the volatile constituents will be present in the "deep steam", unless the inflow is single phase. This will not be addressed in the present report.

In the following sections the deep water concentration will thus only be calculated for the nonvolatile solutes. The fluid enthalpy, Ht, used in the calculations for a given sample is the enthalpy determined from output measurements on the day of sampling. These enthalpy values can be found in Table 2.1. The downhole temperatures used are the reference temperatures discussed in the following section.

4.3 Reference temperature

In order to calculate the deep water composition, a reference temperature is necessary. If a well is fed by a single aquifer, this should be the measured temperature at the point of inflow. Accordingly, a temperature log was included in the original testing program for well NIS-2, in order to provide information about downhole temperatures and feed zones in the well. Due to an obstruction in the well, however, the requisite data could not be obtained and other information will have to suffice. For this reason, chemical geothermometry is used here to establish a reference temperature.

The chemical geothermometer chosen for the purpose is based on the quartz solubility data of Fournier and Potter. It yields temperatures of 279°C and 290°C, respectively, for the NEA reference samples of March 25th and May 26th. These samples are believed to be representative of the chemical composition of the geothermal fluid during the periods before and after, respectively, the event of April 6th, when the wellhead pressure, the total flow, and the fluid enthalpy suddenly changed. The sample of March 25th exhibits a higher concentration of silica than almost all other samples collected during the period before April 6th and thus probably represents a truer value, as pointed out in the section on the silica content in Appendix 2. A similar argument holds for the sample of May 26th, whose silica concentration is higher than that of most other samples collected after April 6th. Accordingly, the temperatures just cited will be taken as reference temperatures in the discussion that follows: 279°C for the period before April 6th, and 290°C for the period after April 6th.

It should be emphasized that these figures do not necessarily represent the true aquifer temperatures; they are used here as a basis for the chemical calculations in the absence of measured values and are considered to be of some inaccuracy. Part of the inaccuracy is due to a discrepancy between quartz solubility values at high temperatures

reported by the various authors. Another source of uncertainty is the high salinity of the Nisyros geothermal fluids. There is little doubt that salinity influences the solubility of quartz, but there is no agreement in the literature as to the extent to which this happens, or even whether the presence of salt increases or decreases the solubility.

4.4 Compositional characteristics

The deep water concentrations of various solutes, computed as described in section 4.2, are listed in Table 4.2. The reference temperatures used in these calculations are those discussed in section 4.3.

The water discharged from well NIS-2 on Nisyros is highly saline. The water in the reservoir contains about 50000 mg/kg of chloride, which is more than double the salinity of seawater. Due to evaporation, water discharged at atmospheric pressure contains some 80000 mg/kg of chloride. Boron levels are relatively high (35 ppm in the reservoir) and Cl/B ratios in the geothermal fluid are about one-third of that in seawater. The concentrations of silica and total dissolved solids in the reservoir are around 640 mg/kg and 85000 mg/kg, respectively, and about 1040 mg/kg and 140000 mg/kg if the fluids are flashed at atmospheric pressure.

The content of major dissolved solids, apart from chloride and boron, which are mobile, appears to be controlled by equilibria with minerals typical of the greenschist metamorphic facies. Simultaneous equilibrium with albite and K-feldspar does not, however, seem to be attained, as discussed in the following section on geothermometry. Calculations show the reservoir water to be close to equilibrium with quartz, calcite, pyrite, and anhydrite. The CO_2, H_2S and H_2 content of the water further suggests equilibrium with epidote, prehnite, and chlorite.

Saline geothermal waters of high temperature, like the Nisyros brine, can be expected to contain relatively high concentrations of various metals and other trace elements as already seen for iron and manganese (Table 4.1). The presence of these and other trace elements is of concern, both with respect to scaling and the environmental impact of utilization. For this reason it is important to analyze the brine for the following elements, at least: Zn, Pb, Cu, Cd, Ag, As, and Hg. To obtain reliable analyses it is essential to filter and acidify the samples immediately after collection and ensure that contamination is avoided during sampling.

4.5 Geothermometry

Various solute and gas geothermometers have been used to estimate the temperature in the feeding aquifer of well NIS-2 on Nisyros (Table 4.3). The quartz geothermometer indicates a temperature of 280-290°C as already discussed. Very similar results are obtained by the various gas geothermometers when slight degassing of the reservoir fluid has been taken into account as discussed later. The Na-K geothermometer yields a low temperature estimate and so does the Na-Li geothermometer of Fouillac and Michard. Since the temperatures derived from the quartz and the gas geothermometers fall in a narrow range, and since the Na-K and Na-Li temperatures differ much from them, it seems likely that the Nisyros brine does not equilibrate with Na- and K-feldspar, nor with the minerals usually governing Na/Li ratios. The geothermometers substantiate the quartz geothermometry results, already discussed, that the producing aquifer (or the main producer) of Nisyros well NIS-2, has a temperature of 280-290°C.

4.6 Theoretical scaling tendency

If the steam from well NIS-2 is to be utilized for electric power generation, it must first be separated from the brine. The temperature and pressure at which this separation occurs is of considerable importance. In particular, if they are too low, the brine becomes supersaturated with respect to silica, which may then precipitate and form scale that, in time, is likely to interfere with the operation of the separator. The temperature and pressure at which flashed brine becomes saturated with respect to silica is therefore of much importance.

For a given well, this temperature and pressure can be calculated when the well fluid enthalpy, the downhole temperature, and the deep water silica concentration, are known. It is, of course, also necessary to know the solubility of amorphous silica as a function of temperature. Because of the high salinity of the Nisyros fluids, the variation of amorphous silica solubility with salt concentration must be taken into account. For this we shall use the solubility data of Chen and Marshall.

The calculated deep water concentration of silica for the Virkir/NEA reference sample of March 25 is 594 mg/kg, and the corresponding reference temperature and enthalpy are 279°C and 1605 kJ/kg, respectively. This yields a temperature of 188°C for the saturation of amorphous silica.

For the reference sample of May 26, the deep water silica concentration is 639 mg/kg, the reference temperature 290°C, and the enthalpy 1330 kJ/kg. The silica saturation temperature calculated from this is 201°C. This temperature corresponds to a water vapor pressure of about 15.8 bar-absolute.

Amorphous silica scaling in the wellbore could be eliminated by operating the well at a sufficiently high wellhead pressure. Whether this is a feasible solution or not depends on the production characteristic curve for the well. Amorphous silica may begin to deposit at a temperature above saturation for the pure phase if it is coprecipitating with other minerals.

The pH of the Nisyros brine is calculated to be 4.4 at 290°C. This is significantly acidic as the neutral pH of pure water at 290°C is close to 6. Upon boiling the pH of the brine increases strongly, (Fig. 4.1), the cause being transfer of the weak acids, CO_2 and H_2S, into the steam phase. As a result of the pH increase, the brine becomes supersaturated with respect to calcite, and the degree of supersaturation increases continuously as boiling proceeds (Fig. 4.2) despite increasing calcite solubility with falling temperature. Calculations show that a fivefold supersaturation is reached at about 200°C (at 16 bar-a steam pressure).

The brine also becomes supersaturated with respect to pyrite because of the pH rise (Fig. 4.3). The degree of supersaturation is further enhanced by the decreasing pyrite solubility with falling temperature. Solubilities of other sulfides, such as galena (PbS) and sphalerite (ZnS) also decrease with increasing pH and decreasing temperature.

Since boiling causes the aqueous phase to become supersaturated with respect to calcite, amorphous silica (if cooled sufficiently), pyrite, and other sulfides, one would expect these minerals to be deposited from the brine, forming a scale. The rate of scale formation is not predicted by this approach, however, and tests are necessary to establish the scaling rate.

For many geothermal waters, the degree of calcite supersaturation caused by boiling is counteracted so strongly by the increasing calcite solubility with falling temperature that the water eventually becomes undersaturated. In such instances, the only tendency for calcite scaling is at the first level of boiling and over a relatively short temperature interval (50°C) after boiling sets in. This is not the case for the Nisyros brine. The boiled water becomes progressively more supersaturated as it cools. The explanation is to be found

in the high salinity of the brine, which, in turn, causes its pH to be so low. Boiling of the initially acid water causes a strong progressive rise in pH due to the limited buffering capacity of weak acids, including H_2CO_3/HCO_3^-, with the effect that the concentration of the carbonate ion (CO_3^{-2}) increases enormously during boiling.

Generally, calcite scaling is only a problem when boiling starts in the well. This may also prove to be so for Nisyros, in which case calcite scaling will not be a problem (since boiling starts in the aquifer). In view of the progressive increase in supersaturation upon boiling, however, it is considered necessary to verify by tests whether calcite scale forms in the well and in surface equipment, and, if so, establish the rate of scale formation.

It is expected that pyrite, and quite possibly other sulfides, will precipitate from the boiled water. This precipitation is expected to occur anywhere after boiling sets in, both in the wellbore and in surface equipment. Generally, the amount of precipitate, i.e. scale formation, is limited in exploited geothermal fields, the reason being to some extent, at least, low concentrations of iron and other base metals in the geothermal water. The high salinity of the Nisyros brine and the concomitant high concentrations of iron suggest that sulfide scaling will be faster than generally encountered in the exploitation of geothermal resources.

4.7 Gas concentrations in steam

The concentrations of gas in steam depend on the separation temperature (pressure) as shown in Fig. 4.4. Except for ammonia, the gases are sparingly soluble in water and are, therefore, practically quantitatively transferred to the steam phase during the early stage of boiling. Accordingly, it is a good approximation to take gas concentrations to decrease in proportion with increasing steam formation. For the analyses in Table 4.1 and taking the separation pressure to be 15.5 bar-a (200°C) and 6 bar-a (159°C), a total gas concentration in the steam of 435 and 375 mmoles/kg is obtained, respectively. This corresponds to 1.9% and 1.6% gas by weight.

It is difficult to predict how gas concentrations in the steam may change with time. Boiling in the aquifer and phase separation would not affect the gas content. If, however, the discharge enthalpy of the well increased through enhanced evaporation by heat transfer from the rock, one would expect the gas content in the steam to decrease at any particular pressure. In view of this, the gas content of the Nisyros well NIS-2 discharge would be expected either to remain con-

stant or to decrease with exploitation time.

The gas content of the well discharge has been used to evaluate boiling processes in the feeding aquifer (Table 4.4), by applying a new method developed by us. The results indicate that the well is withdrawing water that has been somewhat degassed by evaporation and steam loss amounting to about 0.4% steam by weight. It is conceivable that this is so because the well is located away from an upflow zone, and that it is extracting boiling water welling out from this zone.

When initially discharged, the well had an enthalpy of about 1600 kJ/kg but this decreased abruptly in April 1985 to 1400 kJ/kg, which is only slightly above saturated liquid enthalpy at the aquifer temperature of 290°C. The results in Table 4.4 (topmost line) indicate that phase separation in the aquifer was responsible for the high enthalpy of 1600 kJ/kg, involving preferential movement of the steam into the well. This is indicated by an Xe value of close to 0 and an Xd value much in excess of 1. The values given in the topmost line of Table 4.4 were derived from the H_2S and the H_2 content of the steam. Values in the third line, which are based on the same sample, were, on the other hand, obtained from the CO_2 and the H_2 content of the well discharge. Less weight is given to the latter result, since it is subject to greater error, because the difference between the solubilities of CO_2 and H_2S is smaller than between the solubilities of H_2S and H_2.

After the discharge enthalpy of the well decreased, the gas chemistry indicated insignificant phase separation and that a portion of the steam discharged from the well had originated by evaporation due to heat flow from the rock (line 2 in Table 4.4).

Table 4.1. CHEMICAL COMPOSITION OF REFERENCE SAMPLES.

	Sample of March 25	Sample of May 26	
Enthalpy (kJ/kg)	1607	1395	
Separation			
pressure (bar-g)	18.0	11.9	

Brine phase: Concentrations in mg/kg.

SiO_2	718	842	
Cl	56007	66390	
Na	23754	28470	
K	3224	3783	
Ca	8594	9670	
Mg	52.5	102.9	
Sr	110	90	x)
Li	10	10	x)
Fe	26.1	8.2	
Mn	135	140	x)
B	55	55	x)
F	1.76	1.38	
SO_4	24.6	32.6	
Cond./Temp. (°C)	116000/25.0	135000/25.0	
pH/Temp. (°C)	4.47/18.6	4.87/24.	
CO_2	637	1301	
H_2S	1.2	2.9	
NH_3		37.5	
TDS	97408	116588	

Gas phase: Concentrations in volume per cent.

CO_2	97.81	97.68
H_2S	1.73	1.68
H_2	0.05	0.07
O_2 + Ar	0.00	0.01
CH_4	0.32	0.47
N_2	0.09	0.09

Steam phase: Concentrations in mg/kg.

CO_2	40752	13497
H_2S	647	689

Condensate phase: Concentrations in mg/kg.

Cond./Temp. (°C)	0.48/22.0	0.18/-
pH/Temp. (°C)	4.48/16.7	5.05/24.0
CO_2	1561	2269
H_2S	42.8	46.8
Na	2.85	
NH_3	13.7	44.07

x) Based on averages of IGME data, rather than on actual reference samples.

Table 4.2 DEEP WATER COMPOSITION CALCULATED FROM REFERENCE SAMPLES.
All concentrations in mg/kg.

	Sample of March 25	Sample of May 26	
Enthalpy (kJ/kg)	1607	1395	
Inferred aquifer temperature (°C)	279	290	
SiO_2	594	639	
Cl	46300	50400	
Na	19650	21600	
K	2665	2870	
Ca	7100	7340	
Mg	43	78	
Sr	70	55	x)
Li	6	6	x)
Fe	21.5	6.2	
Mn	85	85	x)
B	35	35	x)
F	1.5	1.0	
SO_4	20.3	24.7	
TDS	80370	88350	

x) Based on averages of IGME data, rather than on actual reference samples.

Table 4.3. GEOTHERMOMETRY TEMPERATURES ($°C$) FOR WELL NIS-2, NISYROS. [a]

Sample date Geothermometer	85-03-26	85-05-26	Average
SiO_2 (quartz)	279	290	285
CO_2	317 (325)	286 (293)	302 (309)
H_2S	294 (293)	272 (271)	283 (282)
H_2	267 (292)	260 (281)	264 (286)
CO_2-H_2	248 (278)	252 (277)	250 (278)
H_2S-H_2	243 (289)	250 (288)	246 (288)
Na-K	228	225	226
Na-Li	159	146	152

[a]) Figures in brackets are corrected temperatures based on the calculated degassing (Y) of the reservoir water (see Table 4.4).

Table 4.4. RESERVOIR BOILING PARAMETERS FOR WELL NIS-2, NISYROS.

Sample date	Inflow temp. $°C$	Discharge enth. kJ/kg	Xe	Xd	Xr	Y%
85-03-25	210	1607	-0.05	2.05	1.00	-0.44 [a])
85-05-26	191	1395	0.17	0.52	-0.31	-0.42 [a])
85-03-25	210	1607	0.20	0.84	0.04	-0.39 [b])
85-05-26	191	1395	0.22	0.30	-0.48	-0.39 [b])

Inflow temperature was taken to be equal to the wellhead temperature (pressure).

Xe: Relative mass of steam formed by heat extraction from the rock.

Xd: Relative mass in aquifer of water that boils to yield steam into the well.

Xr: Relative mass of boiled water retained in the aquifer.

Y : Equilibrium steam (by weight) present in the undisturbed aquifer.

[a]) Derived from the H_2 and the H_2S content of the steam.

[b]) Derived from the H_2 and the CO_2 content of the steam.

Figure 4.1 pH in Nisyros brine boiled to various temperatures.
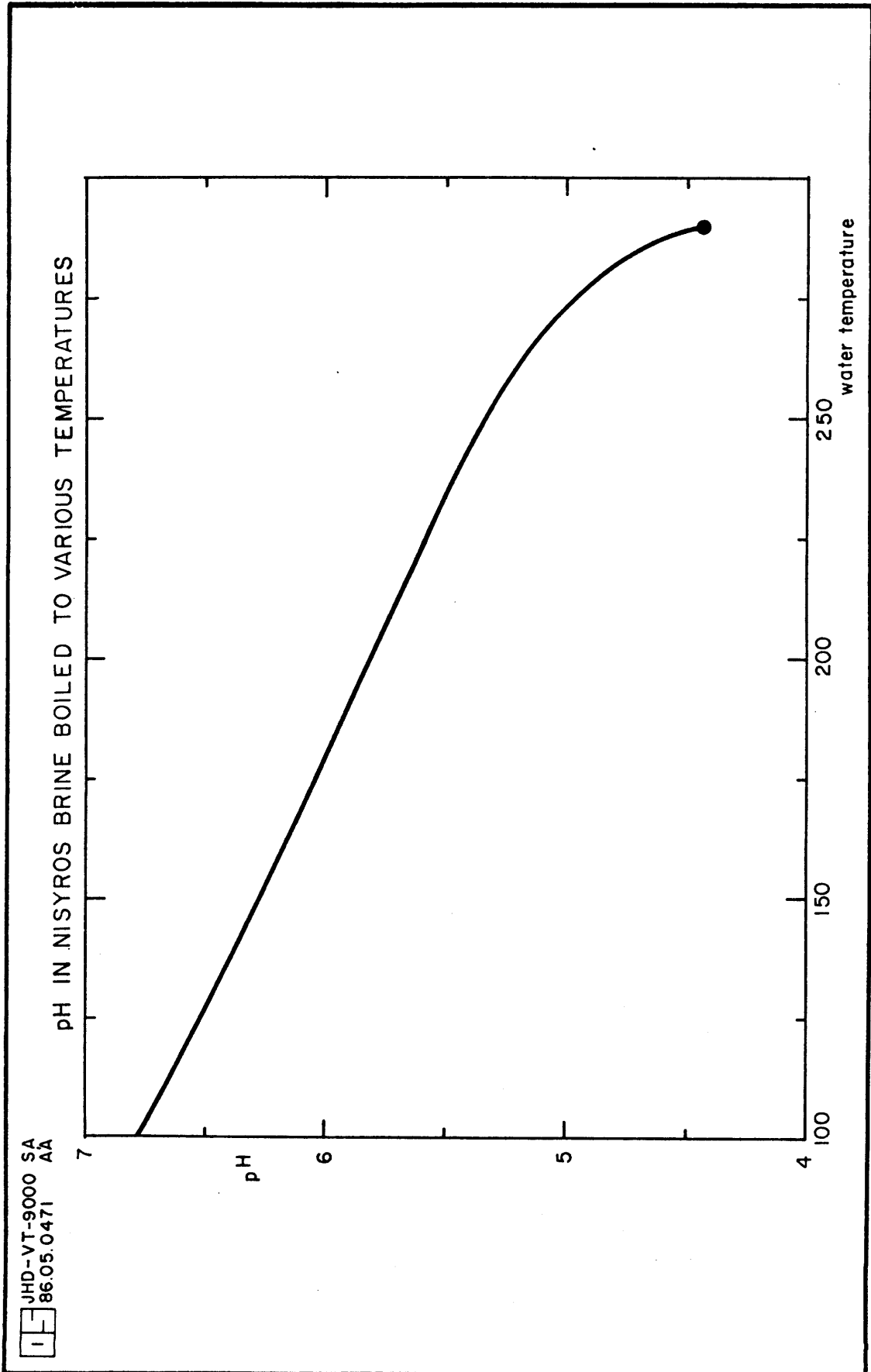
Figure 4.2 Calcite supersaturation.

THE DEGREE OF CALCITE SUPERSATURATION PRODUCED BY
ADIABATIC BOILING OF THE NISYROS BRINE

$CaCO_3 = Ca^{+2} + CO_3^{-2}$
$Q = a_{Ca^{+2}} \cdot a_{CO_3^{-2}}$
$K = Kcalcite$

log Q/K

water temperature °C

JHD-VT-9000 S A
86.05.0472   A A
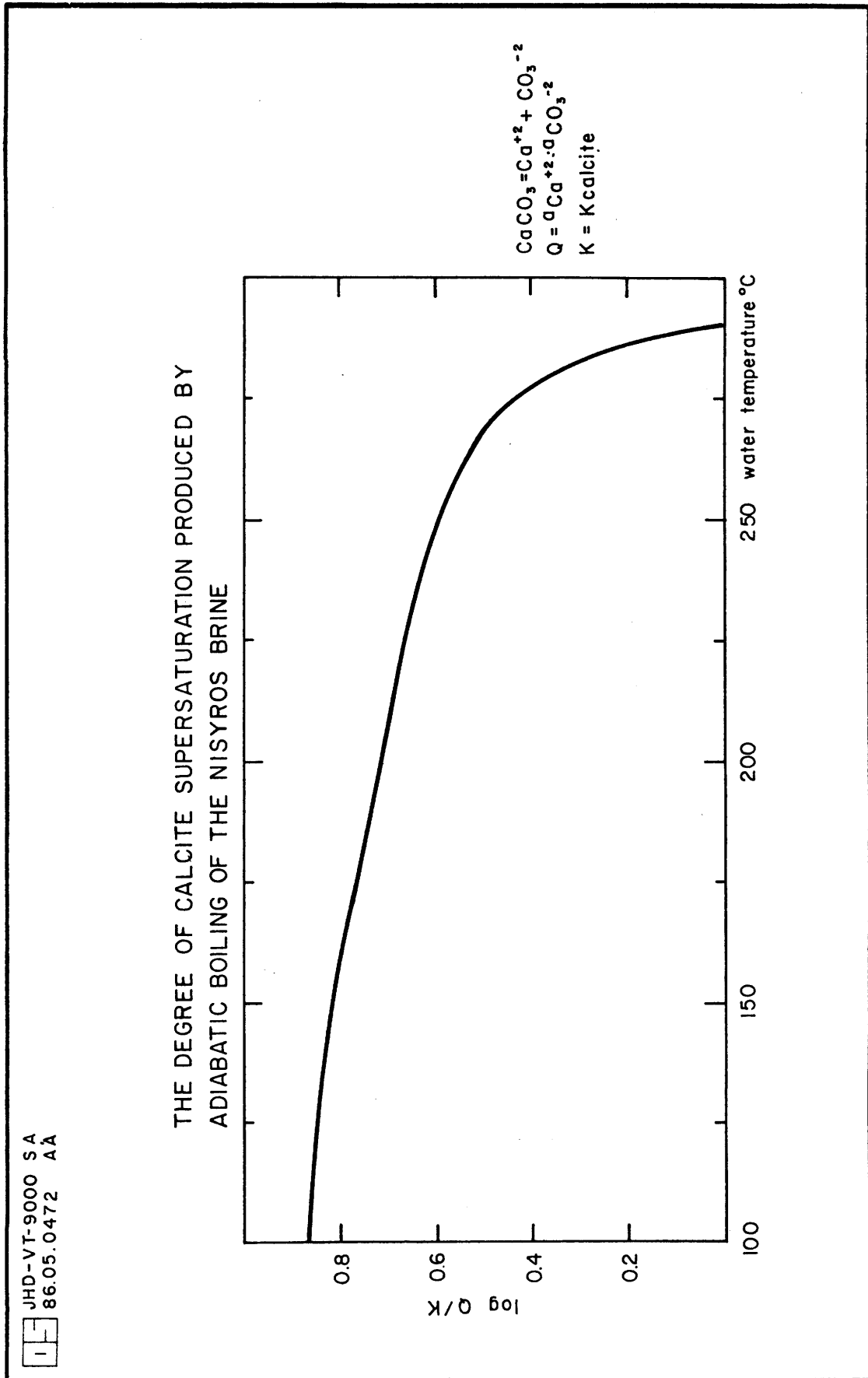
Figure 4.3 Pyrite supersaturation.

THE DEGREE OF PYRITE SUPERSATURATION CAUSED BY
ADIABATIC BOILING OF THE NISYROS BRINE

$8 FeS_2 + 26 H_2O + 10 OH^- = 8 Fe(OH)_4^- + SO_4^{-2} + 15 H_2S$

$Q = a^8 Fe(OH)_4^- \cdot a SO_4^{-2} \cdot a^{15} H_2S / a^{10} OH^-$

$K = Kpyrite$
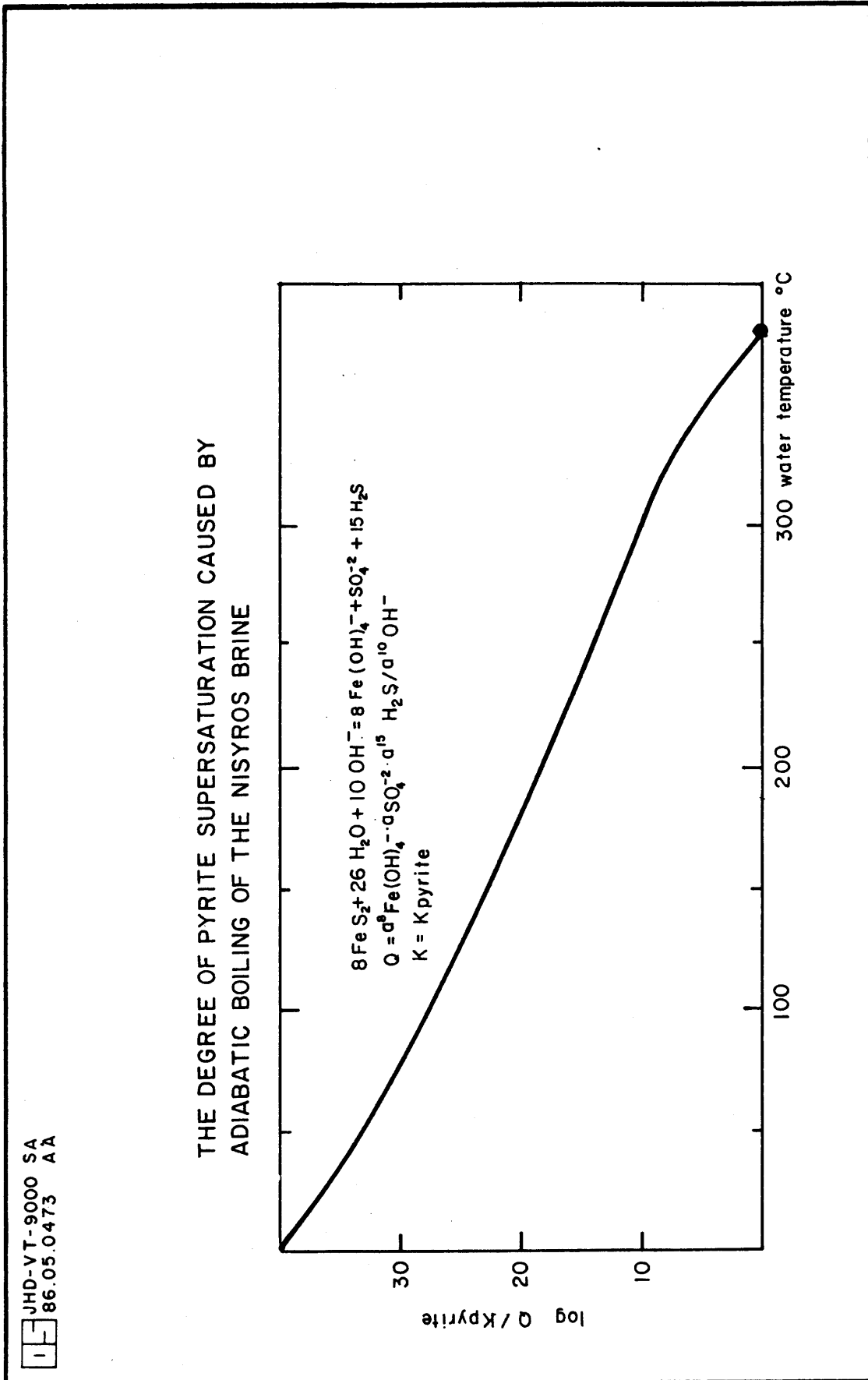
Figure 4.4 Gas in steam from well NIS-2.
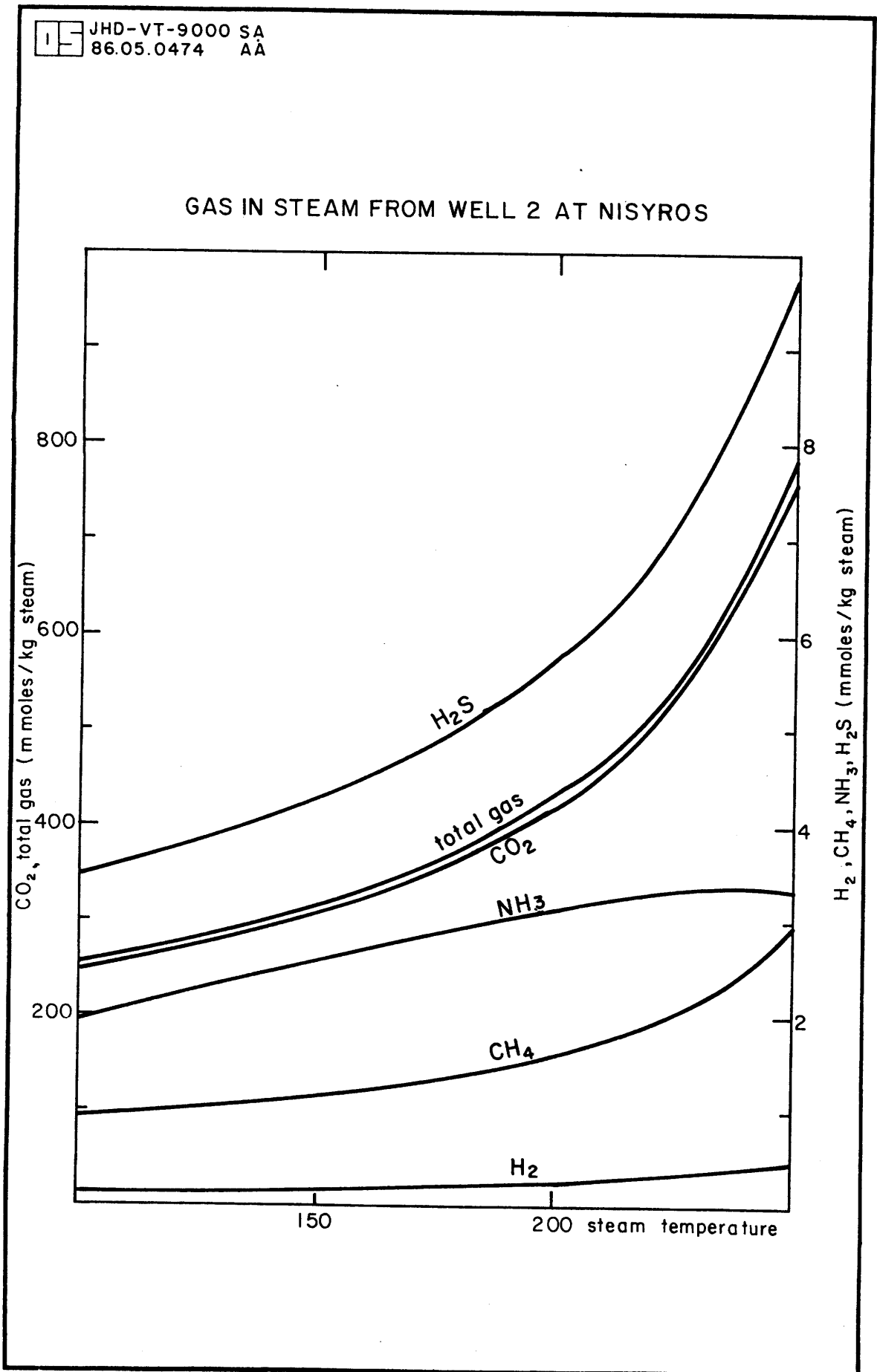
APPENDIX 1

Results of chemical analyses

RESULTS OF CHEMICAL ANALYSES

The following table contains the raw chemical data on which the calcu-
lations and interpretations discussed in this report are based. The
data are from three separate sources, namely the Public Power Corpora-
tion of Greece (PPC), the Institute of Geology and Mineral Exploration
in Athens (IGME), and the contractor, Virkir/NEA. The entry in the
column labeled Lab. indicates the origin of the data, in an obvious
notation.

The data are listed in the table in the form in which they were
received, except for the triplicate analyses of silica from IGME and
Virkir/NEA, which are listed as averages, and the PPC data for CO_2 and
H_2S in brine, condensate, and total steam samples collected by alka-
line condensation. These latter data were received as ml titrant and
have been converted into mg per kg brine, condensate, or steam, as
appropriate. In order to do so it was necessary to know the sample
volumes used in the titrations. Since these were not explictly stated
on the PPC data sheets, except in four cases of brine samples, a rea-
sonable assumption about them was made. This assumption was confirmed
by PPC (Telex dated January 15, sent January 16, 1986) with later cor-
rections (Telex dated March 13, sent March 14, 1986).

The table requires little explanation, but the following should be
pointed out. CO_2 and H_2S denote, respectively, total carbonate and
total sulfide, calculated as CO_2 and H_2S. TDS stands for total dis-
solved solids. The unit ppm refers, of course, to milligrams of the
substance in question per kilogram of brine, condensate, or steam, as
appropriate. The temperatures at which the conductivities and pH are
measured are given. The first 19 data columns in the table, i.e. those
up to and including the one labelled TDS, contain values from brine
analyses. Results of gas analyses are given in the next six columns,
in volume per cent. The following two columns display the results of
analyses of total steam samples collected by alkaline condensation.
The remaining seven columns containing chemical data list the conden-
sate analyses. The very last column gives the pressure at which the
sample was collected, in bar-gauge.

APPENDIX 2

Discussion of analytical results,
with figures

SILICA CONTENT

Figures A-2.1 to A-2.4 display the calculated concentration of silica
in deep water in well NIS-2 during the well-test period. All points in
the first two figures (A-2.1 and A-2.2) represent samples collected at
high pressure. In the latter two figures (A-2.3 and A-2.4) all points
except the stars correspond to samples collected from the silencer at
atmospheric pressure. The squares (Figs. A-2.1 and A-2.3) represent
calculations based on the analytical results reported by IGME, whereas
the octagons are values calculated from PPC data. The results computed
from the NEA analyses appear as stars. Even though the two brine
samples analyzed by NEA were collected at high pressures they are
included in Figs. A-2.3 and A-2.4 also, for comparison.

Several features of these plots emerge at once.

The silica concentration tends to be lower for the silencer samples
than for those collected under pressure. This is not very surprising
since the rate of precipitation and polymerization of silica is quite
high at 100°C when the supersaturation is appreciable. The precipita-
tion rate is further enhanced by the high salinity of the fluid. When
a sample is collected at high pressure, on the other hand, it is
cooled immediately, under pressure, and the process of precipitation
is quenched.

The scatter in the results is large. It is larger for the values cal-
culated from the silencer samples than the high pressure samples. That
the silencer samples should exhibit a larger scatter than the others
is to be expected on the grounds just mentioned. If the silica is in
the process of precipitating rapidly, then it will be difficult to
obtain reproducible results. Why the scatter is larger for the PPC
figures than the ones from IGME is not clear, however.

Analyses of silica frequently yield results that are too low. Only
rarely do errors in the analyses cause values to be too high. The
reason is, of course, that precipitation and polymerization tend to
decrease the amount of silica measured. Thus, high values are more
likely to represent the true concentration of dissolved silica accu-
rately than are low ones, other things being equal. In this context it
should be noted that the results obtained for the two samples analyzed
at NEA are higher than all the values reported by IGME and higher than
all but two of the determinations done by PPC. It may be added that
the two brine samples received by NEA were analyzed again, this time
by a method different from the one normally used by NEA, namely a
method used by Mitsubishi (MHI) for the 2 MW developement on the
island of Milos. The results were virtually identical to those

obtained earlier.

The calculated deep water concentration of silica is 594 ppm for the sample of March 25, and 639 ppm for the sample of May 26.

In light of the above, we believe the silica concentration values obtained by NEA to be the most reliable of those available. Accordingly, these have been used for calculating a reference temperature as described in section 4.3 These are also the values recommended for inclusion in tender documents for a power plant.

CHLORIDE CONTENT

The calculated concentration of chloride in deep water is depicted in figures A-2.5 through A-2.8. The points in the first two of these, A-2.5 and A-2.6, represent samples drawn at high pressure, whereas all points in figures A-2.7 and A-2.8, except those indicated by stars, correspond to samples collected from the silencer at atmospheric pressure. The squares (Figs. A-2.5 and A-2.7) show the results of deep water calculations based on analytical results from IGME, and the octagons are values found from PPC data. As before, deep water concentrations computed from Virkir/NEA data appear as stars in all figures. The two brine samples analyzed by Virkir/NEA, though collected at high pressure, are included in figures A-2.7 and A-2.8 for comparison.

It is immediately clear from these figures that the PPC analyses and those of Virkir/NEA agree quite well. In fact, the Virkir/NEA reference sample of May 26 falls very close to the average of PPC values for high pressure samples. The silencer samples analyzed by PPC yield slightly lower values. For reasons that are not known, the results reported by IGME are generally significantly lower than those of either PPC or Virkir/NEA.

Accordingly, the values that will be adopted here for the deep water chloride concentration are 46300 ppm before the event of April 6, and 50400 ppm for the period after the event.

CONCENTRATION OF ALKALI METALS AND ALKALINE-EARTH METALS.

A number of brine samples were analyzed by IGME for Na, K, Ca, Mg, Sr, and Li, and two reference samples were analyzed by Virkir/NEA for Na, K, Ca, and Mg. Figures A-2.9 through A-2.20 display the concentration of these substances in deep water. As before, the squares represent calculations based on the analytical results of IGME, whereas the

stars are values computed from Virkir/NEA data. The results for each metal are shown in two figures, one for the high pressure samples and another for the silencer samples. For comparison purposes, the two reference samples analyzed by Virkir/NEA, which were collected at high pressure, are also included in the figures with the silencer samples.

It is clear that the IGME data and the Virkir/NEA data agree only moderately well for Ca, and rather poorly for Na and K. The IGME data would indicate some increase in the concentration of Ca, a drop in the concentration of Na by almost a factor of two, but an increase by a similar factor in the concentration of K, during the well-test period. The data of Virkir/NEA, on the other hand, show a slight increase in the concentration of all these elements. The difference between IGME data and Virkir/NEA data is largest in the case of K, for which the Virkir/NEA value is greater, by a factor of 2.5, than the IGME values, for the period before the event of April 6, and about 50% greater for the remainder of the well-test period.

The results for Mg seem to be in better agreement (Figs. A-2.15 and A-2.16), even though the IGME data exhibit considerable scatter.

Strontium shows a decrease during the well-test period according to IGME data (Figures A-2.17 and A-2.18), but the trend for Li (Figs. A-2.19 and A-2.20) is less clear. These two metals were not analyzed by Virkir/NEA.

The discrepancies between the data of IGME and Virkir/NEA call for a closer look at said data. One way of approaching this is to consider the ratio of the concentrations of the metals mentioned to the concentration of chloride. These ratios are depicted in Figures A-2.21 through A-2.24. The IGME data indicate a significant drop in the Na/Cl ratio between the periods before and after the event of April 6, but a considerable rise in the Ca/Cl ratio and an even larger one in K/Cl. The Virkir/NEA data, on the other hand, show virtually no change in these ratios between the two periods. The difference between the two sets of data is probably most dramatically brought out by the Na/K ratio (Figure A-2.25). The IGME data show a drop in this ratio by a factor of four, but the Virkir/NEA data show no change.

It is difficult to see any reason why these ratios should change drastically in the present case. There can be little doubt that the deep water in well NIS-2 is to a large extent of marine origin, in other words, seawater that has boiled and undergone ion exchange with the surrounding rock. Since the ion exchange equilibria involved are presumably the same for the different aquifers, and since the seawater is, of course, the same in all cases, any differences in the Na/Cl,

K/Cl, and Ca/Cl ratios should only reflect temperature differences. As pointed out in the section on the reference temperature, the downhole temperature evidently changed only by 11 degrees or so between the periods before and after the event of April 6. Because of this, and because the Virkir/NEA data show no change in the above three ratios, the IGME data for Na, K, and Ca must be viewed with some scepticism. (The chloride data, which of course influence the behaviour of the ratios mentioned, have been discussed in a previous section.) Accordingly, we shall rely here primarily on the Virkir/NEA data for these constituents. Thus, as deep water concentrations before and after the event of April 6, respectively, we shall take for Na 19650 ppm and 21600 ppm, for K 2665 ppm and 2870 ppm, and for Ca 7100 ppm and 7340 ppm.

The Virkir/NEA data for Mg will likewise be used. They yield 43 ppm and 78 ppm for the deep water concentration before and after April 6, respectively. These values agree tolerably well with averages of corresponding IGME values (Figs. A-2.15 and A-2.16). The Mg/Cl ratios (Figure A-2.24) for the two sets of data are also in reasonably good agreement.

The IGME data yield values of roughly 4 ppm to 7 ppm for the Li deep water concentration, with no clear trend. As an average value, 6 ppm will be used. For Sr the results range from about 50 ppm to about 90 ppm before April 6, and from about 40 ppm to approximately 65 ppm after this time. Averages of 70 ppm and 55 ppm, respectively, will be used. As already stated, neither of these elements were analyzed by Virkir/NEA.

CONCENTRATIONS OF OTHER CHEMICALS

As in the preceeding sections, the squares in the figures to be discussed represent IGME data and stars Virkir/NEA data. There are two figures for each chemical discussed, one for samples collected under pressure and another for the silencer samples. Again, the two samples analyzed by Virkir/NEA, which were collected at high pressure, are also included in the figures with the silencer data, for comparison purposes.

Iron. It is clear from figures A-2.26 and A-2.27 that the concentration of iron in deep water dropped rapidly during the first two weeks of the well-test period. The initial concentration of more than 80 ppm is tremendously high for geothermal water. This high value and the rapid decline suggest that stagnant or nearly stagnant water in the vicinity of the well may have been in the process of being flushed

out. Such water may have dissolved some iron from the well casing. Another likely possibility is that scale in the wellbore, e.g. iron sulfide, was being flushed out. By the latter part of the well-test period the iron concentration had reached a steady state of about 5 ppm. The data of Virkir/NEA and IGME are in good agreement here.

Manganese. Except for a decline in the first two weeks of the well-test period, the concentration of manganese in deep water in well NIS-2 (Figures A-2.28 and A-2.29) shows no clear trend. It averages about 85 ppm.

Boron. Qualitatively, the behaviour of the boron concentration (Figures A-2.30 and A-2.31) is similar to that of the manganese concentration, the only discernible trend being a decline during the early part of the well-test period. The concentration averages roughly 35 ppm.

Fluoride. The fluoride concentration is shown in Figures A-2.32 and A-2.33. The IGME values are somewhat lower than the Virkir/NEA values.

Sulfate. The concentration, calculated from IGME data, of sulfate in deep water ranges from 5 ppm to more than 30 ppm (Figures A-2.34 and A-2.35), so the scatter is large. With about 20 ppm, the Virkir/NEA reference sample of March 25 falls in the middle of the IGME results for the first part of the well-test period. For the period after the event of April 6, the IGME data yield somewhat lower values than does the Virkir/NEA sample of May 26, which contained about 25 ppm.

Total dissolved solids. The total amount of dissolved solids in the deep water of well NIS-2 dropped from about 105000 ppm to about 70000 during the first two weeks of the well-test period and remained stable thereafter, according to IGME data (Figures A-2.36 and A-2.37). The Virkir/NEA reference sample of March 25 agrees with the IGME data, but later the two sets of data diverge somewhat; the Virkir/NEA reference sample of May 26 gives about 88000 ppm.

GAS COMPOSITION

A total of 12 gas samples from well NIS-2 were received by NEA and analyzed by gas chromatography. Of these, two were parts of the complete reference samples of March 25 and May 26. The chemical composition of all twelve samples (given in volume per cent) is presented in the following table.

GAS COMPOSITION (VOLUME PER CENT)

Date	CO_2	H_2S	H_2	O_2+Ar	CH_4	N_2
25-MAR-1985	97.81	1.73	0.05	0.00	0.32	0.09
01-APR-1985	97.50	1.73	0.14	0.02	0.44	0.17
27-APR-1985	97.76	1.57	0.07	0.02	0.43	0.15
04-MAY-1985	97.73	1.57	0.07	0.03	0.44	0.16
09-MAY-1985	97.68	1.67	0.13	0.00	0.43	0.09
26-MAY-1985	97.68	1.68	0.07	0.01	0.47	0.09
27-MAY-1985	94.11	1.58	0.07	0.82	0.44	2.98
10-JUN-1985	88.82	1.47	0.09	2.00	0.39	7.23
12-JUN-1985	97.80	1.57	0.07	0.01	0.43	0.12
13-JUN-1985	7.56	0.03	0.01	20.26	0.02	72.12
15-JUN-1985	25.65	0.34	0.00	16.07	0.11	57.83
16-JUN-1985	11.16	0.21	0.00	19.50	0.04	69.09

The first six samples and the one from June 12 are of excellent quality. The samples from May 27 and June 10 are slightly contaminated by air, but not so as to thwart interpretation. The last three samples, however, are heavily contaminated, due to either imperfect sampling or damage in transit.

If one corrects for atmospheric contamination in the samples of May 27 and June 10, i.e. if one subtracts the oxygen and an amount of nitrogen and argon corresponding to the atmospheric ratio of these gases, and renormalizes the remaining constituents to 100%, one finds that the composition of these samples is essentially identical to that of the uncontaminated samples as shown in the table below.

CORRECTED GAS COMPOSITION (VOLUME PER CENT)

Date	CO_2	H_2S	H_2	O_2+Ar	CH_4	N_2
27-MAY-1985	97.78	1.64	0.07	0.00	0.46	0.05
10-JUN-1985	97.75	1.62	0.10	0.00	0.43	0.10

It is indeed clear that the composition of non-condensible gases from well NIS-2 remained unchanged from March 25 until June 12. Even though the remaining three samples are too heavily contaminated to permit a similar correction, their CO_2/H_2S ratios do not suggest any change in

gas composition during the last few days of the well-test period.

It should be emphasized that this applies only to the relative composition of the dry gases; the absolute, or total, concentration of these in the steam varied greatly over the well-test period as discussed in the following section.

It appears safe to conclude that no significant change in the non-condensible gas composition occurred during the well-test period. The mean gas composition during this time was as follows:

MEAN GAS COMPOSITION (VOLUME PER CENT)

CO_2	H_2S	H_2	O_2+Ar	CH_4	N_2
97.72±0.09	1.64±0.06	0.09±0.03	0.01±0.01	0.43±0.04	0.11±0.04

These figures are means and standard deviations for the seven good samples and the two whose composition was corrected as described above.

TOTAL GAS IN STEAM

In this section the total concentration of gas in steam will be discussed.

Two different methods are commonly used for this determination. One, the volumetric method, involves measuring directly the amount of raw condensate collected along with a given amount of gas. The results of such measurements are usually reported as liters gas collected per kg condensate. This method yields results of acceptable accuracy only when the fraction of gas in the steam is moderately small. When the gas concentrations are high this method is so inaccurate as to be virtually useless. Such seems to be the case with well NIS-2.

The other method involves collecting a sample of steam into a concentrated solution of NaOH. The CO_2 and H_2S are then determined by titration and reported as mg per kg of steam. When the gas concentration is high, as it is in the present case, this is the method of choice.

Five total steam samples were collected by alkaline condensation and analyzed during the consultant visit of Armannsson. The remaining

total steam samples whose composition is presented in this section were collected and analyzed by PPC. Descriptions of the sampling procedures and analytical methods were provided to PPC by Virkir/NEA. Analytical results were transmitted by PPC to Virkir/NEA in a raw form, as ml titrant, but the sample volumes used in the analyses of the alkaline samples were not explicitly reported on the PPC data sheets. A reasonable assumption made by Virkir/NEA about these volumes, however, (see Telex of January 7, 1986) was later confirmed by PPC (see Telex dated January 15, sent January 16, 1986). These volumes were 2 ml for the CO_2 titration and 0.1 ml for the H_2S titration. It may be added here that the total volume (as opposed to the volume for titration) of the alkaline sample of May 27 (sample no. 34) is missing from the PPC data sheets. A good estimate of this volume can be made from other data, however, and this small omission should cause no problems.

A conversation in February 1986, however, between consultants from Virkir/NEA and PPC personnel, raised some questions about the volumes of samples used in the titrations of the alkaline samples, in particular in the determinations of CO_2. An inquiry by Virkir/NEA (Telex of March 4, 1986) elicited the correction (Telex from PPC dated March 13, sent March 14, 1986) that the actual volumes used for titration of those alkaline samples exhibiting high CO_2 values were ten times as large as previously reported. Although the sample numbers involved were not specified we presume these to be the samples of May 1, 26, and 27, and of June 10, 12, and 15. For these samples we use sample volumes of 20 ml.

The total gas concentrations computed from these PPC data are presented in the following table. Included also, at the beginning of the table, are the five samples analyzed during Armannsson's visit. The latter results have already been included in a short interim report by Armannsson.

TOTAL GAS CONCENTRATIONS IN STEAM AT THE PRESSURE OF COLLECTION (mg/kg)

Date	CO_2	H_2S
19-MAR-1985	48458	899
21-MAR-1985	45877	1073
23-MAR-1985	36025	451
24-MAR-1985	28195	334
25-MAR-1985	40752	647
29-MAR-1985	29752	102
01-APR-1985	31962	93.5
01-MAY-1985	5745	5125
04-MAY-1985	42165	5023
09-MAY-1985	-	101
14-MAY-1985	-	520
26-MAY-1985	13497	689
27-MAY-1985	7878	671
10-JUN-1985	10380	675
12-JUN-1985	9096	714
15-JUN-1985	13259	787

Although the interpretation of the gas composition data given in the previous section is straightforward, the results for total concentration of gas in steam are more problematic. Figures A-2.38 through A-2.43, which will be discussed below, illustrate the problem. They depict total concentrations of CO_2 and H_2S in steam samples collected by alkaline condensation.

Figure A-2.38 displays the total concentration of CO_2 in steam. The samples collected up to April 1, the first five of which were analyzed during the consultant visit of Armannsson, as already communicated in his short report, are fairly well grouped; in fact, the relative concentration spread is about what one would expect in determinations of total gas in geothermal steam in a stable well. The sample of May 4 (sample no. 13) falls in the same range. Sample no. 11 of May 1 and all the remaining alkaline samples, however, show a far lower concentration. The total range of concentrations seems rather larger than would be expected of good samples from a stable well, even when the different sampling pressures are taken into account. Although it would be tempting to interpret the data to mean that the gas fraction in steam decreased greatly after the event of April 6, this would leave unexplained the high value of the sample of May 4, which shows a CO_2

concentration in the same range as the samples collected up to April 1.

The concentration of H_2S in steam is shown in figure A-2.39. The first five samples have values ranging from several hundred mg H_2S per kg steam to about one thousand. Results from samples collected from May 14 onwards are in agreement with this. The samples of March 29, April 1, and May 9, however, exhibit quite low values, about 100 ppm or less. By contrast, the values reported for the H_2S concentration on May 1 and May 4 are extremely high: both exceed 5000 ppm. Variations of the kind just mentioned are difficult to correlate with the change that occurred in the well on April 6.

Since the gas fraction in the steam consists mainly of CO_2, it is not surprising that the plot of total gas in steam looks very much like that of CO_2 in steam. For comparison purposes, it is helpful to compute the total percentage of gas in steam at the same separation pressure for all samples. Figures A-2.40, A-2.41, and A-2.42 depict, as weight per cent, the total amount of gas in steam at 12 bars absolute, 6 bars absolute, and at 1.03 bars absolute (atmospheric pressure), respectively. We see that at 6 bar-a, e.g., the steam contained between about 2.7 and 4.5 per cent gas by weight up to the beginning of April. The samples collected from the end of April till the end of the well-test in mid-June, however, exhibit, with one exception, values ranging from about 1.0 to about 1.7 per cent gas by weight. The one exception, around 4 per cent, is in the same range as the samples collected up to April 1.

The scatter in these results, both in the CO_2 analyses and particularly in the H_2S analyses, raises some questions about the integrity of the data.

The CO_2/H_2S ratio provides a way of gauging the quality of the above data. In the previous section it was shown that the gas composition, as analyzed by gas chromatography, had remained constant throughout the well-test period. The sample compositions listed there yield CO_2/H_2S ratios ranging from 57 to 62, approximately. Since analyses of samples collected by alkaline condensation yield the total amounts of CO_2 and H_2S in steam, it follows that the ratio of CO_2 to H_2S in these samples should be identical to that in the samples analyzed by gas chromatography. Figure A-2.43 shows the CO_2/H_2S ratio in the alkaline samples. It is clear that only the first five samples, namely those analyzed during the visit of Armannsson, correspond even approximately to the correct ratio. The remaining samples fall into two different groups, both deviating markedly from the true value.

Because of the change in well characteristics that occurred on April 6, the fraction of gas in steam after this date is of the greatest practical interest, in particular as regards design parameters for a power plant. On their face, the data indicate that the steam, if separated at 6 bar-a, contained approximately 1-1.7 per cent gas by weight during most of the latter part of the well-test period. For the reasons given above, however, it may not be prudent to base the design of a power plant on these values only, and further studies of the gas content of the steam are advisable. It should also be kept in mind that the data from the early part of the well-test period indicate that the well is capable of discharging steam containing up to 4.5 per cent gas by weight (at 6 bar-a) and might therefore do so again.

INTEGRITY OF DATA

The interpretations given and the recommendations offered in this report can obviously never be better than the data on which they are based. The agreement between PPC and Virkir/NEA stipulates that PPC be responsible for the integrity of the Greek data. Thus, PPC must accept responsibility for the interpretations to the extent that they depend on these data.

We are especially concerned about the accuracy of the gas concentration data, i.e. the results of titrations of the gas samples collected by alkaline condensation. The basis for our concern is laid out in the preceeding section.

The silica data show rather large scatter and we believe most of these data to be a bit on the low side. This is understandable since silica can polymerize and precipitate rather easily from supersaturated solutions, especially if they are highly saline as is the case here.

Although agreement between the PPC chloride data and the corresponding Virkir/NEA data is excellent, the IGME values are significantly lower.

The IGME values for potassium are considerably lower than the Virkir/NEA reference values. The IGME data for sodium and potassium furthermore show jumps whose origin is obscure.

We find no reason to question the quality of other data.

Figures A-2.1 and 2.2.
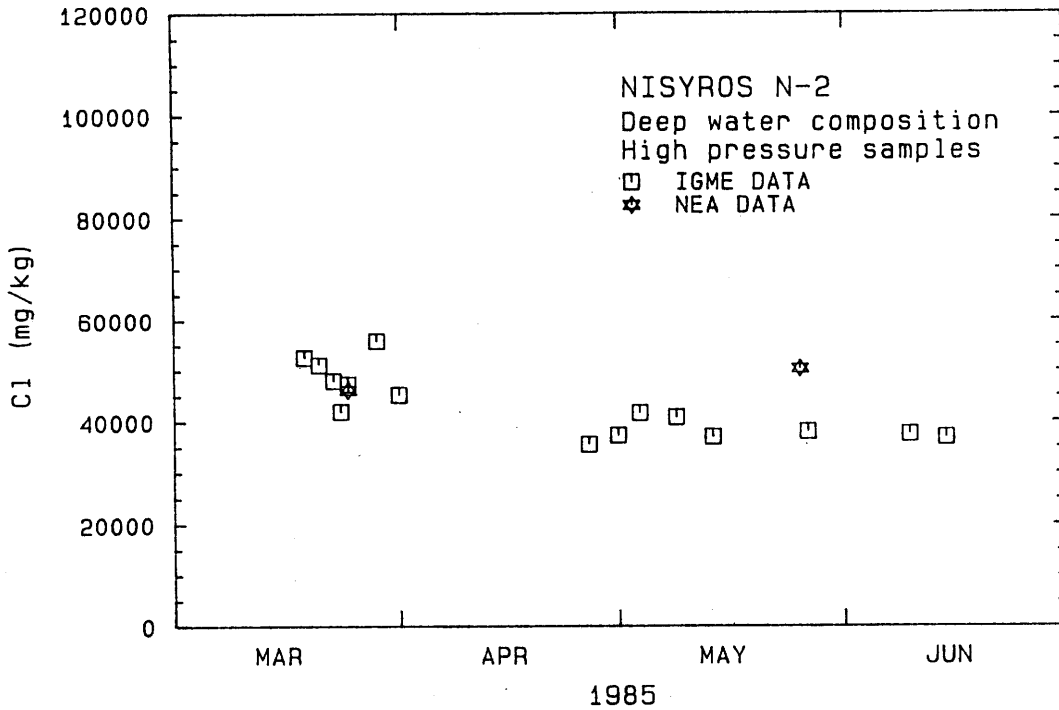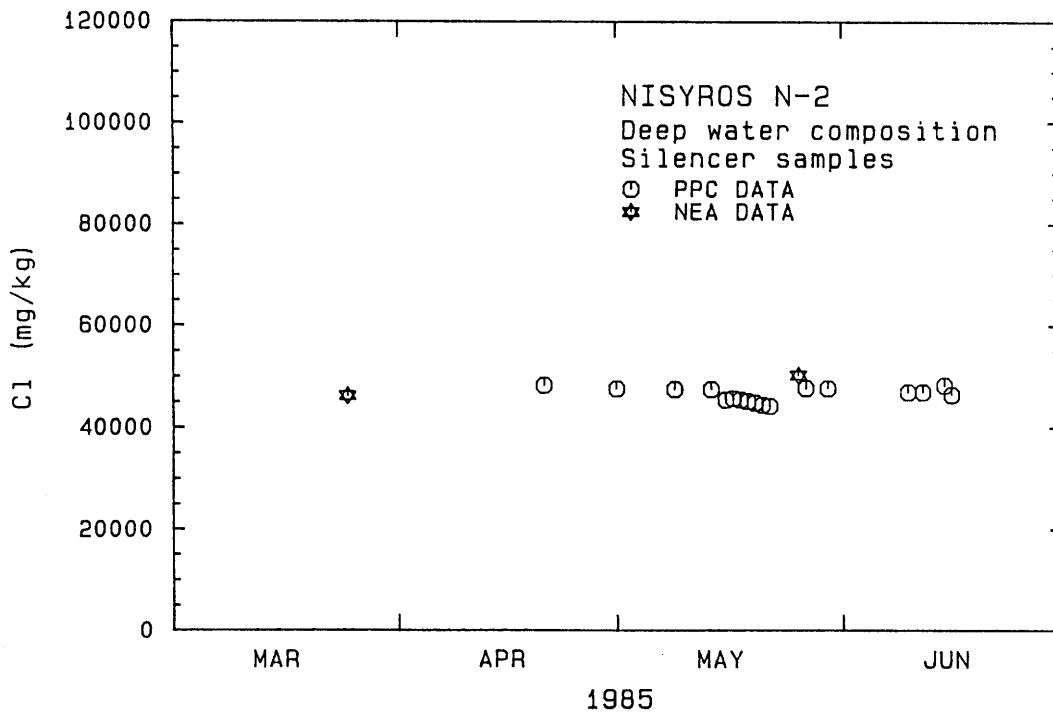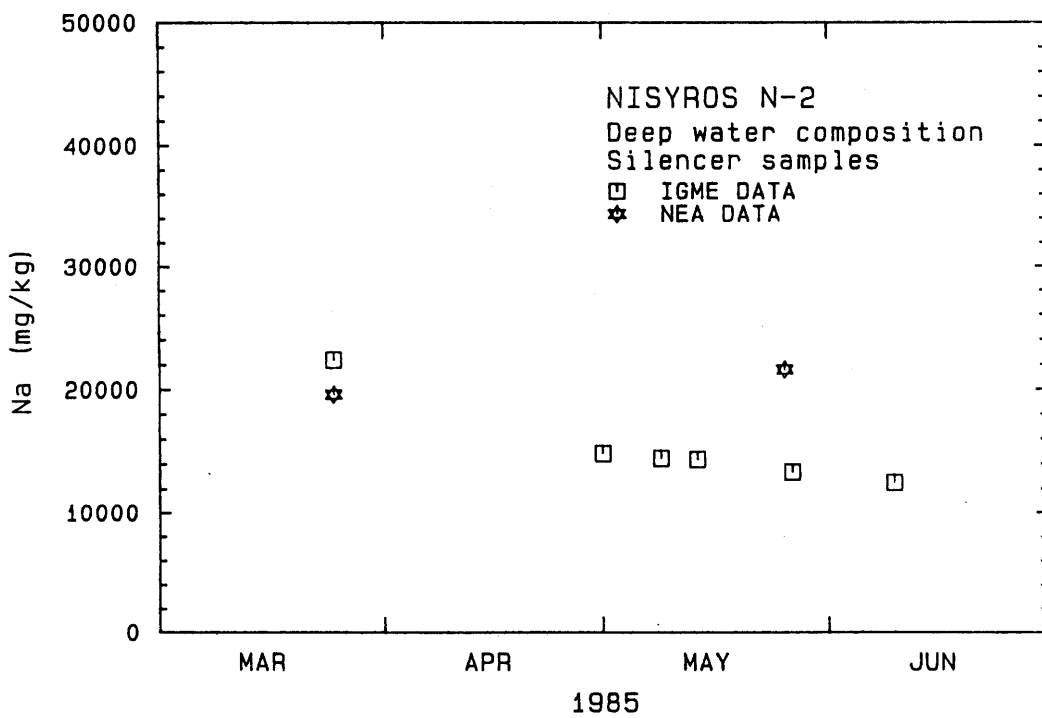
Silica in deep water.

Samples collected at high pressure.

NISYROS N-2
Deep water composition
High pressure samples
⊡ IGME DATA
✿ NEA DATA

NISYROS N-2
Deep water composition
High pressure samples
⊙ PPC DATA
✿ NEA DATA
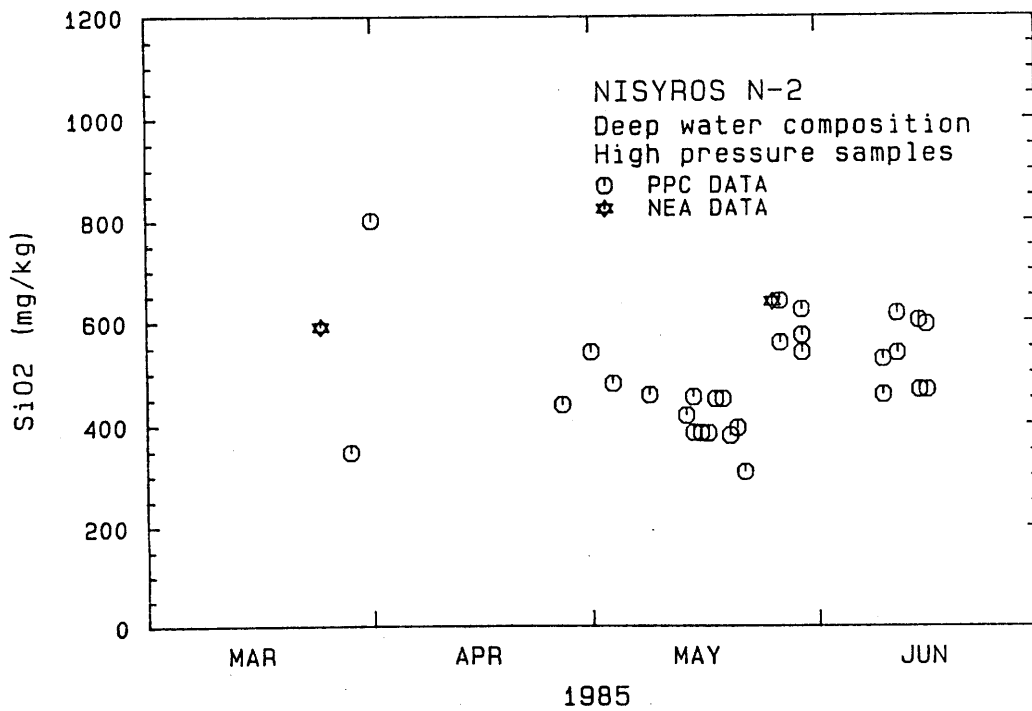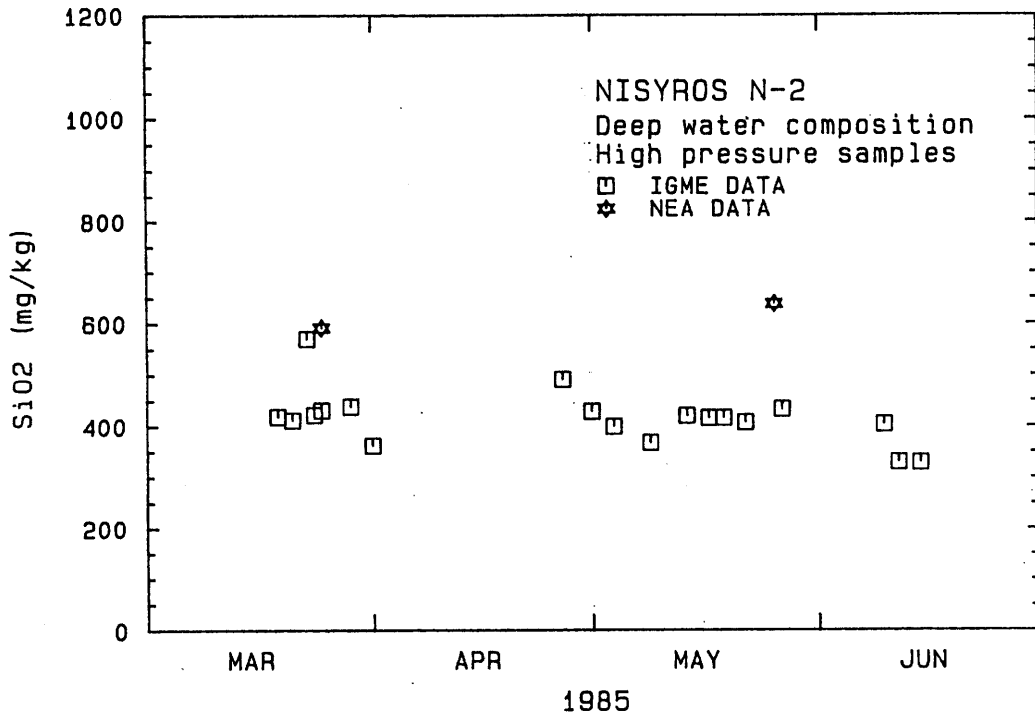
Figures A-2.3 and 2.4.

Silica in deep water.

Samples collected at atmospheric pressure.

NISYROS N-2
Deep water composition
Silencer samples
□ IGME DATA
✪ NEA DATA

NISYROS N-2
Deep water composition
Silencer samples
⊙ PPC DATA
✪ NEA DATA
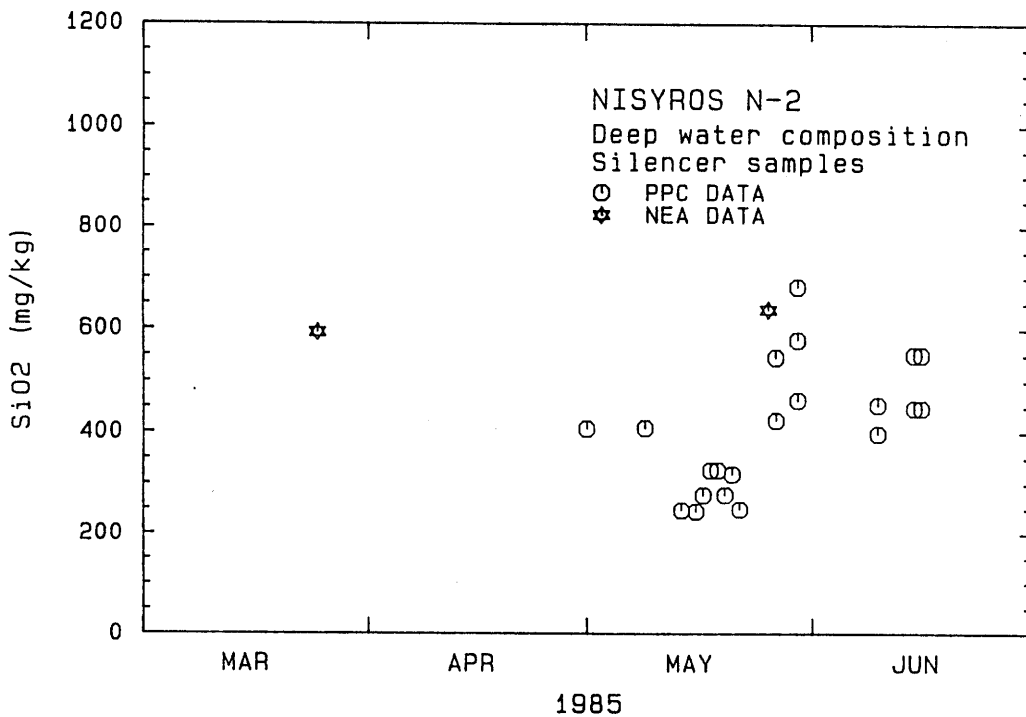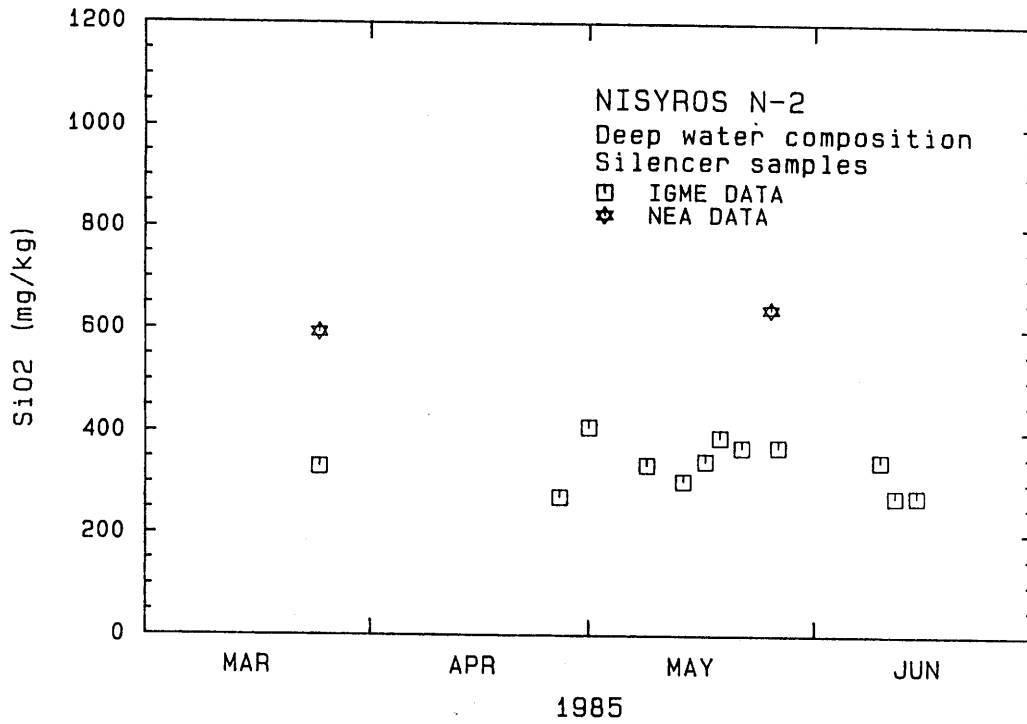
Figures A-2.5 and 2.6.

Chloride in deep water.

Samples collected at high pressure.
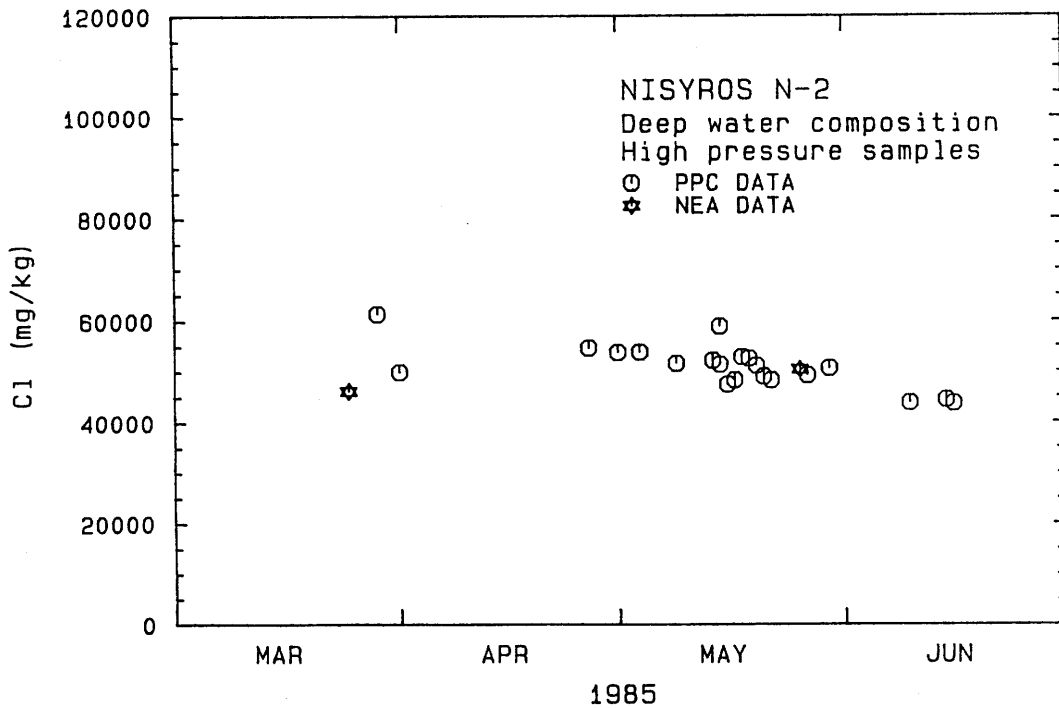
Figures A-2.7 and 2.8.

       Chloride in deep water.

       Samples collected at atmospheric pressure.

NISYROS N-2
Deep water composition
Silencer samples
⊡ IGME DATA
✿ NEA DATA

NISYROS N-2
Deep water composition
Silencer samples
⊙ PPC DATA
✿ NEA DATA
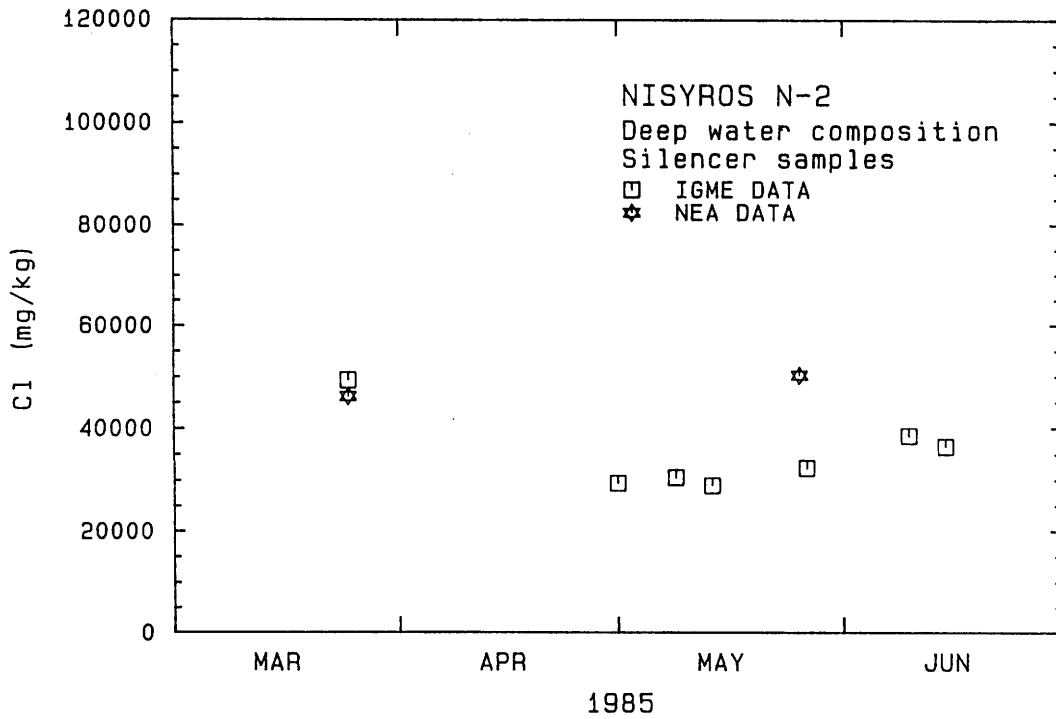
Figures A-2.9 and 2.10.

       Sodium in deep water.

NISYROS N-2
Deep water composition
High pressure samples
⊡ IGME DATA
✿ NEA DATA

NISYROS N-2
Deep water composition
Silencer samples
⊡ IGME DATA
✿ NEA DATA
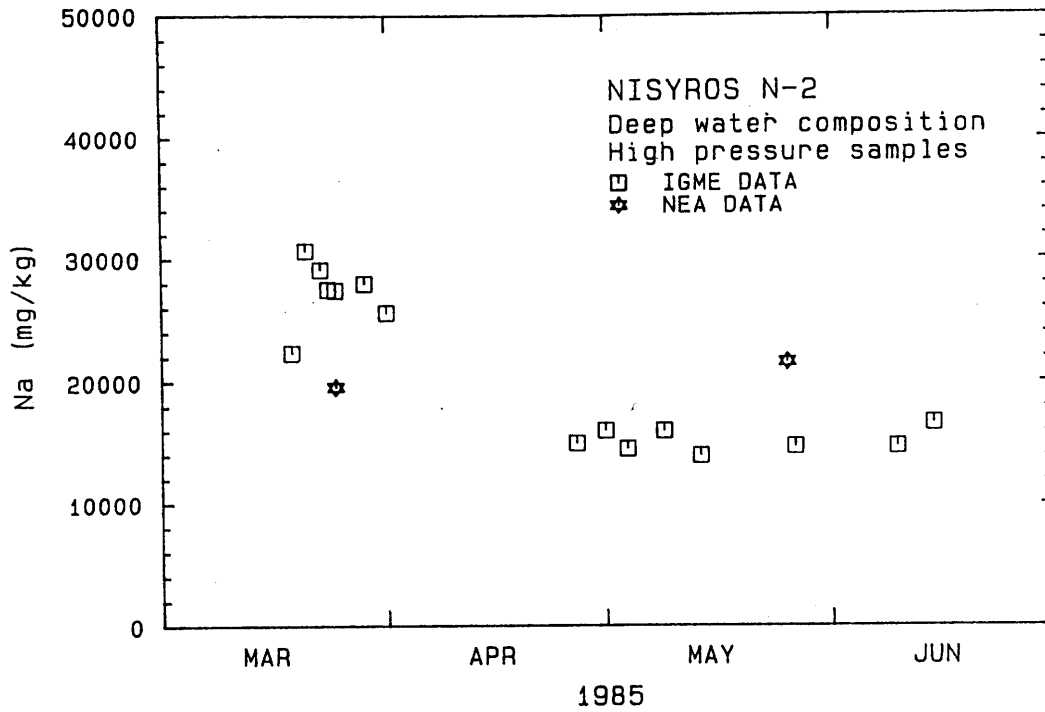
Figures A-2.11 and 2.12.

      Potassium in deep water.

Figures A-2.13 and 2.14.
        Calcium in deep water.
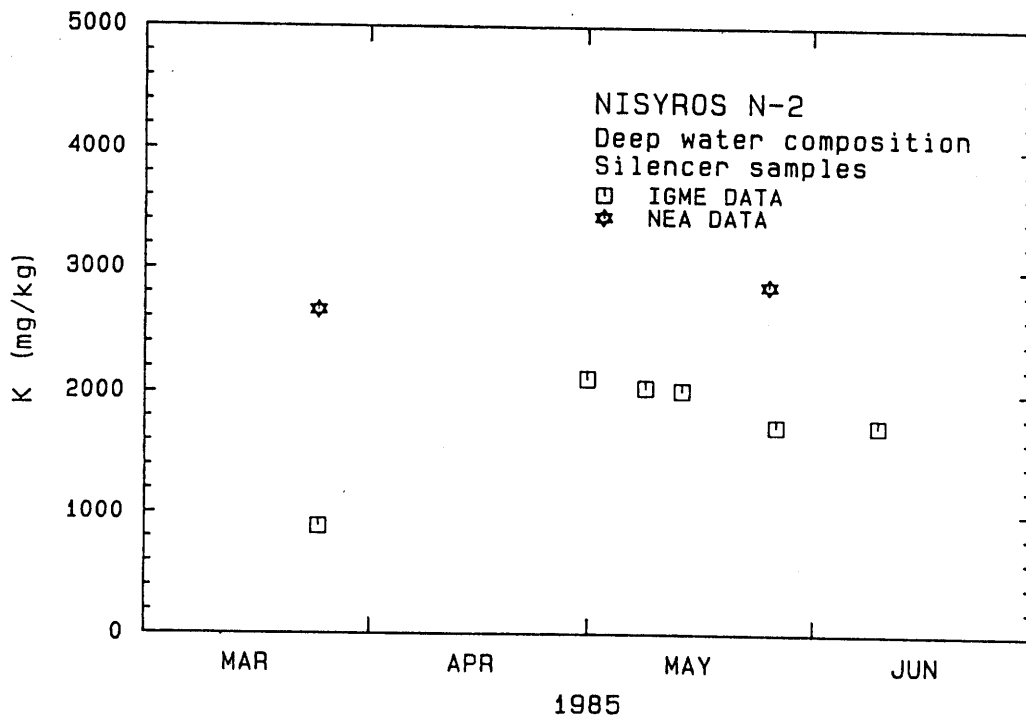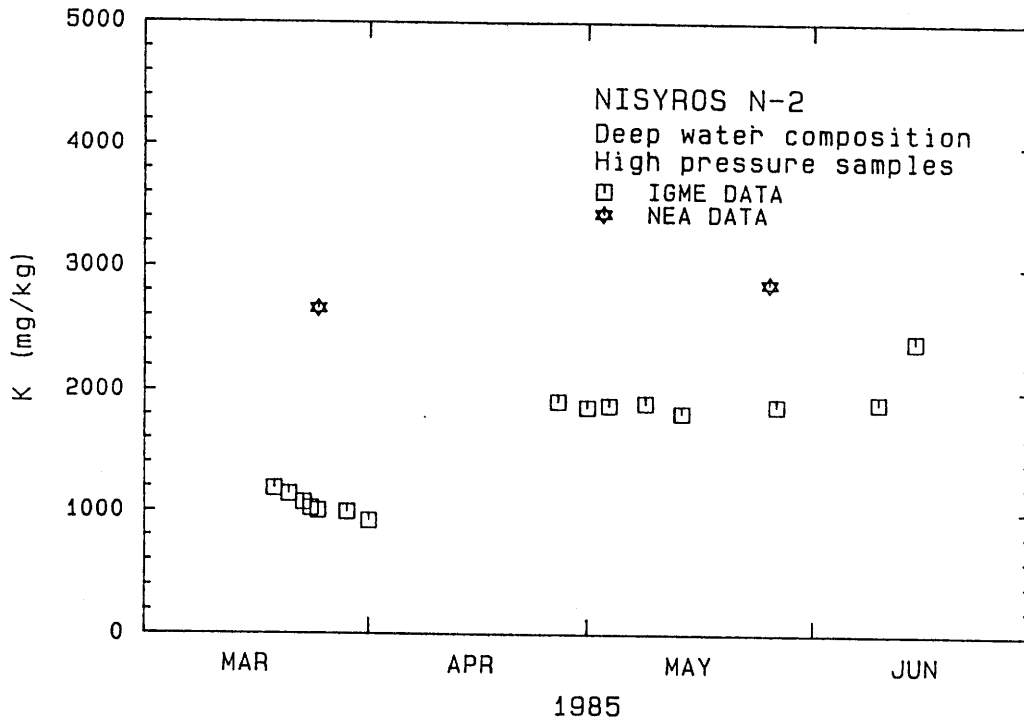
Figures A-2.15 and 2.16.

      Magnesium in deep water.

NISYROS N-2
Deep water composition
High pressure samples
☐ IGME DATA
✿ NEA DATA

NISYROS N-2
Deep water composition
Silencer samples
☐ IGME DATA
✿ NEA DATA
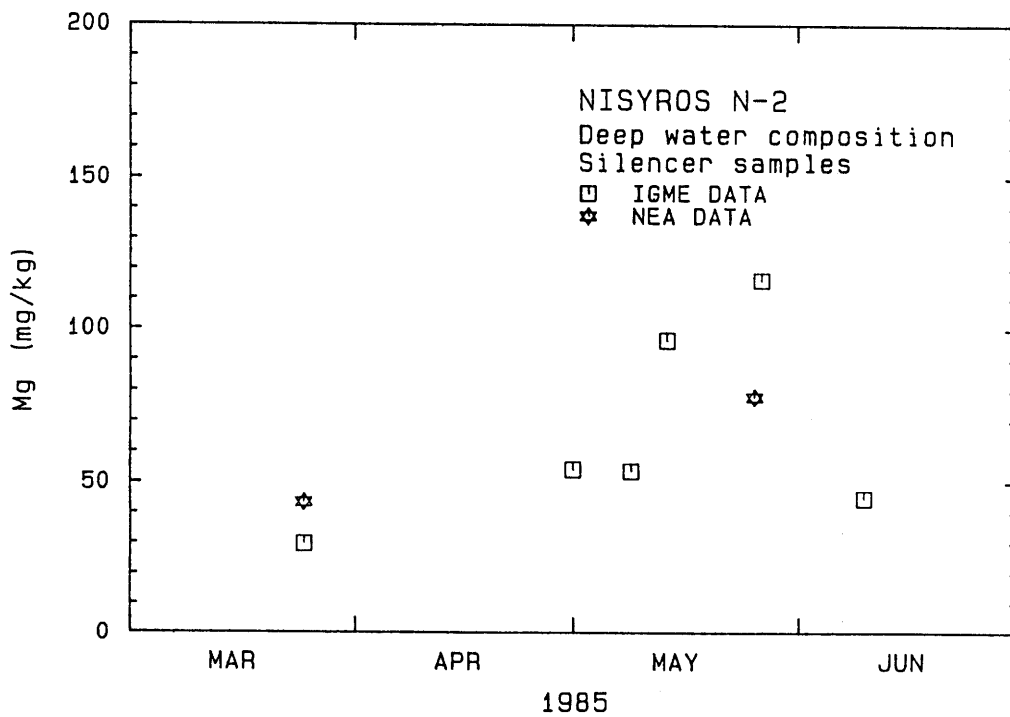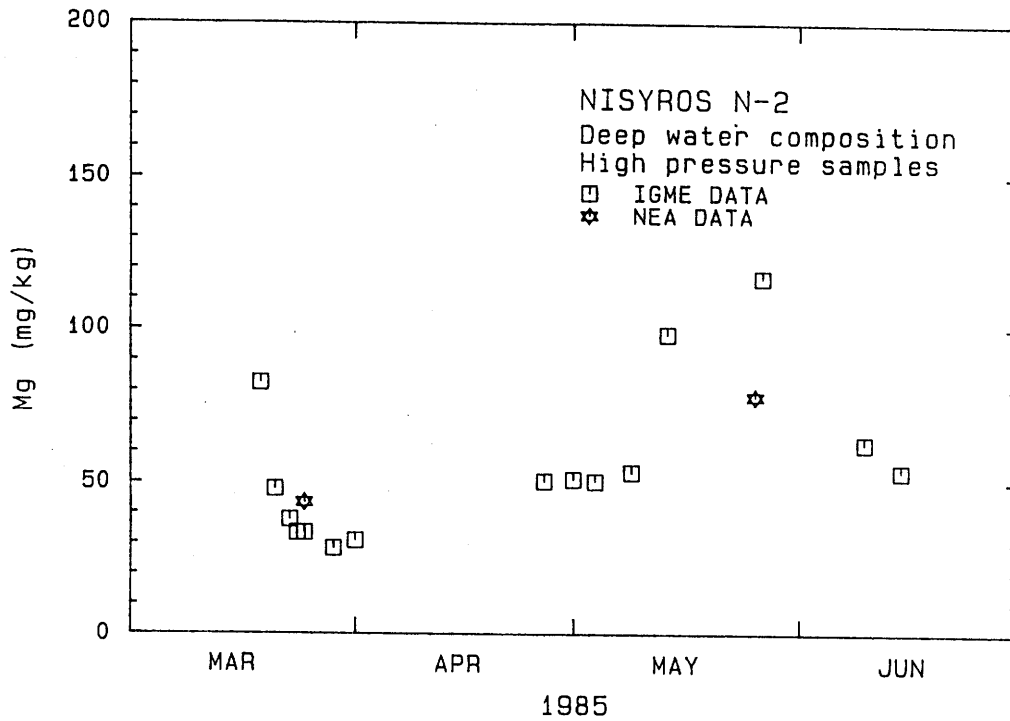
Figures A-2.17 and 2.18.
        Strontium in deep water.

NISYROS N-2
Deep water composition
High pressure samples
☐ IGME DATA

NISYROS N-2
Deep water composition
Silencer samples
☐ IGME DATA

Figures A-2.19 and 2.20.

     Lithium in deep water.
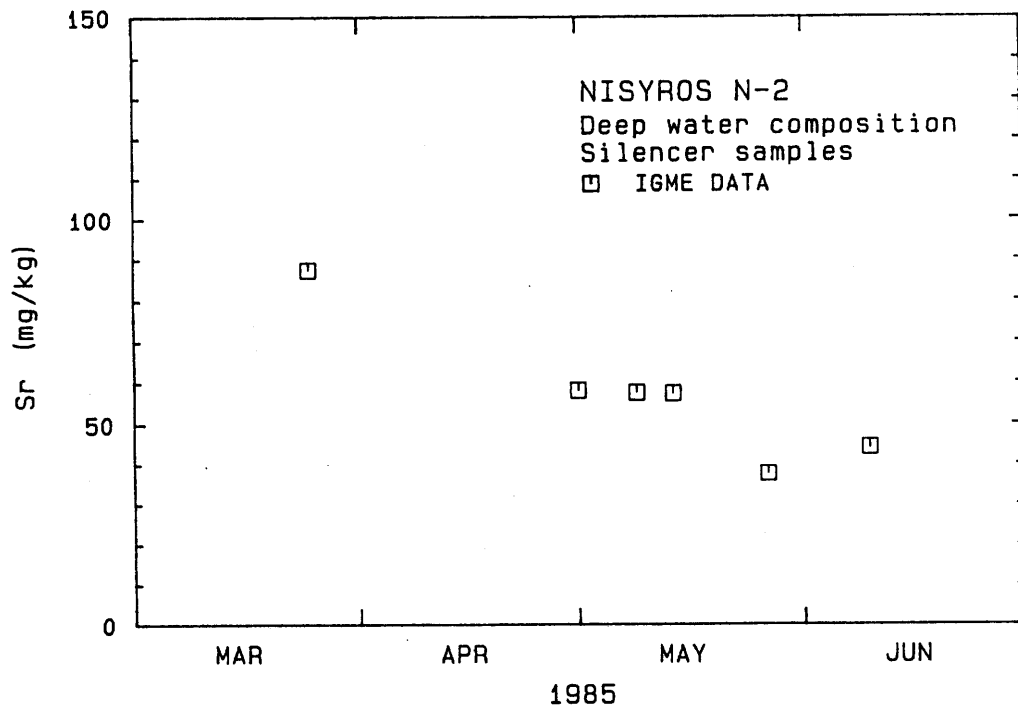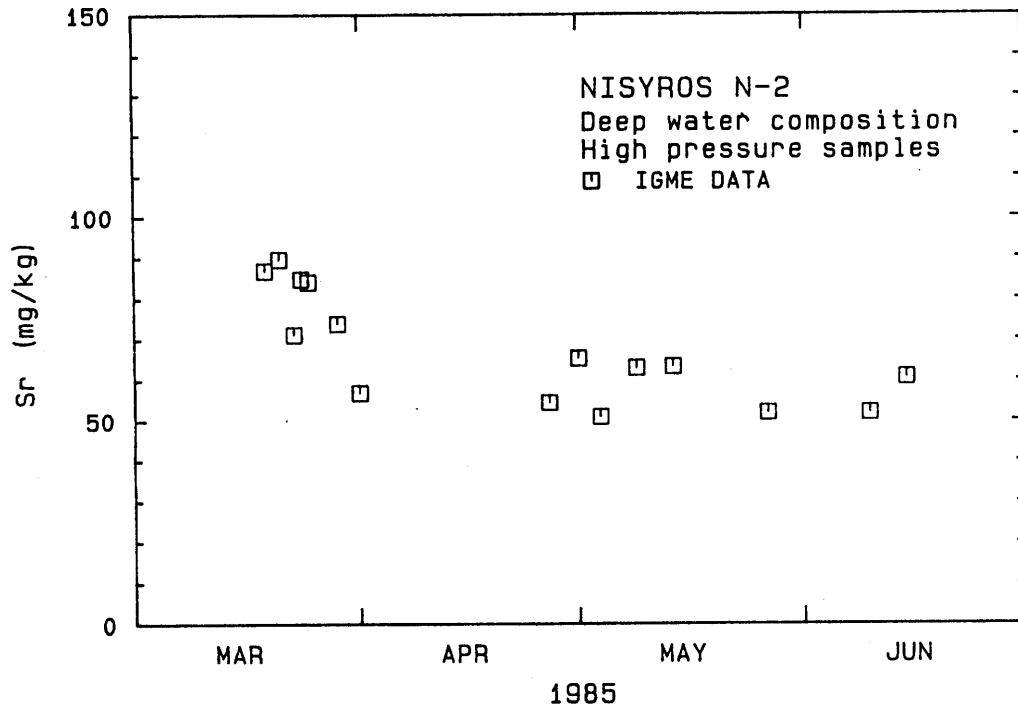
Figures A-2.21 and 2.22.
      Ratio of sodium and potassium to chloride.

Figures A-2.23 and 2.24.
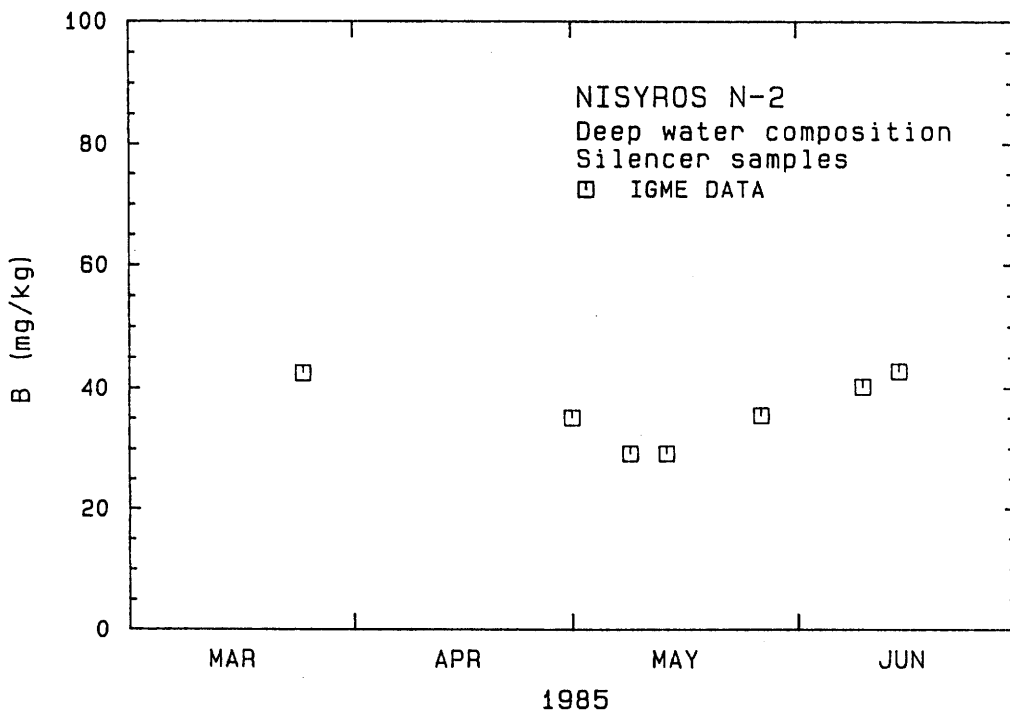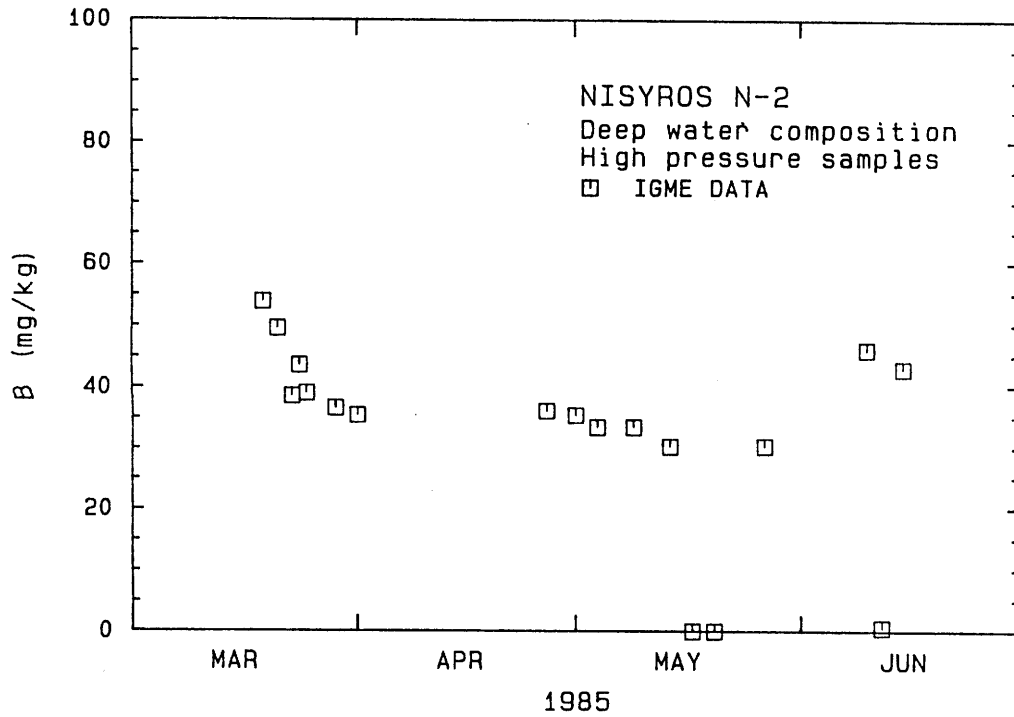   Ratio of calcium and magnesium to chloride.
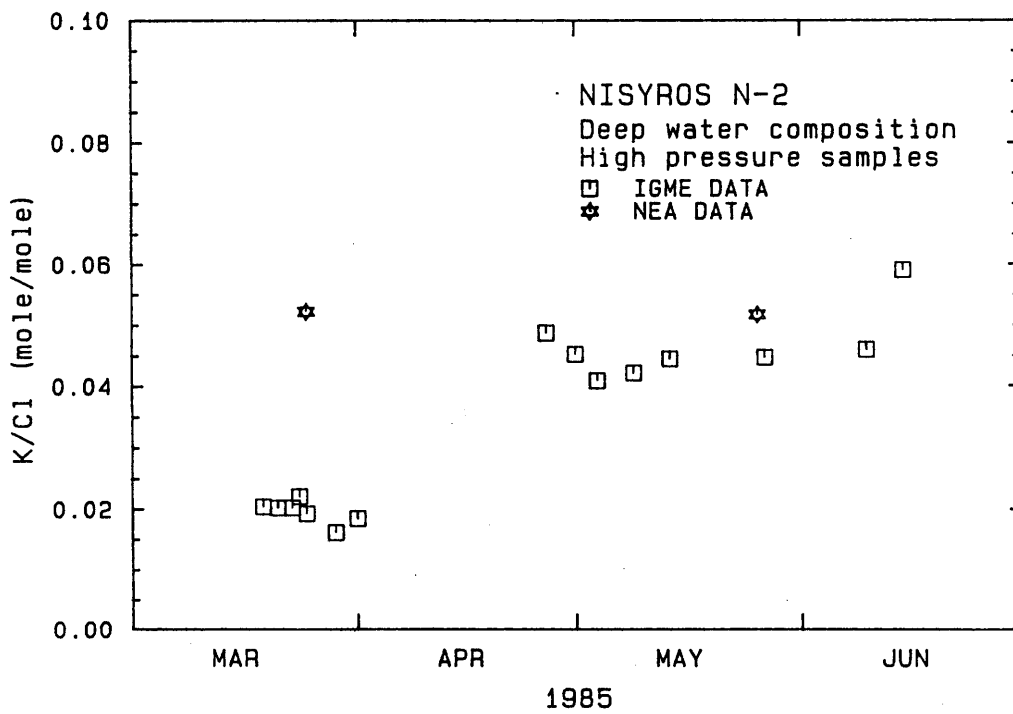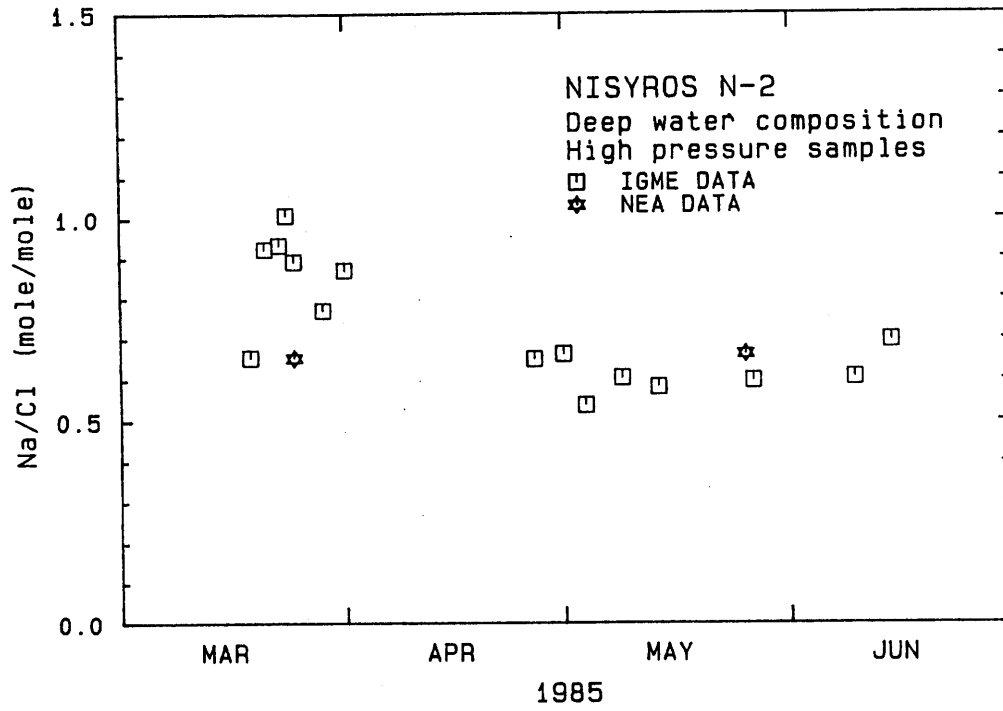
Figure   A-2.25.

Ratio of sodium to potassium.
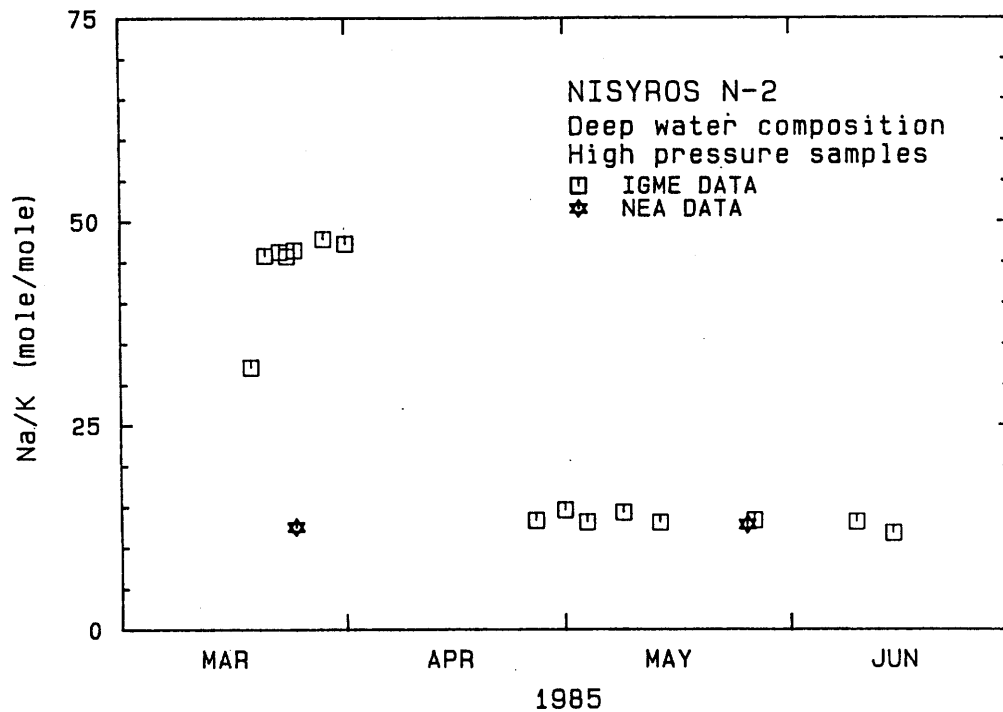
Figures A-2.26 and 2.27.
        Iron in deep water.

NISYROS N-2
Deep water composition
High pressure samples
☐ IGME DATA
✿ NEA DATA

1985

NISYROS N-2
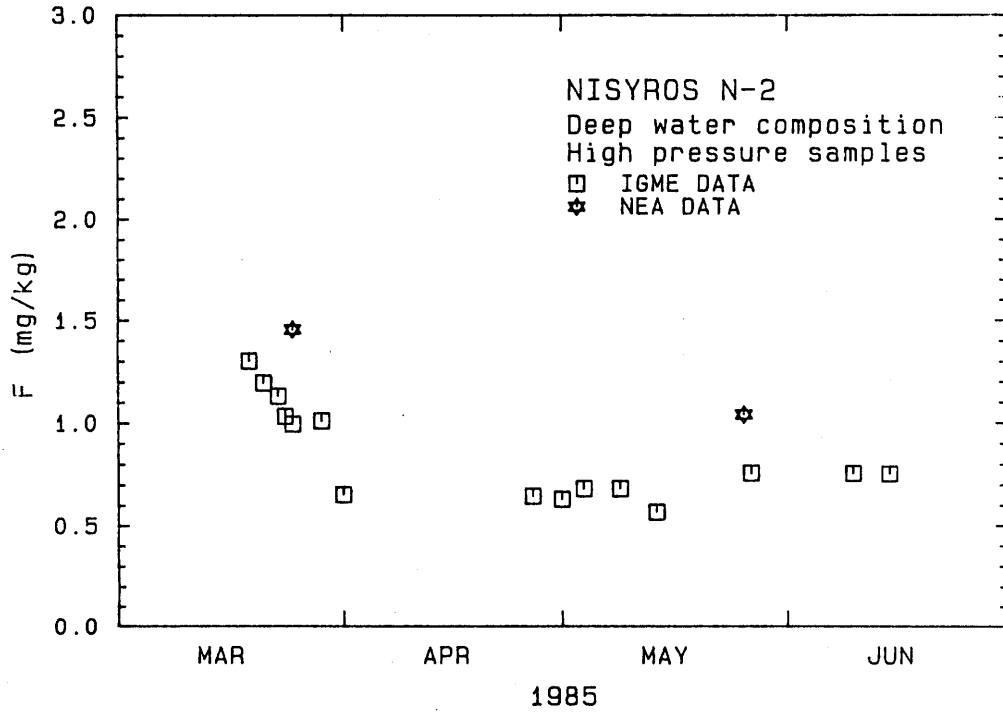Deep water composition
Silencer samples
☐ IGME DATA
✿ NEA DATA

1985
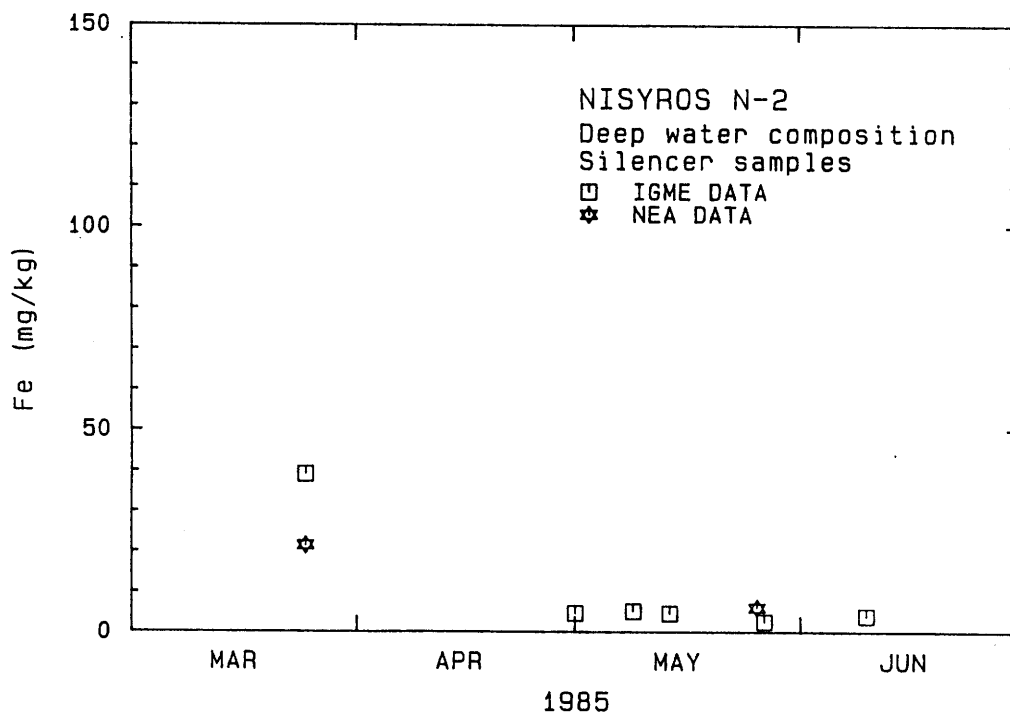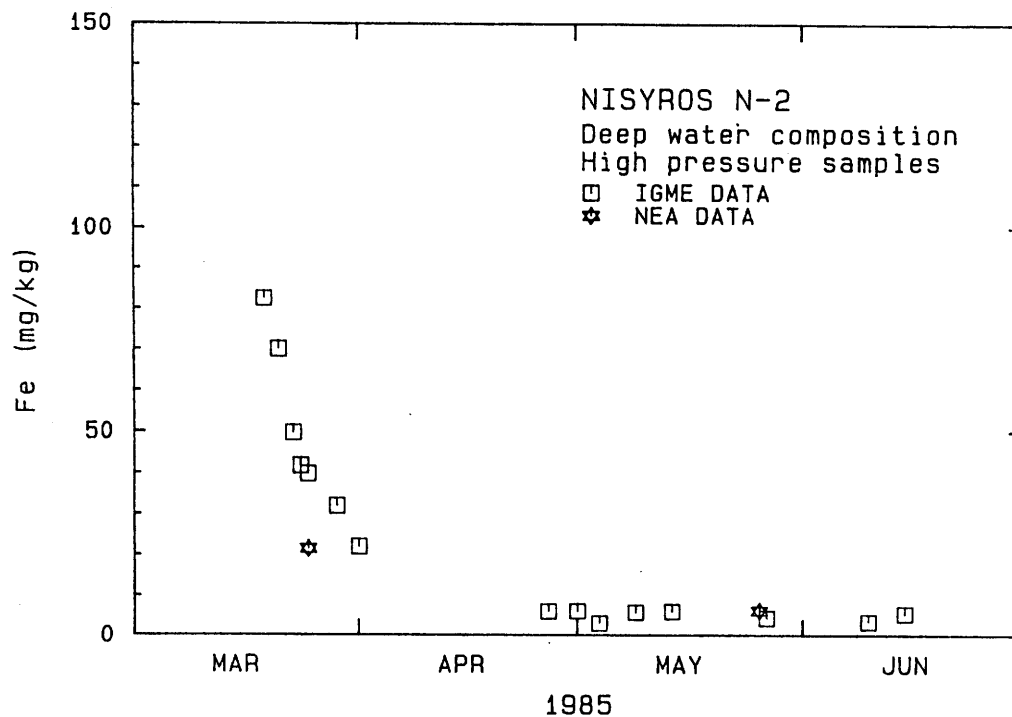
Figures A-2.28 and 2.29.
        Manganese in deep water.

NISYROS N-2
Deep water composition
High pressure samples
▫ IGME DATA

Mn (mg/kg)

200

150

100

50

0

MAR   APR   MAY   JUN

1985

NISYROS N-2
Deep water composition
Silencer samples
▫ IGME DATA

Mn (mg/kg)

200

150

100

50

0

MAR   APR   MAY   JUN

1985
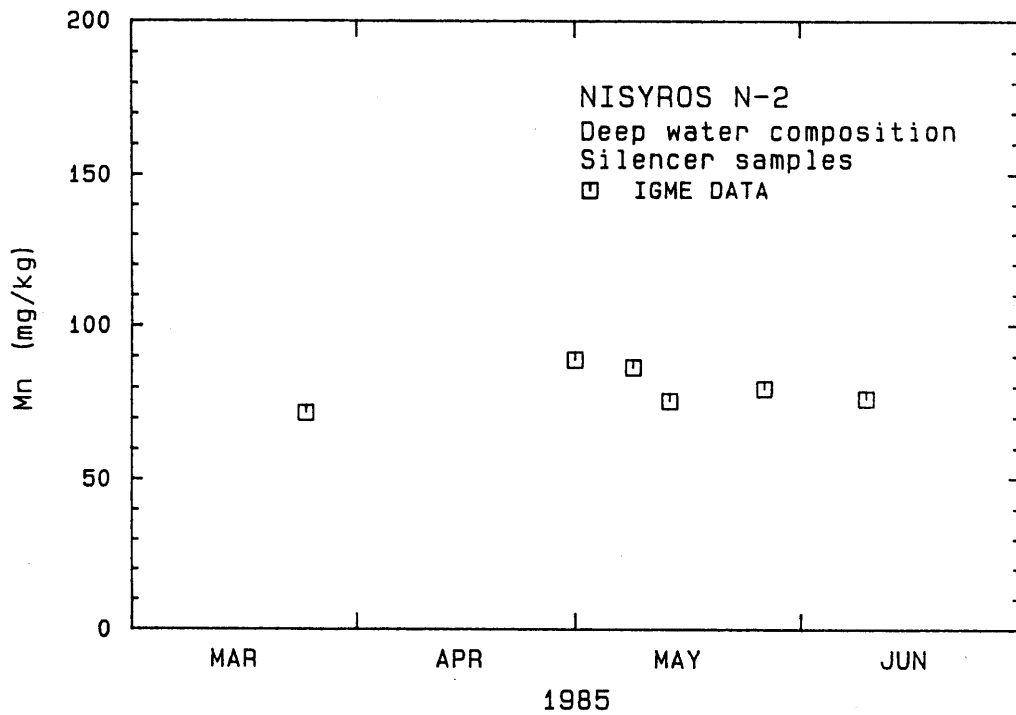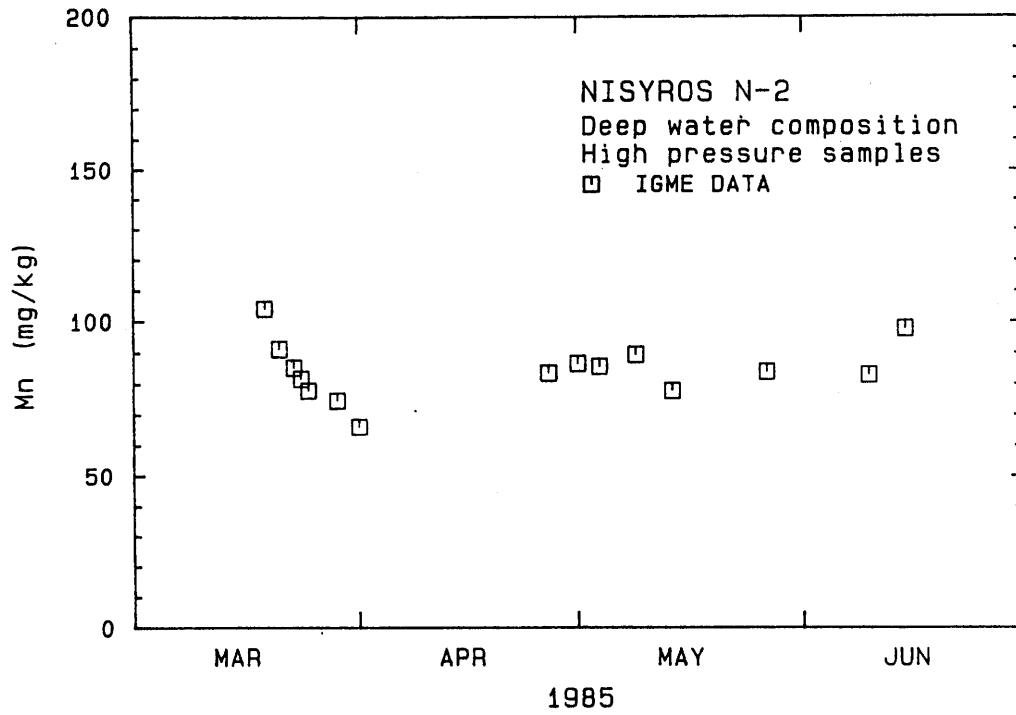
Figures A-2.30 and 2.31.
    Boron in deep water.

Figures A-2.32 and 2.33.

     Fluoride in deep water.
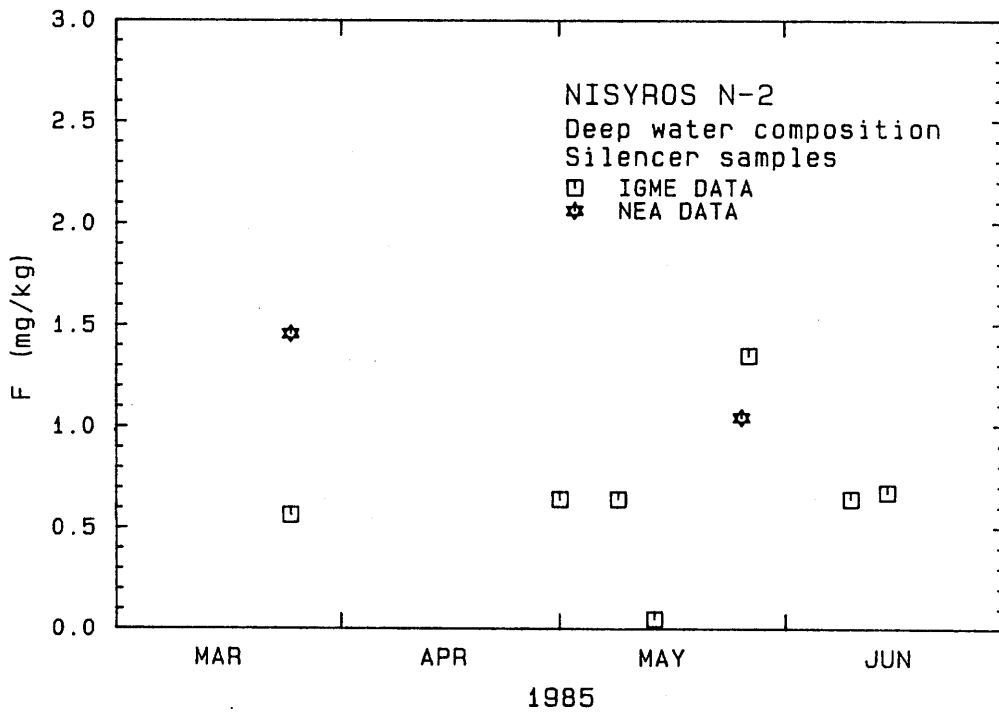
Figures A-2.34 and 2.35.
        Sulfate in deep water.

NISYROS N-2
Deep water composition
High pressure samples
☐ IGME DATA
✿ NEA DATA

NISYROS N-2
Deep water composition
Silencer samples
☐ IGME DATA
✿ NEA DATA
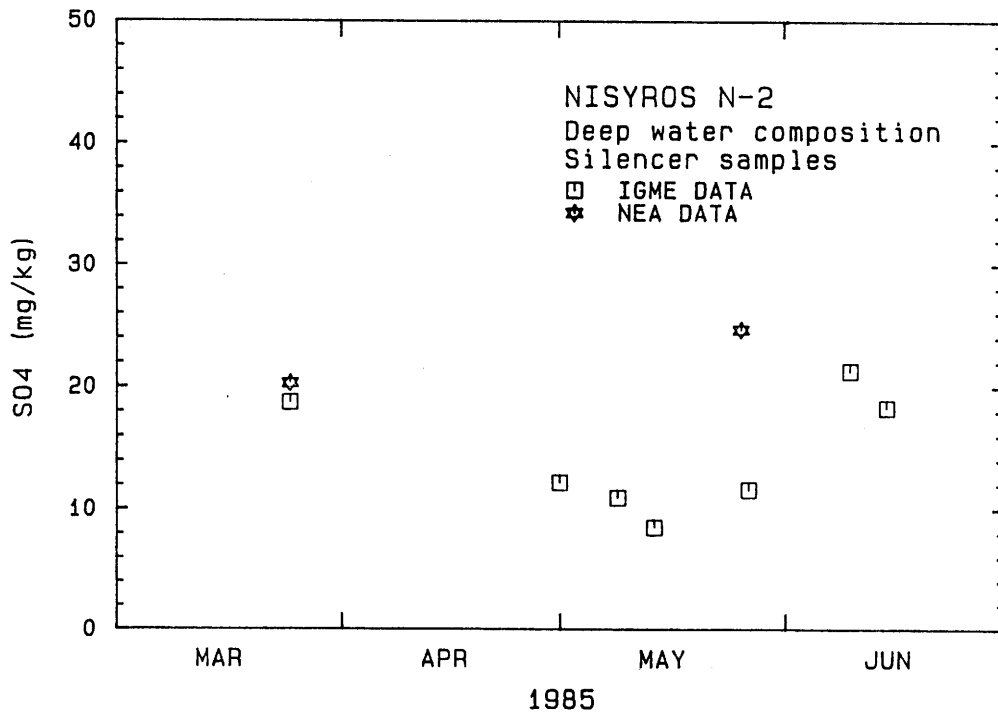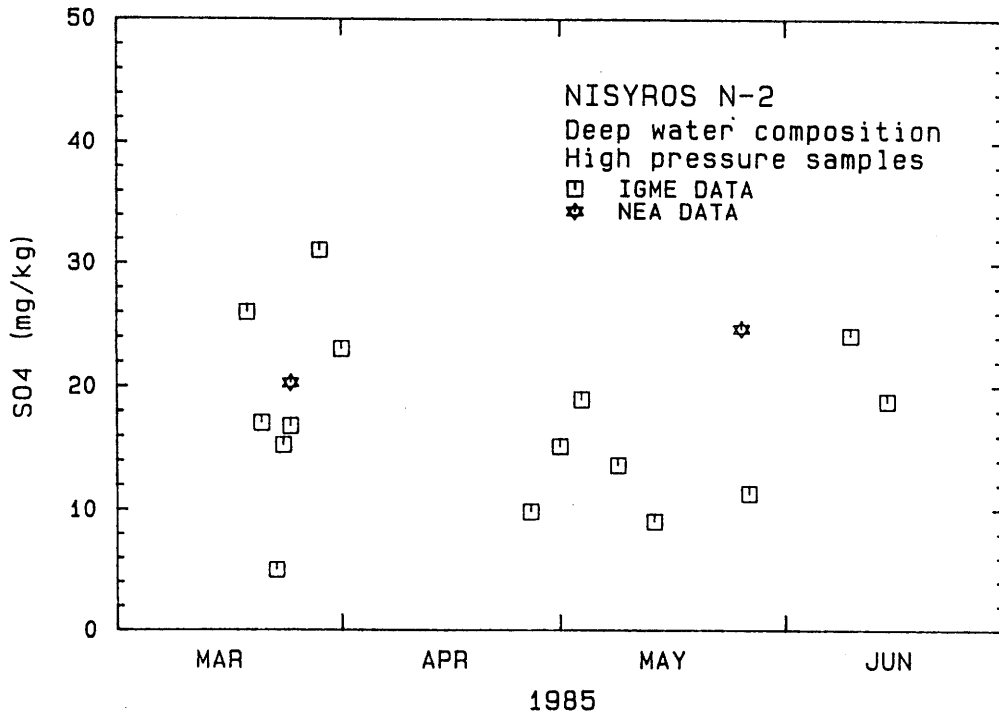
Figures A-2.36 and 2.37.

      Total dissolved solids in deep water.

NISYROS N-2
Deep water composition
High pressure samples
▣ IGME DATA
✿ NEA DATA

NISYROS N-2
Deep water composition
Silencer samples
▣ IGME DATA
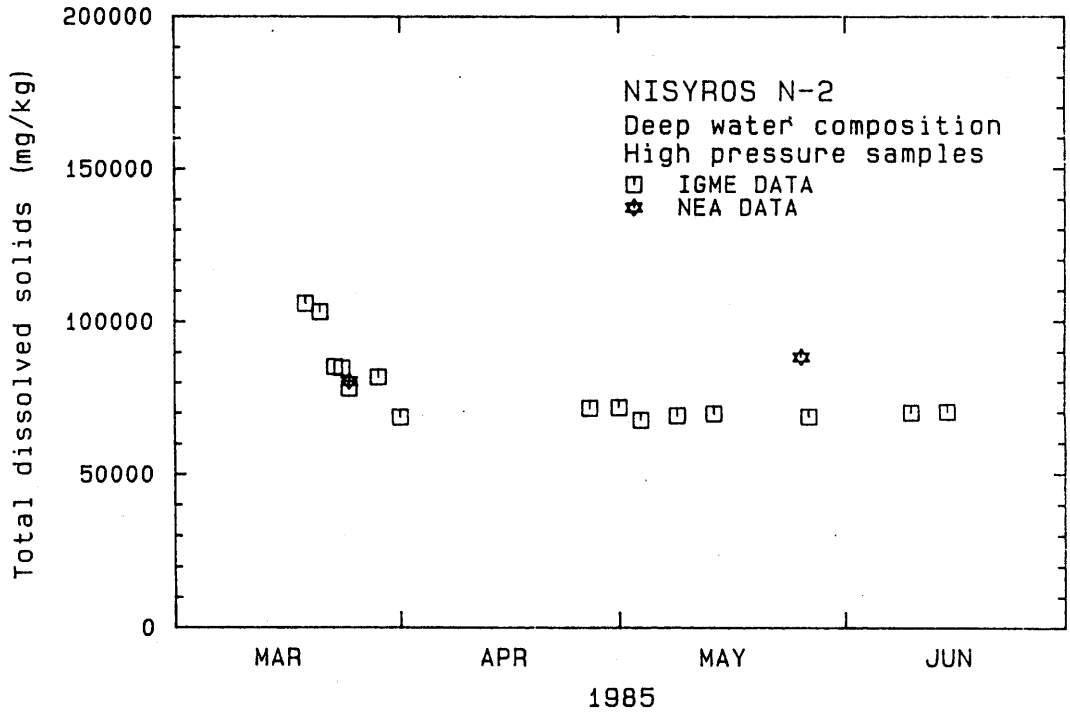✿ NEA DATA
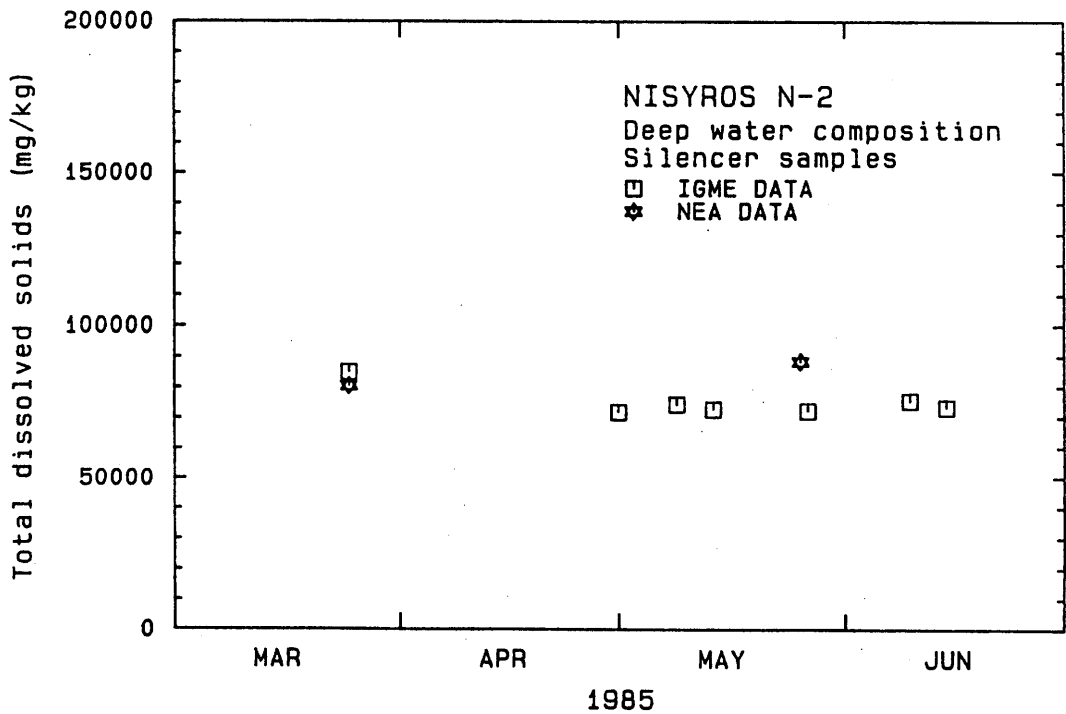
Figure A-2.38.
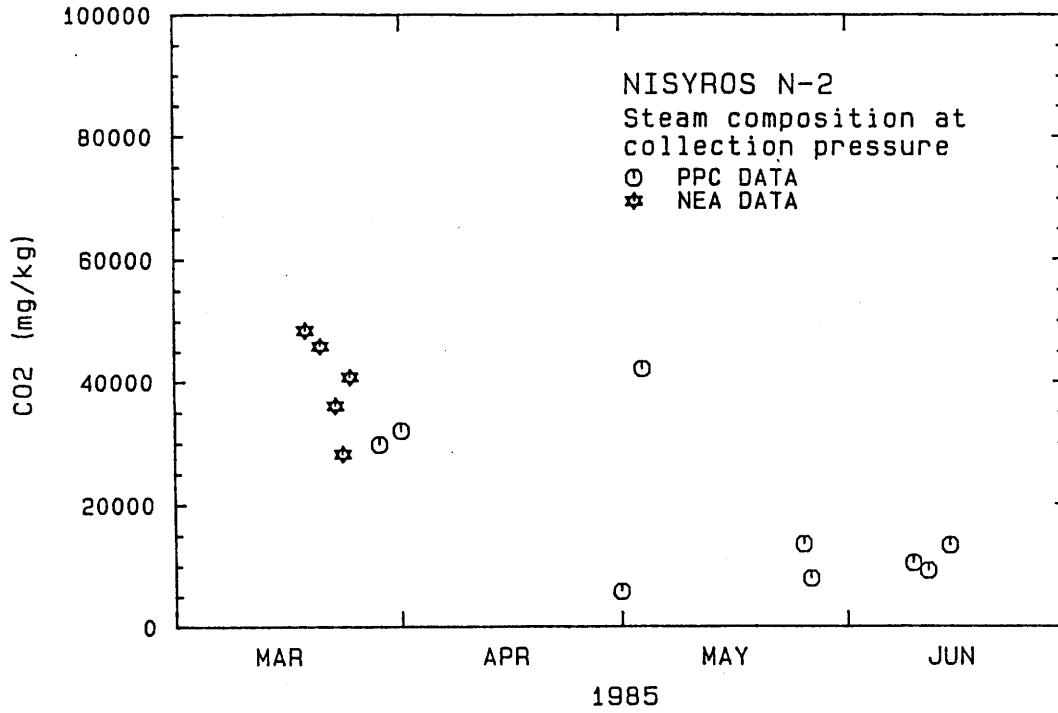   Carbon dioxide in steam.
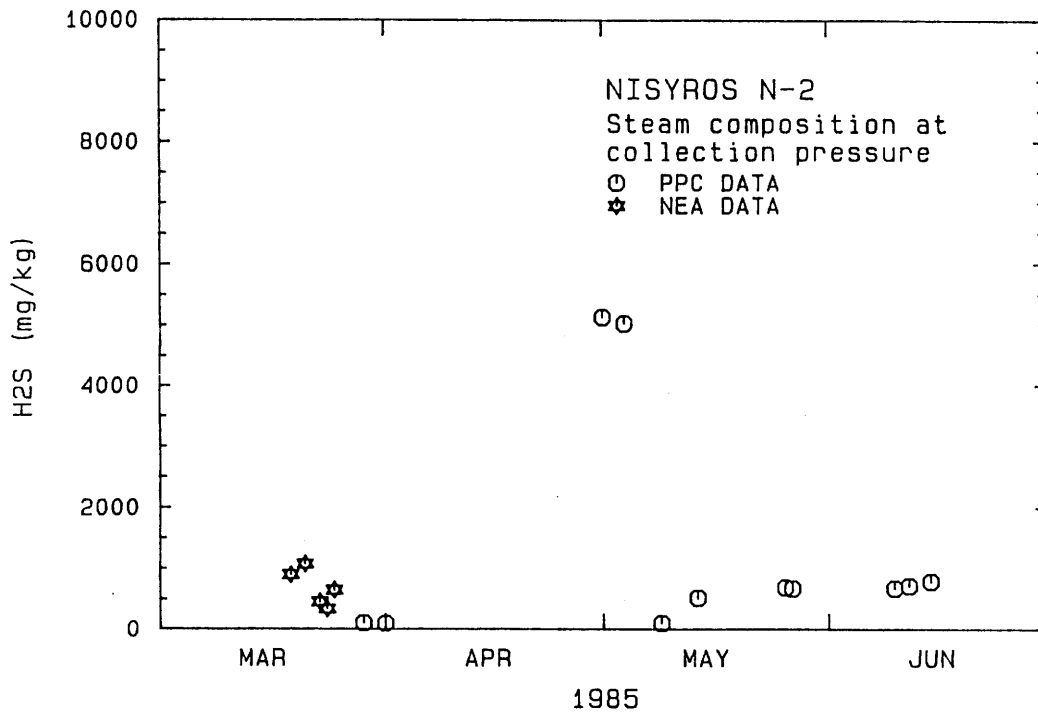

Figure A-2.39.
        Hydrogen sulfide in steam.

Figures A-2.40 and 2.41.

Total gas in steam.
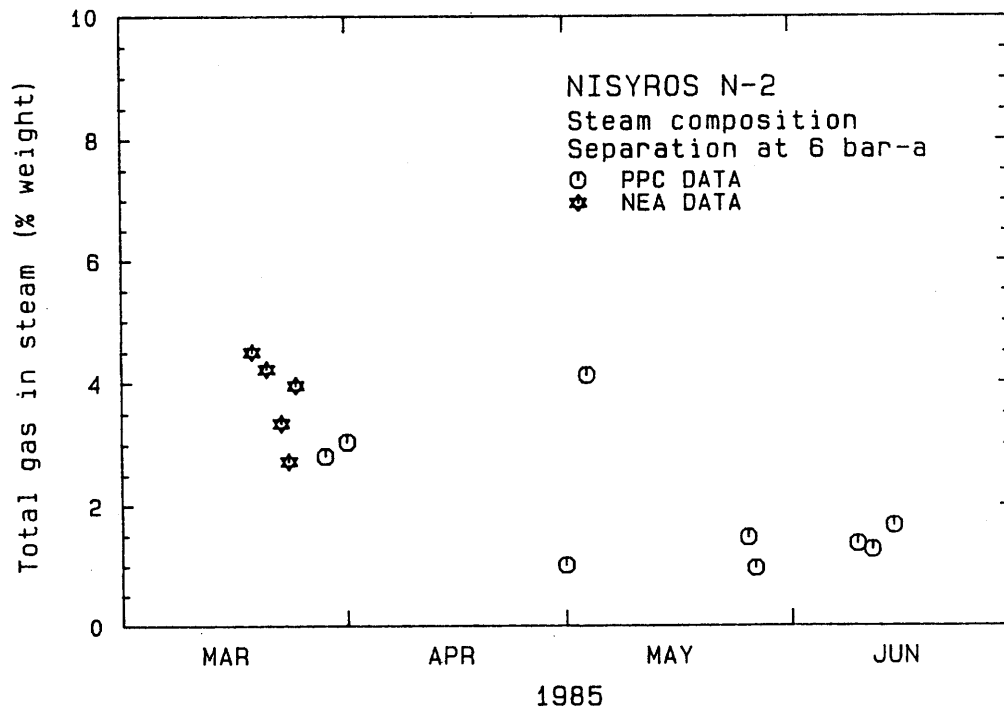

NISYROS N-2
Steam composition
Separation at 12 bar-a
⊘ PPC DATA
✿ NEA DATA

NISYROS N-2
Steam composition
Separation at 6 bar-a
⊘ PPC DATA
✿ NEA DATA
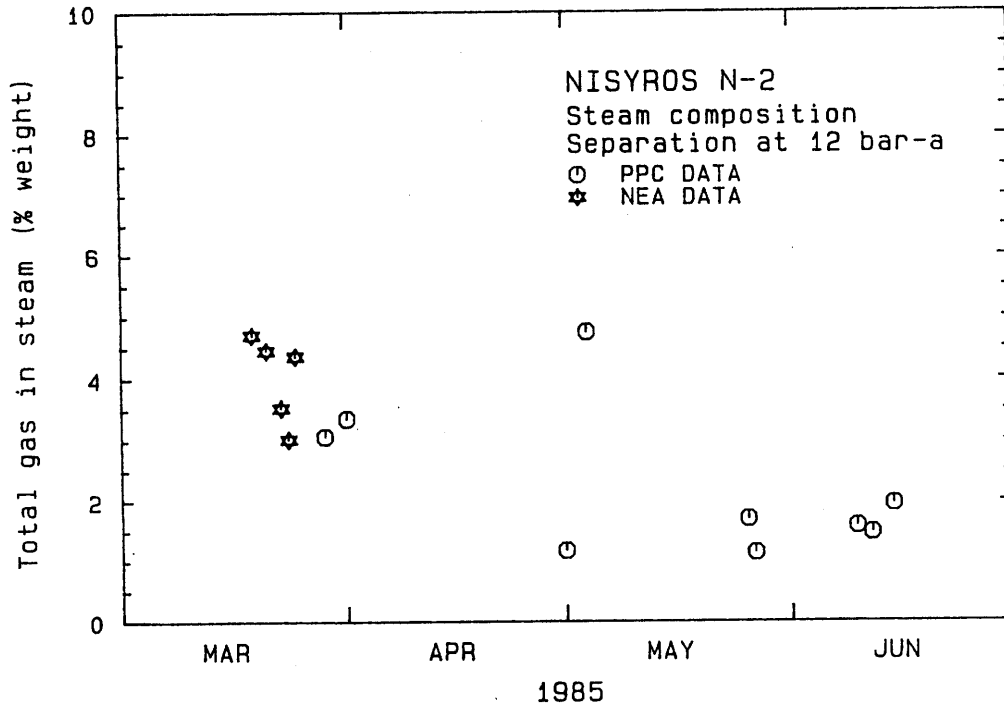
Figure A-2.42.

  Total gas in steam.

NISYROS N-2
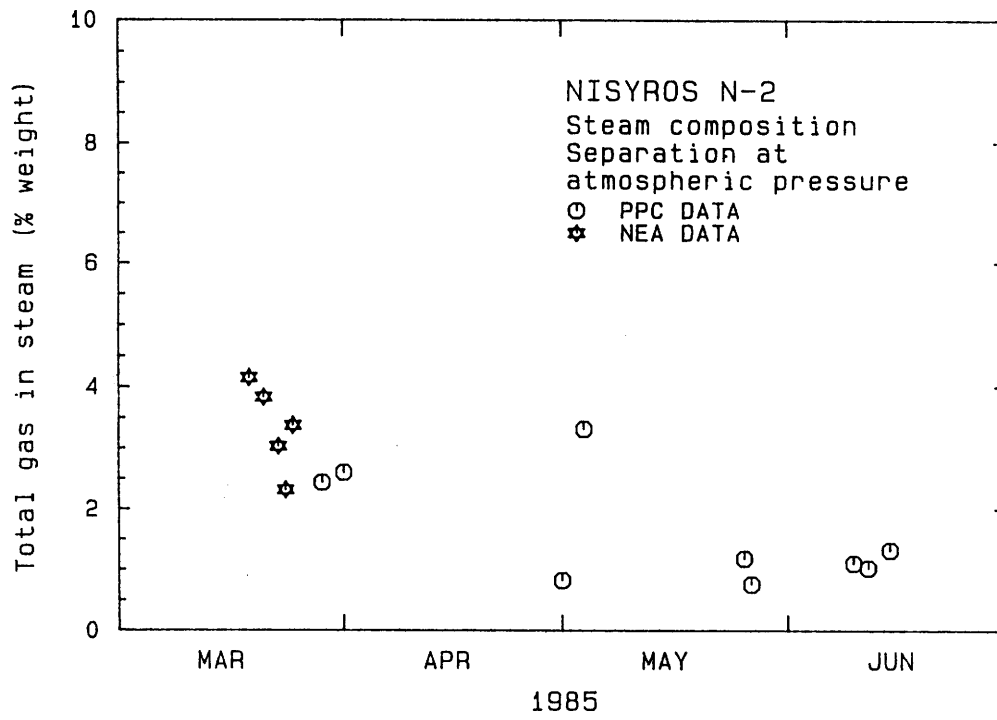Steam composition
Separation at
atmospheric pressure
⊙ PPC DATA
✿ NEA DATA

Figure A-2.43.

CO_2/H_2S ratio.